Using three-dimensional point clouds to improve characterizations of forest structure across spatial and temporal scales in mixedwood forest stands

by

Christopher William Mulverhill

B.S. University of Oregon, 2016

A DISSERTATION SUBMITTED IN PARTIAL FULFILLMENT OF

THE REQUIREMENTS FOR THE DEGREE OF

DOCTOR OF PHILOSOPHY

in

THE FACULTY OF GRADUATE AND POSTDOCTORAL STUDIES

(Forestry)

THE UNIVERSITY OF BRITISH COLUMBIA

(Vancouver)

July 2020

The following individuals certify that they have read, and recommend to the Faculty of Graduate and Postdoctoral Studies for acceptance, the dissertation entitled:

Using three-dimensional point clouds to improve characterizations of forest structure across spatial and temporal scales in mixedwood forest stands

submitted by Christopher William Mulverhill in partial fulfillment of the requirements for the degree of Doctor of Philosophy in Forestry

Examining Committee:

Nicholas C. Coops, Professor, Forestry, UBC
Supervisor

Peter L. Marshall, Professor, Forestry, UBC
Supervisory Committee Member

Joanne C. White, Research Scientist, Canadian Forest Service
Supervisory Committee Member

Sean M. Smukler, Associate Professor, Land and Food Systems, UBC
University Examiner

Julie Cool, Assistant Professor, Forestry, UBC
University Examiner

Van R. Kane, Research Professor, College of the Environment, University of Washington
External Examiner

Abstract

Sustainably managing the world's forests requires detailed inventories of the resource at varying spatial and temporal scales. The structural and compositional diversity of the boreal mixedwood forest, one of Canada's largest forest types, provides valuable timber resources and ecological services. However, the extent and complexity of this forest type poses challenges for inventories. The objective of this dissertation was to develop and assess the utility of three-dimensional remote sensing techniques for enhancing forest inventories by characterizing forest structure in boreal mixedwood forests. These technologies are scalable and adaptable for use in forest inventory as they provide consistent spatial and temporal detail.

Digital terrestrial photogrammetry from spherical cameras at known locations was used to model individual tree stems and sample plots. For individual trees, stem diameters at different heights were estimated very accurately (RMSE < 1 cm for stem heights below 10 m), which matched or exceeded the accuracy of conventional ground-based inventories. Plot-level point clouds based on a relatively small set of images were used to locate and model trees on sample plots to an accuracy that was comparable to other studies on homogeneous plots (mean 72% detection and 19% RMSE of diameter at breast height).

At broader scales, airborne laser scanning (ALS) was used to characterize forest structure by estimating stem size distributions (SSD) across a large forest management unit. First, ALS was used to differentiate unimodal and bimodal stands. Next, parameters of functions describing the SSDs were estimated with ALS metrics ($r^2 \approx 0.5$) and the resulting functions were more accurate in characterizing field-measured SSDs than without differentiating stands by modality. For assessing temporal patterns of forest structure, photo-interpreted polygons of fire and harvesting were used with the derived SSDs to characterize structural development following

stand-replacing disturbance. It was determined that stands that had burned had significantly more trees in larger diameter classes than harvested stands (at $\alpha = 0.05$). This dissertation outlined the methods required when applying three-dimensional remote sensing technologies to enhancing forest inventories in mixedwood stands and demonstrated the utility of these technologies for deriving information to inform responsible decision-making for management of these forests.

Lay summary

Forest inventories are critical for sustainable management. Current challenges such as the consistency of acquisition, level of detail, and forest access have led to the adoption of three-dimensional remote sensing techniques such as photogrammetry and laser scanning for use in deriving detailed forest structural attributes. In this dissertation, three-dimensional remote sensing methods were adapted for use at different scales in a large, diverse, and important forest type in Canada, the boreal mixedwood forest. For information on individual trees and sample plots, terrestrial photogrammetry was used to characterize individual tree stems. Moving up to the landscape scale, airborne laser scanning was used to determine variation within forest stands. Finally, this variation was used to characterize the patterns of structural development over time. The role and prospects of the resulting data for enhancing forest inventories was discussed, emphasizing the value for heterogeneous forest types such as boreal mixedwood.

Preface

The objectives of this dissertation were developed through a series of discussions between me and my supervisory committee. Much of the research presented in the dissertation has been published in peer-reviewed publications, which are listed below. For each publication, I developed the methods, processed and analyzed the data, interpreted the results, and prepared the manuscripts for publication. Co-authors for each publication provided critical feedback and recommendations for each manuscript and, in some cases, provided data.

<u>Chapter 3:</u>

Mulverhill, C., Coops, N. C., Tompalski, P., Bater, C. W., & Dick, A. R. (2019). The utility of terrestrial photogrammetry for assessment of tree volume and taper in boreal mixedwood forests. *Annals of Forest Science*, *76*(3). https://doi.org/10.1007/s13595-019-0852-9

<u>Chapter 4:</u>

Mulverhill, C., Coops, N. C., Tompalski, P., & Bater, C. W. Digital terrestrial photogrammetry to enhance field-based forest inventory across stand conditions. *Submitted.*

<u>Chapter 5:</u>

Mulverhill, C., Coops, N. C., White, J. C., Tompalski, P., Marshall, P. L., & Bailey, T. (2018). Enhancing the estimation of stem-size distributions for unimodal and bimodal stands in a boreal mixedwood forest with airborne laser scanning data. *Forests*. https://doi.org/10.3390/f9020095

<u>Chapter 6:</u>

Mulverhill, C., Coops, N. C., White, J. C., Tompalski, P., & Marshall, P. L. (2019). Structural development following stand-replacing disturbance in a boreal mixedwood forest. *Forest Ecology and Management*, *453*. https://doi.org/10.1016/j.foreco.2019.117586

With support and guidance from co-authors, results were presented at the following conferences:

Mulverhill, C., Coops, N. C., White, J. C., Tompalski, P., & Marshall, P. L. Using 3-Dimensional Point Clouds to Improve Characterizations of Tree Stems Across Scales in Boreal Mixedwood Forest Stands. *New Frontiers in Forecasting Forests.* Stellenbosch, South Africa. September 2018.

Mulverhill, C., Coops, N. C., Tompalski, P., Bater, C. W., & Dick, A. R. (October 2019). Terrestrial Photogrammetric Measurements at the Individual Tree and Plot Levels in a Boreal Mixedwood Forest. *Silvilaser*. Foz do Iguaçu, Brazil.

Table of contents

List of tables

List of figures

List of abbreviations

ABA – Area-based Approach

ALS – Airborne Laser Scanning

AVI – Alberta Vegetation Inventory

CAD$ – Canadian dollars

DAP – Digital Aerial Photogrammetry

DBH – Diameter at Breast Height

DTP – Digital Terrestrial Photogrammetry

EI – Error Index

EFI – Enhanced Forest Inventory

FMM – Finite Mixture Model

FR – Filling Ratio

GAMM – Generalized Additive Mixed Models

GPS – Global Positioning System

LAD CV – Leaf Area Density – Coefficient of Variation

LiDAR – Light Detection and Ranging

MLE – Maximum Likelihood Estimation

NFI – National Forest Inventory

NN – Nearest Neighbor

PDF – Probability Density Function

PSP – Permanent Sample Plot

RMSE – Root Mean Square Error

RMSE% - Relative (%) Root Mean Square Error

SD – Standard Deviation

SSD – Stem Size Distribution

TLS – Terrestrial Laser Scanning

VCI – Vertical Complexity Index

Acknowledgements

First, I would like to thank my supervisor, Dr. Nicholas C. Coops, to whom I owe much of my success in this degree. Dr. Coops shows an unmatched level of support and appreciation to his students and I am thankful for the trust and guidance he has shown me in the last four years. Under his supervision, I have learned and grown very much, and I would have never made it this far without him. Also, my other supervisory committee members, Dr. Joanne C. White and Dr. Peter L. Marshall have been instrumental in helping me to develop many of the projects in this thesis. I thank them for the patience and care that they have shown me to help me to communicate and strengthen my work. Thanks also goes to Dr. Adam Dick at the Canadian Wood Fibre Centre for his help in developing components of this dissertation. Christopher Bater helped to develop components of this dissertation and also helped coordinate critical portions of the fieldwork, for which I am very grateful. I am also thankful to Dr. Christopher Bone, who supported my early research endeavors at the University of Oregon and encouraged me to venture out of my comfort zone and into the open arms of Canada.

The Integrated Remote Sending Studio has shown me an unimaginable amount of friendship and support, for which I am eternally grateful. Particular thanks go to Dr. Piotr Tompalski, Dr. Txomin Hermosilla, Dr. Douglas Bolton and Dr. Tristan Goodbody who have never hesitated to help me when I needed it and have shown a great deal of support both in and out of the lab. I was fortunate to go on fieldwork in my study area in 2016 and 2018 with amazing field crews from the IRSS, and I am thankful to them for their diligence and helping me to find a balance between work and play.

Nothing in my life would be possible without my mom, dad, sister, and the rest of my family who have been pillars of strength, support, love, and help in my life. I am also grateful to those I am lucky to call my friends who have been there for me throughout this ups and downs of my degree. Particular thanks go to Alexandria Borseth who has challenged, cared for, and supported me in more ways than she knows.

Finally, I would like to thank NSERC and West Fraser for their contributions throughout this research as a part of the AWARE project. Further thanks to all of the team members on the AWARE project at many different universities, government entities, and companies across Canada. I have thoroughly appreciated and enjoyed your support and camaraderie during the project.

Dedication

To Steve Simon and Lauren Ray

Chapter 1 – Introduction

1.1. – Background and motivation

1.1.1. – Forest information

Forests cover about one third of global land surface, and provide many valuable ecological goods and services (FAO 2010). Collecting detailed information of the forest at different scales is critical for measuring and monitoring the resource. Generally, forest inventory information is collected using a combination of terrestrial and airborne data, but there may be issues with the representativeness, consistency, timeliness, and detail of conventional inventories. This dissertation aims to develop methods for deriving forest structural information with three-dimensional remote sensing technologies across scales in a heterogeneous boreal forest.

Nearly one-third of the world's 4 billion hectares of forested area is found in the boreal forest, making it the world's largest terrestrial biome (FAO 2010). The boreal forest occurs at high latitude regions with relatively shorter growing seasons and a limited range of tree genera present such as *Abies*, *Picea*, *Pinus*, *Populus*, and *Betula* (Brandt 2009). Due to their extent and complexity, boreal forests perform a wide range of ecosystem services. Despite the short growing season, the boreal forest has global importance in the carbon cycle, and was estimated to have been responsible for 22% of terrestrial carbon sequestered in global forests between 1990 and 2007 (Pan et al. 2011). Boreal forests regulate and support the local environment, and are valuable for services such as water purification, nutrient cycling, and soil production (Hassan, Scholes, and Ash 2005). The boreal forest also provides cultural goods and services as long as humans have existed in the region (Johnson and Miyanishi 2012). Canada has 28% of the world's boreal forest, which comprises almost 80% of the nation's total forested area (Brandt et al. 2013). In addition to its vast ecological benefits, forest resources contribute a substantial amount to Canada's economy, supporting over 300,000 jobs and adding $24.6 billion to Canada's gross domestic product in 2017 (Natural Resources Canada 2018).

1.1.2. – Boreal forest ecology

The boreal mixedwood forest region represents an important and extensive component of the Canadian boreal forest, generally occupying the southernmost extent of the boreal. Forests in this region are defined by their compositional and structural diversity which can differ from other boreal forest types. These forests generally support trembling aspen (*Populus tremuloides*), paper birch (*Betula papyrifera*), black spruce (*Picea mariana*), white spruce (*Picea glauca*), and balsam fir (*Abies balsamea*). Boreal mixedwood forests also vary substantially across an east–west gradient. The eastern portions of the boreal mixedwood tend to get more moisture, meaning the dry western portions are more susceptible to fire from lightning strikes (Krawchuk and Cumming 2009), and generally have fires with higher intensity and frequency than the east (Bergeron et al. 2014; Bergeron and Fenton 2012). The stand dynamics of the western mixedwood forests are therefore primarily driven by fire (Krawchuk and Cumming 2009). In fact, many boreal mixedwood species have adapted to frequent disturbances in the form of root suckering in aspen or cone serotiny in some conifers (e.g. *Pinus spp.* and *Picea mariana*; Chen and Popadiouk 2002). Soil types and geology also differ along this gradient (Fulton 1989). Different environmental conditions across the region influence the presence and mixtures of species in boreal mixedwood stands (Lenihan 1993). For example, the eastern boreal tends to have more coniferous species, and paper birch (*Betula papyrifera*) is one of the most common broadleaf species. In the west, however, trembling aspen (*Populus tremuloides*) is more abundant. The mixture of species and disturbances leads to a wide variety of structural types and many different pathways between the successional stages in boreal mixedwood forests (Bergeron et al. 2014).

Increased structural and compositional heterogeneity of mixedwood stands can have different consequences. For example, heterogeneous stands may have slower overall growth rates than pure-species stands as species compete for resources (del Río et al. 2016). However, heterogeneous mixedwood stands may provide increased ecosystem services to the surrounding area (Turner, Donato, and Romme 2013). Structural and compositional diversity can lead to higher potential habitat for species such as birds and understory flora (Cavard et al. 2011). At the landscape-level, they influence a variety of ecosystem services and processes such as nutrient retention and the presence of migration corridors (Turner et al. 2013). Furthermore, increased structural and compositional diversity will lead to an increase in forest resilience, or ability to tolerate change while retaining its function, structure, identity, and feedbacks (Walker et al. 2004). For example, landscape heterogeneity can have a strong influence on wildfires (when fire weather is not extreme) by potentially providing fire breaks or low fuel connectivity. Increased forest heterogeneity also impacts the post-disturbance structure as a result of increased diversity of seed sources or coarse woody debris on which regeneration can take place (Brassard and Chen 2010).

Changes in global climate are likely to have a prominent impact on the condition of the boreal forest, such as growth rates and disturbance regimes (Seidl et al. 2017). Therefore, ecosystem resilience to change will become increasingly important, making the structural and compositional diversity of the boreal mixedwood important to measure and assess. The extensive, dynamic, and complex nature of boreal mixedwood forest pose challenges to measuring and monitoring; however, in order to sustainably manage these forests, detailed, up-to-date information on the status of the forest at different spatial scales is required.

1.2. – Forest inventory

1.2.1. – Scales of forest inventory

An essential component for understanding forested landscapes is undertaking inventories of the resource at various spatial and temporal scales. At the broadest scale are strategic inventories, which inform long-term forest strategies or policies (White et al. 2016). This includes National Forest Inventories (NFIs), which have been undertaken globally in order to measure and monitor forest cover and condition to support a national-level forest policy and information needs (Stinson and White 2018). Countries such as Canada, the United States, and Finland have NFI programs in place to "assess and monitor the extent, state and sustainable development [of the forest] in a timely and accurate manner" (Gillis, Omule, and Brierly 2005). At the finest scale are operational forest inventories, which are primarily focused on logistics of short-term wood supply to satisfy prevailing demand (Bourgeois et al. 2018). Operational forest inventories use a combination of field-based techniques and aerial data to monitor changes or to directly plan management interventions of forest units which may be as many as hundreds of thousands of hectares in size. Tactical inventories aim to reconcile the two scales – that is, to spatially disaggregate strategic inventory targets or guidelines (e.g., annual allowable harvest amounts) in order to allocate management interventions to specific areas (e.g., forest management units or blocks; Gautam, Lebel, and Beaudoin 2017).

Conventional methods for deriving forest inventory attributes require field measurements of various structural and compositional attributes of forest stands (Gillis and Leckie 1996). In operational inventories, the estimates are then scaled up to a larger area using aerial data or existing maps. Manually delineated aerial photography, frequently using digital aerial images, is a common source of inventory information. Stand boundaries are first delineated and digitized, after which attribute estimation can be performed by a trained interpreter (Leckie and Gillis 1995). Typical stand-level attributes can include height, species mixtures, and age. These stand polygons can then be used to provide an input for biometric modeling approaches to extrapolate field-measured data. Strategic inventories may make use of field data to calibrate airborne estimates, although use of field data for this scale may be infrequent (Leckie and Gillis 1995).

Forest managers rely on detailed and up-to-date information on the state of the forest. However, increasing financial pressures and uncertain future environmental conditions have exacerbated challenges with data acquisition for conventional forest inventories (Barrett et al. 2016; Kangas, Gobakken, et al. 2018). Despite the importance of aerial data for augmentation of forest inventory needs, there are increasing difficulties with the use of aerial photography for deriving inventory information. Manual delineation of stands requires a trained interpreter, and labor costs can be high. Data demands are also changing, particularly with forest management increasingly focusing on a broader range of ecosystem goods and services. In its current capacity, aerial photography has challenges in providing information such as below-canopy forest structure, which is a primary component of forest inventory. Photo-interpretation is limited to describing attributes at the stand level, while some operational forest inventories may require information with a finer spatial resolution. Furthermore, the accuracy of photo-interpreted attributes may vary depending on the interpreter and it usually has a low probability of having a completely correct stand description (Leckie and Gillis 1995). Due to these increasing challenges, enhanced information and auxiliary data sources are required to meet the level of detail needed for accurate and robust characterization of forest structure.

1.2.2. – Components of forest inventory

Forest structure, defined as the arrangement of the physical and biological components of a forest, is a primary target of forest inventories. The value of forest structural measurements is multifaceted, as their derivatives have important relationships to a variety of ecological and operational information needs. A major component of structural attributes is the size of tree stems, characterized by the diameter at breast height (DBH) and height of individual trees, which are related to many other structural attributes. Using height and DBH, attributes such as total tree volume and merchantability can be estimated using a variety of models (Huang 1994). Both DBH and volume have strong relationships to estimates of biomass or carbon storage. In fact, DBH is among the most important considerations of estimating biomass, even more so than height (Lambert, Ung, and Raulier 2005). Understanding the relationships between age and DBH or height informs site productivity or growth models, which can provide estimates of future yield and optimal harvest times (Liang, Buongiorno, & Monserud, 2005). Taper, the pattern of decreasing diameter measurements with increase in height up a stem, is another attribute which can inform volume, stem form, and merchantability. Taper is typically either estimated using functions requiring DBH, height, and species, or directly measured by felling the tree and taking manual measurements at fixed intervals along the stem.

Aggregation of diameter measurements across a given area yields the stem size distribution (SSD), which represents the relative frequency of tree sizes in a given area (e.g. plot or stand; Taubert et al. 2013). A SSD can be used directly to describe stand attributes such as its structure, age, and volume (Gobakken and Næsset 2004; Niklas, Midgley, and Rand 2003), or used as inputs to models that can describe product quality (Landsberg et al. 2005) or forecast growth (García 1992). Similarly, the distribution of tree heights forms vertical structure of an area, which provides insights into stand history and successional stage, as disturbance, growth, and competition drive vertical structure as stands develop (Latham, Zuuring, and Coble 1998). These inventory attributes provide valuable insights to inform stand- and landscape-level forest management decisions, so their complete and accurate estimation is critical for maximizing both the economic and ecological capacity of forest resources.

1.3. – Three-dimensional remote sensing data for enhanced forest inventories

1.3.1. – Enhanced forest inventory

Developments in data acquisition and processing methods have led to an increase in the use of three-dimensional remote sensing technologies for developing enhanced forest inventories (EFIs). One such technology is Light Detection and Ranging, or LiDAR. LiDAR sensors emit high-energy pulses (typically in the near-infrared wavelengths) that reflect from surfaces they intercept and return to the sensor (Baltsavias 1999). The LiDAR sensor records the return time of each pulse and uses the device's three-dimensional position and direction of the pulse to calculate the location of and distance to each surface that was intercepted. The resulting product provides a three-dimensional array of points of the scanned area, known as a point cloud (Wulder et al. 2008). Acquiring LiDAR data from a unit mounted on an aircraft is referred to as Airborne Laser Scanning, or ALS, which is the most common for broad-scale forest inventories due to its ability to accurately and continuously characterize large areas (Hudak, Evans, and Smith 2009). As such, ALS point clouds are used to generate descriptive metrics characterizing height, volume, and biomass on broader scales (Næsset 2002), as well as fine-scale descriptions such as crown dimensions, and vertical and horizontal canopy structure (Coops et al. 2007). Digital Aerial Photogrammetry (DAP) is another possible source of airborne data. DAP aligns sets of overlapping images to build dense point clouds of the resulting targets using advanced image matching techniques.

One key method for generating information in an EFI is the use of airborne data in an area-based approach (ABA; Figure 1.1), in which airborne ALS or DAP data is used with co-located measured field data to build predictive models and then the relationships are used to apply predictive models across an area of interest (Næsset 2002). The ABA uses metrics such as height, cover, or variability of ALS returns on a geolocated sample plot to determine the relationship between ALS metrics and measured plot attributes such as the dominant height, mean diameter, stem number, basal area, or volume (White, Wulder, Varhola, et al. 2013). Once these relationships are determined, they are applied across the entire area for which airborne data (ALS or DAP) exists, representing grid-cell level estimates of the attribute of interest (typically at a 20-meter resolution). These attribute layers then become a valuable information source in an EFI. It has been demonstrated that forest inventory attributes can be estimated using ALS data in combination with a sample of ground plots such that they satisfy (or exceed) required levels of accuracy for forest inventory (van Leeuwen and Nieuwenhuis 2010). Goodbody et al. (2019) reviewed 18 studies comparing estimation accuracies for ALS and DAP, showing that ALS produced ABA estimates that were slightly more accurate than DAP (< 4%; Table 1.1).

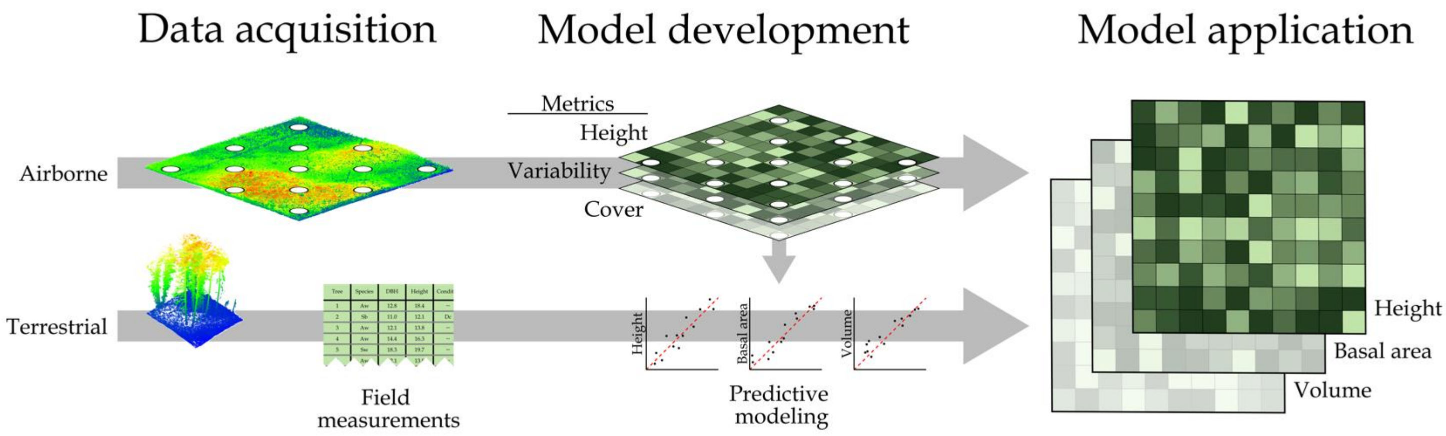

Figure 1.1 - An example workflow for forest inventory attribute estimation using ALS and an area-based approach

Table 1.1 – A comparison between ALS and DAP metrics in predicting forest inventory variables, based on the review of Goodbody et al. (2019). Values are in terms of the RMSE% of predictions.

Variable	ALS (RMSE%)			DAP (RMSE%)			Difference (DAP – ALS)
	Mean	Range	SD	Mean	Range	SD	
Basal Area	20.0%	10 – 35.4%	8.1%	24.3%	12.6 – 37.7%	9.02%	3.85%
Diameter	16.0%	11.4 – 25.3%	6.07%	18.5%	12.0 – 33.7%	9.39%	2.52%
Height	7.4%	3 – 18.6%	3.97%	11.0%	6.8 – 28.2%	5.42%	3.29%
Volume	20.3%	11.0 – 33.2%	7.03%	25.0%	13.0 – 40.3%	8.15%	3.59%

Recent years have seen photogrammetric principles undergoing a digital revolution, as low-cost digital cameras and advanced computing algorithms and methods have become available (Leberl et al. 2010). This has led to an increased use of digital aerial photogrammetry (DAP) as a data source in EFIs (White et al. 2013b). DAP generates point clouds from overlapping sets of aerial images based on image alignment and dense point matching approaches. The result is a point cloud with both structural and spectral detail, with spectral information resulting from the matched pixel values from source images. DAP has been used to derive accurate wall-to-wall predictions of forest structural attributes when the ground surface is known (Bohlin, Wallerman, and Fransson 2012). The passive nature of DAP limits its ability to penetrate the forest canopy and provide points below the outer canopy envelope. However, DAP has been shown to provide data at a cost of one-third to one-half that of ALS, with valuable use in updating forest inventories (regardless of scale) with detailed structural information (Goodbody et al. 2019).

1.3.2. – Field-based data acquisition

Three-dimensional remote sensing technologies also have the capacity to augment field-based data acquisition for EFIs. Auxiliary data collection can be performed with terrestrial laser scanning (TLS) or digital terrestrial photogrammetry (DTP), which have been shown to satisfy the detail required for inventory estimates (Liang et al. 2018; Liang, Jaakkola, et al. 2014). In addition to standard inventory measures such as stem location and DBH, these TLS and DTP can derive non-destructive estimates of more detailed measurements such as the taper or volume (Liang et al. 2016; Piermattei et al. 2019). Typically, TLS point clouds provide slightly more accurate estimates of forest attributes than DTP (Liang, Jaakkola, et al. 2014). However, the use of DTP has increased in recent years with the decrease in the cost of cameras and improvements in computing power and photogrammetric algorithms, leading to the generation of cost-effective point clouds for characterizing trees and plots.

1.4. – Challenges and opportunities

Three-dimensional remote sensing from both airborne and terrestrial platforms have the capacity to augment forest inventory. However, there are challenges to implementation of these products in forest inventories, particularly in mixedwood forests. Area-wide SSD estimates provide detailed and spatially- explicit information, and SSDs have been used to demonstrate the patterns of stand dynamics (e.g. Zenner 2005), or determine the drivers of change (Toledo, Magnusson, and Castilho 2013). While ALS has previously been used to estimate SSD, it has primarily been used in homogeneous forests requiring relatively simple techniques (Maltamo et al. 2005) or heterogeneous forests requiring more complex ones (Penner, Woods, and Pitt 2015). However, less is known about the application of techniques when the complexity of neighboring stands may differ, as is the case in boreal mixedwood forests. Additionally, previous studies estimating SSD often required auxiliary information such as species mixtures (Packalen and Maltamo 2008), thereby reducing the ability of the technique to be applied in areas where the species is not known. Furthermore, the capacity of ALS-derived SSDs for characterizing temporal patterns in forest structure is relatively unknown. In particular, patterns of structural development could be valuable information to managers implementing ecosystem-based management techniques since they may differ with stand conditions (Brassard and Chen 2010; Grumbine 1994).

There is also opportunity to improve field data acquisition for deriving additional ground-based structural estimates or calibration and validation of airborne estimates. While terrestrial three-dimensional remote sensing techniques have been used to derive detailed characterization of individual trees and sample plots, the cost-effectiveness of these methods is an important consideration that needs to be addressed. The high input cost of TLS devices (Eitel, Vierling, and

Magney 2013) and challenges with occlusion (Pueschel et al. 2013) and merging scans (Newnham et al. 2015) may impede their adoption into forest inventories. DTP often uses hundreds to thousands of photographs to characterize trees and plots, thereby increasing the time spent acquiring images and processing into a point cloud. Finally, previous studies have been limited to relatively homogeneous stands with low stem densities and few species. Further study into the patterns of accuracy of DTP in different stand and acquisition conditions is required before this technology can be applied in more complex forests.

1.5. – Research objectives and questions

The primary objective of this dissertation is to determine the utility of three-dimensional remote sensing techniques for deriving structural information across spatial and temporal scales in heterogeneous boreal forests (Figure 1.2). To accomplish this, methods were developed for estimation of structural attributes from both aerial and terrestrial datasets and the derived products are used to enhance understanding of forest structural processes. To meet this objective, this dissertation addressed the following core questions:

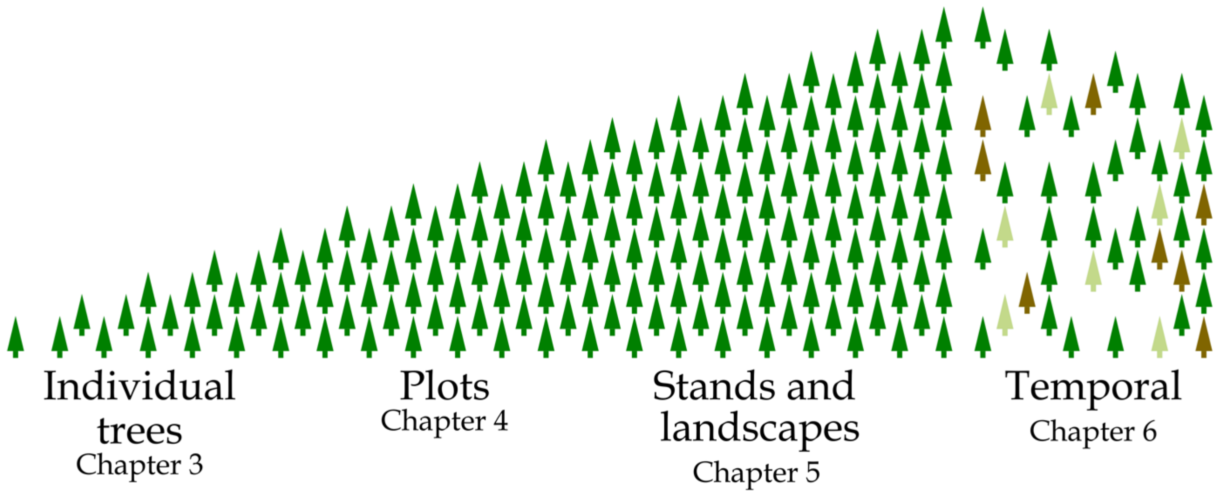

Figure 1.2 - The scales at which structural information is required in forest inventory and the structure of the research undertaken in this dissertation

1. What is the potential of DTP for assessing tree-level taper and volume and how do these compare to conventional field-based estimates?
2. How can DTP point clouds be used to cost-effectively augment conventional ground-based surveys, and how do detection and estimation accuracies depend on field and acquisition conditions?
3. How can ALS be used to model and predict SSD in structurally heterogeneous forests?
4. What information do ALS-derived SSDs provide regarding structural development following stand-replacing disturbance?

1.6. – Dissertation overview

The remainder of this dissertation is composed of six chapters (Figure 1.2), representing the different spatial and temporal scales at which forest structural information is required:

- Chapter 2 describes Canadian boreal mixedwood forests and provides an overview of the remote sensing datasets collected for this dissertation;
- Chapter 3 focuses on deriving estimates of diameter at different heights and total volume for individual trees;
- Chapter 4 expands the methods developed in Chapter 3 to the plot scale, and examines patterns of detection and attribute estimation accuracy across different forest types and acquisition conditions;
- Chapter 5 develops methods for estimating SSDs in a heterogeneous mixedwood forest;
- Chapter 6 applies derived structural information to support the temporal component of forest inventory and enhance understanding of stand structural development over time;
- Chapter 7 is a synthesis of the work developed across the different spatial and temporal scales and provides examples of how terrestrial and airborne data could be combined into a next-generation forest inventory which incorporates the strengths of multiple sources of input data.

Chapter 2 – Study area and data

2.1. – Boreal mixedwood forests

Boreal mixedwood forests represent a large proportion of the Canadian boreal forest (Bergeron et al. 2014), and over 60% of the forested area in Alberta (Strong 1992). In addition to providing resources such as timber or pulp, they also provide valuable ecosystem services across both regional (e.g. nutrient regulation) and global scales (e.g. carbon sequestration). Naturally diverse stands such as those in the boreal mixedwood harbor biodiversity in species such as understory plants and songbirds (Cavard et al. 2011). Increased productivity and growth in mixedwood stands also means that more carbon could potentially be stored in these stands (Zhang, Chen, and Reich 2012) and their structural and compositional diversity makes them resilient to disturbances and changes in climate (Cumming 2001; Terrier et al. 2013). Despite their importance, there has been limited work in deriving estimates of structural attributes in these forest types with three-dimensional remote sensing technologies. This may be due to the structural and compositional heterogeneity of these forests, which pose a range of challenges for attribute estimation with remotely sensed data.

2.1.1. – Slave Lake study area

The study area for this dissertation is an approximately 700,000 ha forest management unit near the towns of Slave Lake and Swan Hills in central-northern Alberta, Canada (Figure 2.1). Human activities in the area are primarily related to timber harvesting and oil and gas extraction. There are at least 8 common tree species present, with white spruce (*Picea glauca*), black spruce (*Picea mariana*), trembling aspen (*Populus tremuloides*) and lodgepole pine (*Pinus* *contorta*) as the most common (Table 2.1). Other species present are balsam fir (*Abies balsamea*), balsam poplar (*Populus balsamifera*), paper birch (*Betula papyrifera*), and tamarack (*Larix laricina*).

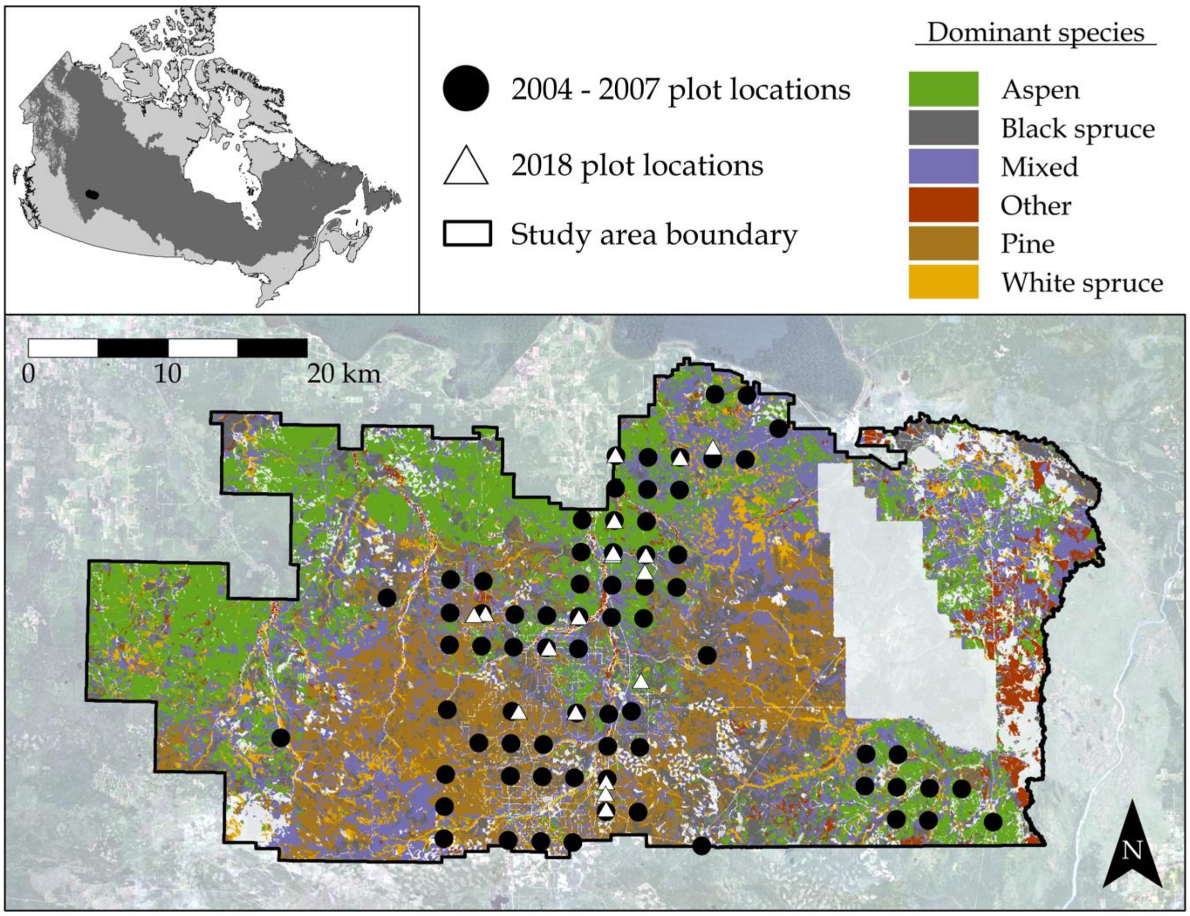

Figure 2.1 - The Slave Lake study area, with its position (black outline) in the Canadian boreal forest (dark grey on inset map). Species information comes from AVI polygons.

Table 2.1 - Species composition of stands in the study area as determined by photo-interpretation (Government of Alberta 2005)*. Mixed stands are those with the dominant species representing less than 80% of the stand. Aspen is* Populus tremuloides, *pine is* Pinus contorta, *black spruce is* Picea mariana*, and white spruce is* Picea glauca*. Volume predictions are based on data from* Tompalski et al. (2018).

Dominant Species	Total number of stands	% of study area (stands)	Total area (ha)	% of study area (area)	% by total volume (predicted)
Mixed	14,309	30.50	179,740	30.57	32.12
Aspen	9,329	19.89	157,322	26.76	36.10
Pine	8,142	17.36	113,370	19.28	16.26
Black spruce	8,867	18.90	77,506	13.18	6.68
White spruce	4,240	9.04	38,304	6.52	7.12
Other	2,026	4.32	21,633	3.68	1.71

Part of the Slave Lake management area is located within the eastern foothills of the Canadian Rocky Mountains, with an elevation ranging from 545 to 1575 m above sea level. The area has an average annual precipitation of 600 mm and has mean temperatures of -21° C in the winter and 20° C in the summer (Natural Regions Committee 2006). Three distinct ecoregions exist in the study area. The Central Mixedwood ecoregion, which composes 33.7% of the study area, is found primarily at lower elevations. This ecoregion is dominated by stands composed of aspen and spruce, with some mixed stands. The Upper Foothills ecoregion, which represents 13.6% of the study area, occurs at higher elevations. This ecoregion is dominated by stands with lodgepole pine and black spruce understory, generally with few or no deciduous species. The Lower Foothills ecoregion occurs in the middle of the study area's elevation range and composes 52.7% of the study area. This ecoregion is among the most diverse in the province and the large proportions of mixed stands represent a gradient between the other ecoregions in the study area. Photos of sample plots are shown in Figure 2.2.

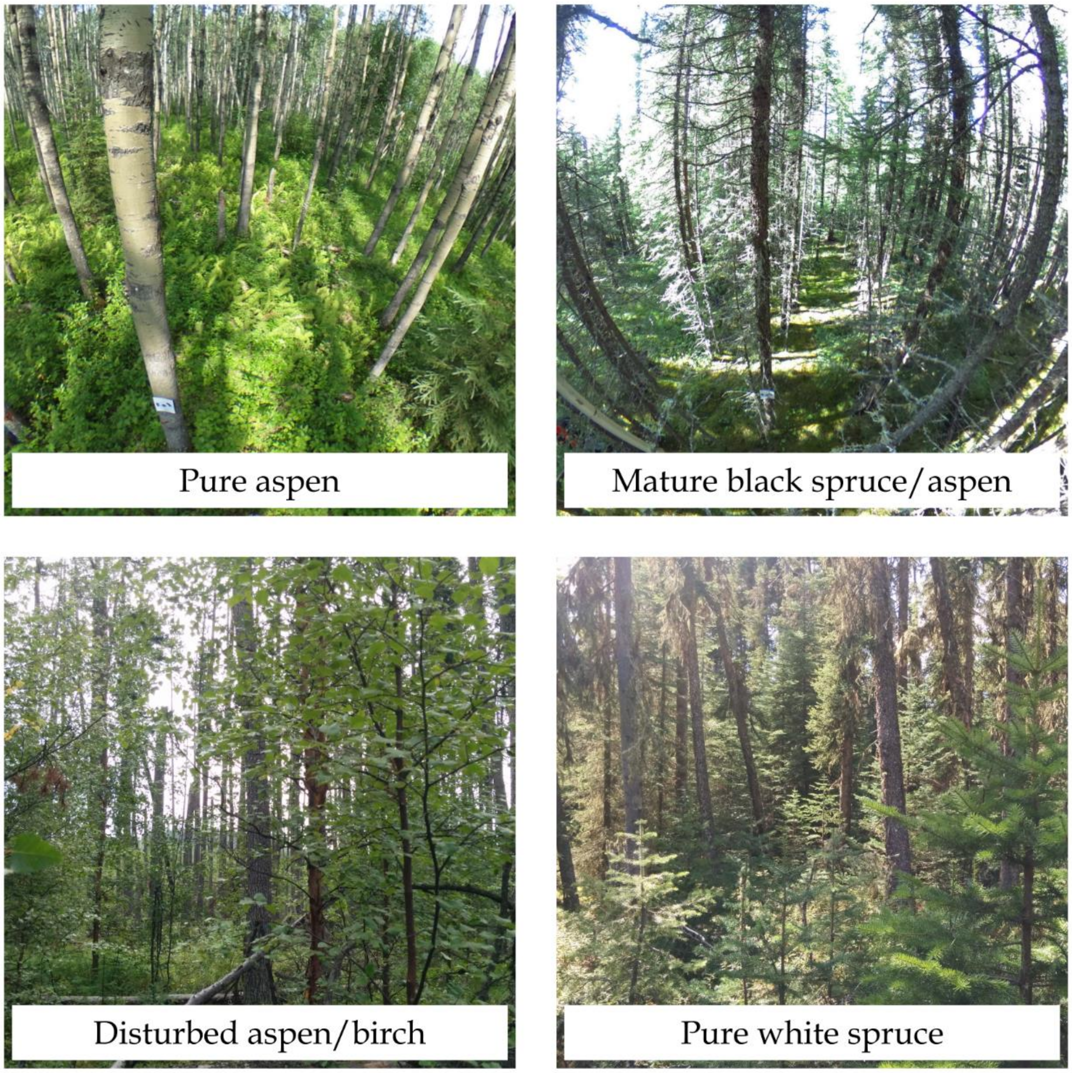

Figure 2.2 – Examples of the forest types in the study area.

Similar to other boreal mixedwood forests, the study area experiences a marked amount of both stand-replacing and non-stand replacing disturbances. Based on a provincial dataset of photo-interpreted stand polygons, 24% of the study area had a stand-replacing disturbance between 1956 and 2008, with 21% attributed to stand-replacing fires and 3% to clearcut harvests (Government of Alberta 2005). Including non-stand-replacing disturbances, 35% of the stands experienced a disturbance during this same time period, with 21% being from fires, 13% from harvesting activities, and 1% from other causes (e.g. windthrow or insect defoliation).

2.2. – Field data

Two field data acquisition campaigns were carried out in the study area. The first was undertaken by Woodlands Forest Management Inc. and occurred between 2004 and 2007 to coincide with ALS data acquisition. The field data acquisition followed provincial guidelines for the provision of permanent sample plot (PSP) data across the region (Alberta Sustainable Resource Management 2005). All plots were circular and had a fixed radius of 11.28 m, with a corresponding area of 400 m^2. Standard provincial inventory procedures were followed, which included the plot center being recorded with a GPS and tagging and measuring each tree having a DBH larger than 7 cm. Five representative trees per plot were cored to determine the age of each tree, and the average of these was used to summarize the plot age. For all trees (≥ 7 cm DBH), measured tree attributes included height, species, DBH, height to live crown, location, and condition or health. While up to 25 attributes were measured for each tree, only 8 attributes were relevant for this research and therefore used in this dissertation (Table 2.2).

Table 2.2 – The attributes measured for each tree on the sample plots.

Attribute	Measurement technique	Units / Classes
Species	Visual assessment	Aspen (*Populus tremuloides*) Balsam fir (*Abies balsamea*) Birch (*Betula papyrifera*) Balsam poplar (*Populus balsamifera*) Black spruce (*Picea mariana*) Dead Jack pine (*Pinus banksiana*) Lodgepole pine (*Pinus contorta*) Tamarack (*Larix laricina*) White spruce (*Picea glauca*)
DBH	DBH tape	Centimeters
Height	Clinometer	Meters
Crown class	Visual assessment	Dominant Codominant Intermediate Suppressed Veteran
Height to live crown	Clinometer	Meters
Distance from plot center	Laser hypsometer	Meters
Azimuth from plot center	Compass	Degrees
Condition code	Visual assessment	Healthy Insects Disease Rabbit browsing Shepherd's crook Other browsing Mechanical Climate Flooding Poor planting Suppression Erosion

In addition to the provincial dataset collected in 2004-2007, more sample plots were measured in 2018 to support this research, specifically the DTP acquisition, in 2018. This involved visiting 18 plots, which were a combination of remeasured PSPs (n = 5) and additional established plots (n = 13) by field crews. Existing PSPs were located by using GPS coordinates and triangulating the known locations of tagged trees closest to plot center. With the exception of determining the age, all trees were remeasured according to the provincial standards and guidelines, including those which were not previously recorded but had grown above the minimum DBH (7 cm) since the last measurement. The remaining 13 new plots were selected to increase the range species and structures found in the study area, determined by an analysis of photo-interpreted stand polygons and ALS structural metrics. These plots were the same size and followed the same measurement protocol as the PSPs. Plot center was recorded with a GPS with an accuracy of 3 m and the position (distance and azimuth from plot center) of each tree in the plot was measured with a TruPulse 360 laser hypsometer. A summary of plot measurements for both acquisition periods is shown in Table 2.3.

Table 2.3 – A summary of the plot measurements collected during the 2006-2008 (n = 71) and 2018 (n = 18) field seasons. QMD = quadratic mean diameter.

	Characteristic	Minimum	1st quartile	Median	Mean	3rd quartile	Maximum	SD
2006-2008	Lorey's height (m)	6.13	12.71	16.27	15.99	19.83	28.39	4.97
	QMD (cm)	3.88	11.00	14.14	13.48	17.08	25.42	4.72
	Total volume (m^3)	16.99	154.1	280.83	248.2	348.8	809.1	181.96
	Density (n/ha)	1075	1875	2644	2650	3138	8325	1194.65
2018	Lorey's height (m)	15.79	18.60	21.87	22.49	24.22	28.98	3.80
	QMD (cm)	15.22	20.20	22.80	22.01	25.79	25.79	4.28
	Total volume (m^3)	231.1	387.8	457.2	484.0	457.2	660.2	135.12
	Density (n/ha)	750	1000	1428	1288	1682	2525	549.59

2.3. – Remotely sensed data

The research reported in this dissertation was based on three sources of remotely sensed data to characterize forest structure at multiple spatial scales. DTP was used to characterize the structure of individual trees and plots. ALS was used to characterize the structure of stands and to predict SSDs for the study area. Photo-interpreted stand inventory polygons were used to provide information on the disturbance history and composition of delineated stands (Government of Alberta 2005). Methods for DTP acquisition are described in Chapters 3 and 4, and ALS processing methods are described in Chapters 5 and 6.

2.3.1. – Airborne laser scanning data

The ALS data for the study area was acquired across multiple flights between 2006 and 2008, with the majority of the coverage occurring in 2008. Coverage of the area by year represented 8.83%, 24.37%, and 66.80% of the study area for 2006, 2007 and 2008 flights, respectively. Acquisition parameters for the different flight years are found in Table 2.4. The combination of these datasets resulted in complete coverage of the study area with an average point density of 1.5 points per m^2. Further detail about the processing methods for the ALS data are found in Chapter 5.

Table 2.4 - ALS acquisition parameters for the three different acquisition years

Characteristic	Collection Year 2006	Collection Year 2007-2008
Acquisition months	July	October 2007 July-September 2008
Sensor	Optech ALTM 3100	
Flying height	1250 m	1400 m
Flight speed	160 kts	
Pulse repetition frequency	50 kHz	70 kHz
Scan frequency	30 Hz	33 Hz
Scan angle	50°	
Beam divergence	0.3 mrad	
Average point density	1.5 points / m^2	

2.3.2. – Alberta vegetation inventory polygons

As a part of the provincial inventory program, aerial photographs are acquired (at 1:60,000 or 1:40:000 scale) and interpreted by experts to delineate stand boundaries and estimate attribute information. The photo-interpretation includes compositional attributes such as species mixtures and structural attributes such as height classes. The most recent assessment was undertaken with imagery from between 2006 and 2008, coinciding with the ALS acquisitions and fieldwork. Research in chapter 6 is based on a dataset of over 50,000 photo-interpreted polygons for the study area, completed to provincial standards (Government of Alberta 2005). According to these standards, there are up to 65 attributes derived for each delineated stand polygon. Of these attributes, the species mixtures and the type of stand-initiating disturbance are used in Chapter 6. This dataset of over 7,000 stand polygons is also used to determine the patterns of structural development in the study area.

Chapter 3 – The utility of terrestrial photogrammetry for assessment of tree stem volume and taper in boreal mixedwood forests

3.1. – Introduction

In an operational forest inventory, many attributes are manually measured where all, or a sample, of the trees above a given diameter threshold in a sample area are measured (Liang et al. 2016). Traditional inventory methods of measuring tree stem taper is difficult and typically requires felling the tree (Huang 1994). For trees with unconventional stem shapes resulting from varying growth patterns or environmental conditions, traditional ground-based inventory methods and equations based on diameter and height as inputs may fail to provide accurate estimates of tree volume or biomass.

In order to meet increasing demands of data accuracy and robustness, recent years have seen the incorporation of remote sensing technologies to enhance forest inventories (Leckie and Gillis 1995; White et al. 2016; Wulder and Franklin 2003). One such technology is terrestrial laser scanning (TLS), which uses LiDAR from a ground-based sensor to more effectively characterize individual stems at a plot or individual tree scale, providing accurate estimates of tree DBH, height, stem volume, and stem biomass (Liang et al. 2016). However, TLS units are expensive and often unwieldy (Eitel et al. 2013). A faster and inexpensive alternative to derive similar data for use in forest inventory is digital terrestrial photogrammetry, or DTP. Recent research has shown the success of DTP in the reconstruction of individual trees for attributes such as DBH (Forsman, Börlin, and Holmgren 2016), location within a plot (Liang, Jaakkola, et al. 2014), and stem shape (Bauwens et al. 2017).

Despite advancements in DTP technology and associated methods, there are current limits to its operational use. The need for manual intervention or trial-and-error in point cloud generation has limited the application of DTP within forest management and ecological modeling. The advances in automation of point cloud generation was an important in making the technology useful as an operational tool (Berveglieri, Oliveira, and Tommaselli 2014; Hapca, Mothe, and Leban 2007; Mikita, Janata, and Surovỳ 2016). However, previous studies using DTP have relied on either the acquisition of hundreds to thousands of images over a given area (Mokroš et al. 2018), or tens to hundreds of images of single trees (Bauwens et al. 2017; Miller, Morgenroth, and Gomez 2015), which raises issues of time or data storage requirements in operational capacities. Point cloud-derived upper stem measurements, such as those from Fang and Strimbu (2017), could provide better estimates of attributes such as taper, volume, or biomass (Bauwens et al. 2017). However, most studies focus on relatively even-sized stands or a single primary species (Fang and Strimbu 2017). As a result, an additional analysis of point cloud accuracy across species and environmental gradients is needed to understand the utility of DTP in irregular stands such as those present in boreal mixedwood forests.

In this Chapter, I evaluate a methodology for DTP estimation of DBH, upper stem diameter (> 1.3 m), and volume of individual trees in a boreal mixedwood forest. Limited sets of photographs taken at known locations were used to automatically generate photogrammetric point clouds for trees across a range of sizes and species. Estimates of diameters at varying heights were derived from the point clouds and used as inputs to estimate taper and volume. The accuracy of DTP-derived estimates was assessed based on field-measured taper from felled trees and compared to traditional methods (based on height-diameter allometries) for estimation of taper and tree volume.

3.2. – Methods

3.2.1. - Field data

The trees measured in this study were located within plots established in July 2018. Across the sample plots, 15 individual trees were randomly selected and photographed as outlined in section 3.2.2. Trees were later felled and diameters were measured in 1-m increments up the stem. Field-measured volume was calculated as the sum of section volumes between diameter measurements up each stem. Smalian's formula was used to calculate the volume of each section as a function of its length and the top and bottom area. The topmost section was treated as a cone and the stump was treated as a cylinder. Attributes for each tree are shown in Table 3.1.

*Table 3.1 - Characteristics of trees (n = 15) used in this study. Species codes are as follows: Aw = trembling aspen (*Populus tremuloides*), Sw = white spruce (*Picea glauca*), Pl = lodgepole pine (*Pinus contorta latifolia*), Sb = black spruce (*Picea mariana*), Fb = balsam fir (*Abies balsamea*).*

Tree ID	Species	Height (m)	DBH (cm)	Volume (m^3)
1	Aw	28.6	28.6	0.9296
2	Aw	22.3	15.7	0.2028
3	Sw	25.9	30	0.9071
4	Sw	26.3	40.4	1.696
5	Pl	17.0	17.1	0.2078
6	Sw	22.2	38.1	1.140
7	Sw	18.7	29.5	0.5952
8	Pl	17.0	16.1	0.1689
9	Pl	26.2	26.4	0.7626
10	Pl	18.2	15	0.1962
11	Sb	18.0	20.7	0.3487
12	Pl	19.8	26.1	0.5437
13	Sb	21.8	31	0.7288
14	Sb	9.70	10.8	0.0525
15	Fb	26.0	25.5	0.6668
Overall Mean	-	21.18	24.73	0.6098
Species Means	Aw	25.45	22.15	0.5662
	Fb	26.00	25.5	0.6668
	Pl	19.64	20.41	0.3758
	Sb	16.50	20.83	0.3767
	Sw	23.27	34.50	1.085

3.2.2. - Image acquisition

Before images were taken, 5 coded targets were positioned on and around each tree (4 on the ground and one on a tree approximately 2 m high. In some cases, targets were placed on the selected tree but were filtered from resulting point clouds. The coded targets were generated in the Agisoft Photoscan software (Agisoft 2018) for automatic detection during image matching, and each target was printed such that it took up approximately the width of a standard letter-sized page (22 x 28 cm). The targets were used to enhance image alignment, both within and among image locations.

Figure 3.1 details the image acquisition method. Images were acquired using two RICOH Theta S (RICOH 2017) cameras mounted on a telescoping pole. Each camera was equipped with two fisheye lenses whose images are stitched together to generate a single spherical image with a 360˚ field of view. The mount ensured the two cameras remained at a fixed distance apart (70.0 cm), which allowed this distance to be inputted as a scale bar during point cloud processing, outlined in Section 3.2.3 Using two adjacent cameras (placed ~ 70 cm from each other) allowed for high (close to 100%) overlap between image pairs. Sets of images taken at two locations meant that approximately half of the circumference of the tree was visible in the set of images. Sets of simultaneous images, acquired with both cameras, were taken at each of three heights, approximately 2, 3, and 5 m above the ground, and at each of two locations around the tree. The result was a set of 12 images (2 cameras, 3 heights above the ground, 2 locations). Preliminary testing showed that this methodology provided sufficient coverage around the tree for circle-fitting techniques to accurately estimate stem diameter. The locations of cameras and coded targets were recorded relative to ground level at the location of the first image set, which was defined as the center of a local coordinate system (with xyz coordinates of 0,0,0). Table 3.2 compares the methodology presented in this study to that of previous work producing photogrammetric point clouds from ground-based images.

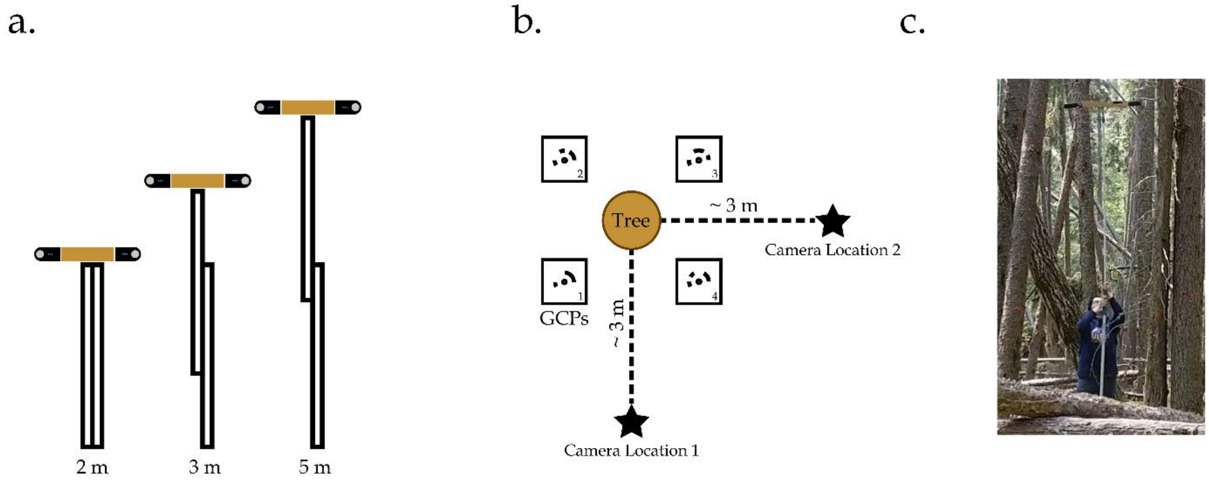

Figure 3.1 - Image acquisition methodology used in this Chapter. a. outlines the camera mount setup, b. details the approximate location of photos and coded targets in relation to the tree, and c. shows the camera in use during field acquisition.

Table 3.2 - A comparison of selected studies detailing previous work with DTP to that of the proposed methodology. Single asterisk indicates values not explicitly reported but calculated based on values presented in study. Double asterisk indicates values not reported but estimated based on figures in study. NR = not explicitly reported but calculated based on available data

Study	Goal	Scale	# of species	# of trees	# of images	Avg. # images/tree	RMSE of DBH – cm (RMSE%)	Mean DBH (SD; cm)
Liang et al. 2014	Tree detection and	Plot	2+ (NR)	25	973	38.9	2.39 (6.60)	31.86 (NR)
Miller et al. 2015	Crown and stem	Tree	4	30	150 - 180	150 - 180	.021 (9.60)	2.198 (.013)
Forsman et al. 2016	DBH and tree location	Plot	3+ (NR)	12 - 38	36	0.95 – 3	7.4 (33.8*)	21.92 * (NR)
Mikita et al. 2016	DBH and volume	Stand	1	118	1774	15	.911 (2.39)	38.16 (7.01)
Bauwens et al. 2017	Trunk shape	Tree	3	37	188	188	< 1 (NR)	122.5 (53.57*)
Fang & Strimbu 2017	DBH, taper	Tree	1	18	32 **	32 **	1.71 (5.60)	30.61 (6.85)
Mokroš et al. 2018	DBH, detection	Plot	1	74	440 - 1271	6 – 17.2	4.41 - 5.98 (16.7 - 20.9)	25.30 (NR)
Proposed	DBH, taper, volume	Tree	6	15	12	12	-	24.73 (8.93)

3.2.3. – Point cloud generation

Point clouds were processed using an automated Agisoft Photoscan workflow (Agisoft 2018). First, camera and target locations were entered and targets were automatically detected. Next, a scale bar between each pair of photographs was set as the distance between the images taken in the field (~ 70 cm). Photos were aligned using a "high" setting and the resulting tie points were filtered to remove those with high reconstruction uncertainty. Finally, dense point clouds were generated using a "high" setting and were then exported to be used in further processing, which was performed on a computer with an Intel Xenon E5-2630 (24 cores @ 2.3 GHz), 64 GB of DDR3 RAM, and an NVIDIA Quadro P4000 GPU.

3.2.4. - Attribute extraction

Generated point clouds were analyzed in Computree (Piboule et al. 2015), a collaborative and open-source software to derive detailed tree-level estimates from ground-based point clouds. Analysis followed a standard Computree workflow, beginning with detection and removal of ground points, followed by noise removal (Belton, Moncrieff, and Chapman 2013). In the next step, horizontal clustering of points and vertical aggregation into logs was performed. For resulting logs, cylinders were fit at various heights up the stem using a least squares fitting technique (e.g. Berveglieri et al. 2017). Finally, smoothed diameters were calculated at breast height and 1-meter intervals by averaging diameters of neighboring cylinders (e.g., 1.2 – 1.4 m for DBH).

3.2.5. - Taper and volume assessment

As heights of the point cloud measurements did not reach the full height of the stem, estimates of taper were determined by matching point cloud-derived diameters to a database of all possible taper curves for the area. In Alberta, variable-exponent taper equations are used (Kozak 1988), and parameters of these curves are adapted to various ecoregions of the province (Huang 1994). Generation of the curve database and associated matching techniques are described below.

3.2.5.1. - Curve database

Taper curves were generated for all possible tree dimensions in the study area based on parameters used throughout the province (Huang 1994). To generate each curve, taper equations required inputs of species, ecoregion, DBH, and total height, while outputting the diameter of the tree at any given height. All possible taper curves were thereby created using all possible combinations of the variables in my study area – all three ecoregions, six species, DBH values from 4 to 40 cm in 0.1 cm increments, and height values from 5 to 35 m, in 0.1 m increments. For each combination, equations output the diameter values at height increments of 10 cm up the stem. The list of curves was then filtered to remove trees whose allometries were unlikely to exist in the study area (e.g., trees that were 30 m tall and had a 4 cm DBH), by removing curves from the database whose height values were not within ± 5 m of the predicted height from the specified allometric equation. This limited the database to allometrically valid taper curves (e.g., those that could exist in the study area) and resulted in a final database of 1,652,778 taper curves.

3.2.5.2. – Curve matching

Point cloud measurements of diameter at different vertical heights were used to match with possible taper curves. Two different curve matching approaches were evaluated in this study, outlined in Figure 3.2. In the first method (1), diameters were not weighted and the curve was chosen based on having the smallest residual between the point cloud-derived diameters and diameters from possible taper curves. The second method (2) applied weighting factors to the residuals of diameters closest to 3.28 m. This height was chosen as it was the average of the three camera heights, and all cameras are expected to have the lowest residual distance to this point on the stem, potentially making it the portion of the stem most accurately reconstructed by the point clouds.

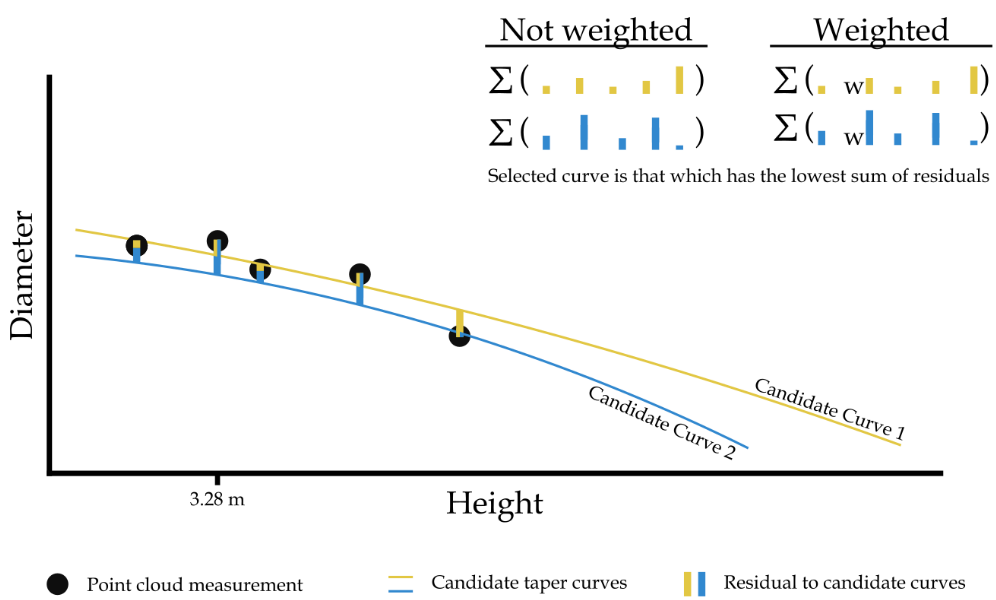

Figure 3.2 - A representation of the two different curve matching techniques (Not Weighted and Weighted) used in this Chapter. w in the equations indicates the weight applied to the residual closest to 3.28 m. In this simplified example, the blue and yellow lines represent two candidate curves coming from the generated taper curve database. There were approximately 90,000 candidate curves for each species in each ecoregion in the curve database.

3.2.5.3. – Verification and accuracy assessment

As a comparison, estimates from the point cloud curve matching were compared to three other methods: (3) the selection of a taper curve based on measured DBH, height (from laser hypsometer), and species before trees were felled; (4) field-measured DBH and species were used as inputs to height-diameter allometric equations (Huang 1994) to predict a tree height, which was then input to select a taper curve; (5) the fifth dataset was similar to the fourth, but used DBH as estimated from the point cloud as an input to a height-diameter equation to predict height. In summary, five methods were compared, two of which used field measurements to match a taper equation (3 and 4), and three which were based on point cloud estimates of diameter (1, 2, and 5). An overview of these methods is shown in Figure 3.3. The accuracies of the DBH, volume, and taper were evaluated by using the Root Mean Squared Error (RMSE), RMSE relative to the mean (RMSE%), bias, and bias relative to the mean (bias%). Results of the methods were tested to see if estimates differed significantly from one another using a t-test. The equations for these statistics are below.

$$RMSE = \sqrt{\frac{1}{N}\sum_{i=1}^{N}(\hat{y}_i - y_i)^2}\ , \tag{1}$$

$$RMSE\% = \frac{RMSE}{\bar{y}} * 100\ , \tag{2}$$

$$bias = \frac{1}{N}\sum_{i=1}^{N}(\hat{y}_i - y_i)\ , \tag{3}$$

$$bias\% = \frac{bias}{\bar{y}} * 1, \quad (4)$$

where N is the number of trees, y_i is the reference measurement for tree i, $\hat{y}_i$ is the predicted measurement for tree i, and $\bar{y}$ is the mean of reference measurements on all trees.

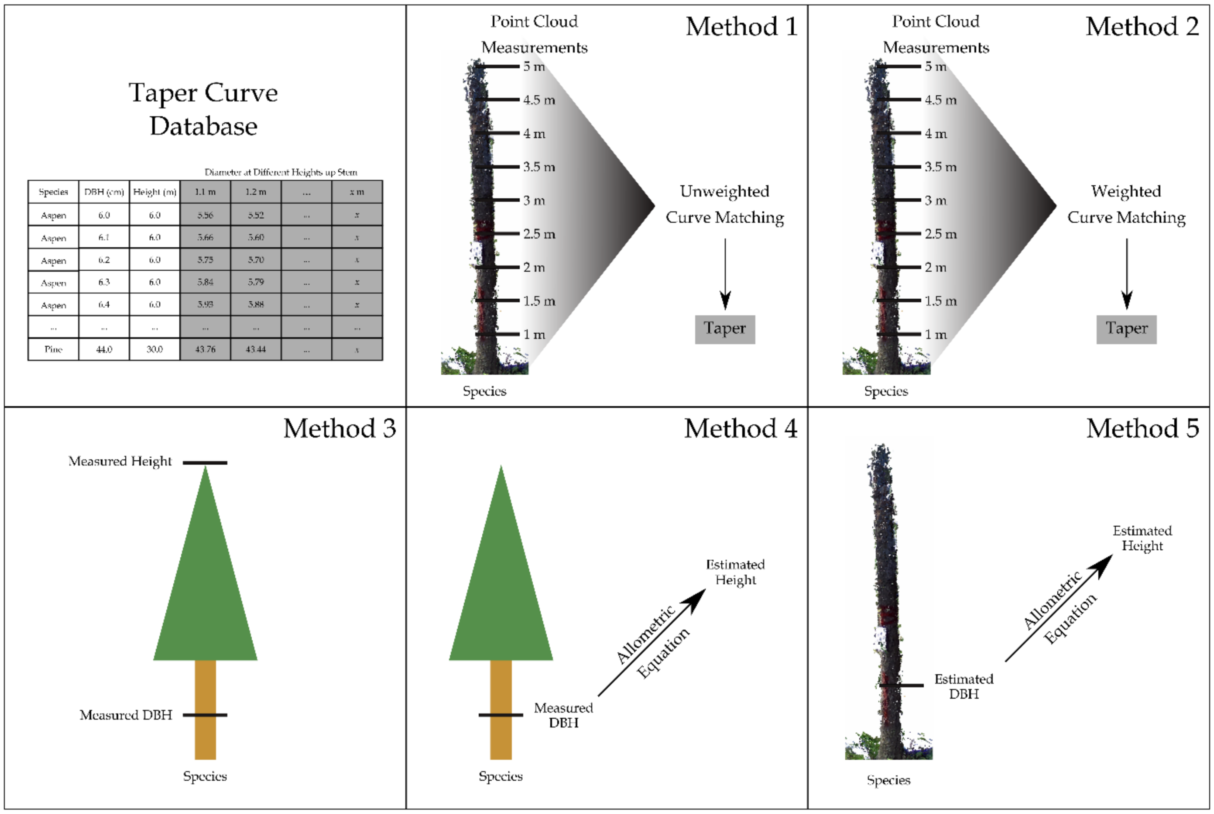

Species	DBH (cm)	Height (m)	1.1 m	1.2 m	...	x m
Aspen	6.0	6.0	5.56	5.52	...	x
Aspen	6.1	6.0	5.66	5.60	...	x
Aspen	6.2	6.0	5.75	5.70	...	x
Aspen	6.3	6.0	5.84	5.79	...	x
Aspen	6.4	6.0	5.93	5.88	...	x
...	...	...	...	...	...	...
Pine	44.0	30.0	43.76	43.44	...	x

Figure 3.3 - An overview of the 5 methods used: curve matching (methods 1 and 2), inputting field measurements (methods 3 and 4), and using the DBH as estimated from the point clouds (method 5).

3.3. – Results

3.3.1. – Point cloud reconstruction and diameter estimates

Once an efficient processing workflow was produced, the total amount of time taken for all steps was, on average, 8 minutes per tree (3 minutes for setup of locations and targets, 1 minute for image acquisition, 3.5 minutes for point cloud generation, 0.25 minutes for deriving measurements from CompuTree, and 0.25 minutes for curve matching). The resulting point clouds contained between 10,000 and 62,000 stem points for the shortest (Tree 14) and tallest (Tree 1) trees, respectively. Points covered an area immediately around the stem and ranged from ground level to a maximum height of 4 to 8 m. Diameter estimates were derived from DTP point clouds, shown in Figures 3.4 and 3.5, and showed good, unbiased correspondence with manual measurements (1.28 cm RMSE, 5.15 RMSE% for DBH). This degree of correspondence was observed at other heights along the stem, although the DTP-derived point clouds rarely allowed extraction of diameter measurements above five meters. For example, for one of the tallest measured trees (Tree 9, a large lodgepole pine, 26.4 cm DBH, 26.2 m height; Table 3.1), the generated point cloud allowed stem reconstruction up to 9 m above the ground. The shortest stem reconstruction was to a height of 3.5 m on a small black spruce (Tree 14, 10.8 cm DBH, 9.7 m height). In general, lower stem heights (e.g., < 3 m) had approximately 50% of the circumference of the tree represented by points. However, point clouds further up the stem generally became more obscured by canopy or branches, resulting in less direct observation from some of the camera perspectives. This resulted in approximately 25% of the stem circumference being represented by points. Despite this, points coming from one camera location were often enough to derive a sufficiently accurate diameter estimate. For example, a separate analysis using only 6 images at a single location for point cloud reconstruction yielded an RMSE of 2.00 cm, or 8.10 RMSE%, for DBH estimation.

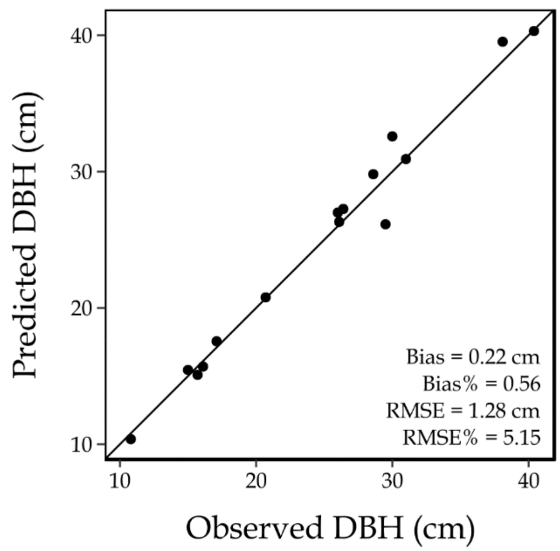

Figure 3.4 - Comparison between observed and predicted DBH measurements (n = 15) from DTP point clouds.

3.3.2. – Upper stem diameters and taper assessment

The relationship between measured and predicted stem diameters for all trees and all evaluation methods is shown in Figure 3.5. For comparison across trees of different heights, the relationship is shown as both the measurement error by absolute height up the stem and the percentage of total tree height for individual trees. For diameters at lower sections of the stem (< 8 m), both curve matching techniques (methods 1 and 2) performed better than other approaches (~ 0.5 cm RMSE). Above 10 m, or approximately 30% of total tree height (across stems), method 3 (using the field-measured DBH and height) yielded the most accurate diameter estimates (< 1 cm RMSE). In some cases, either the curve matching or the allometric equation yielded inaccurate estimates of total tree height, producing larger discrepancies at upper parts of stems (> 75% of total tree height). Despite this, all methods were generally successful at characterizing stem diameter, with the most accurate measurements coming at points in the bottom 13 m or 50% of the stem (< 1.5 cm RMSE).

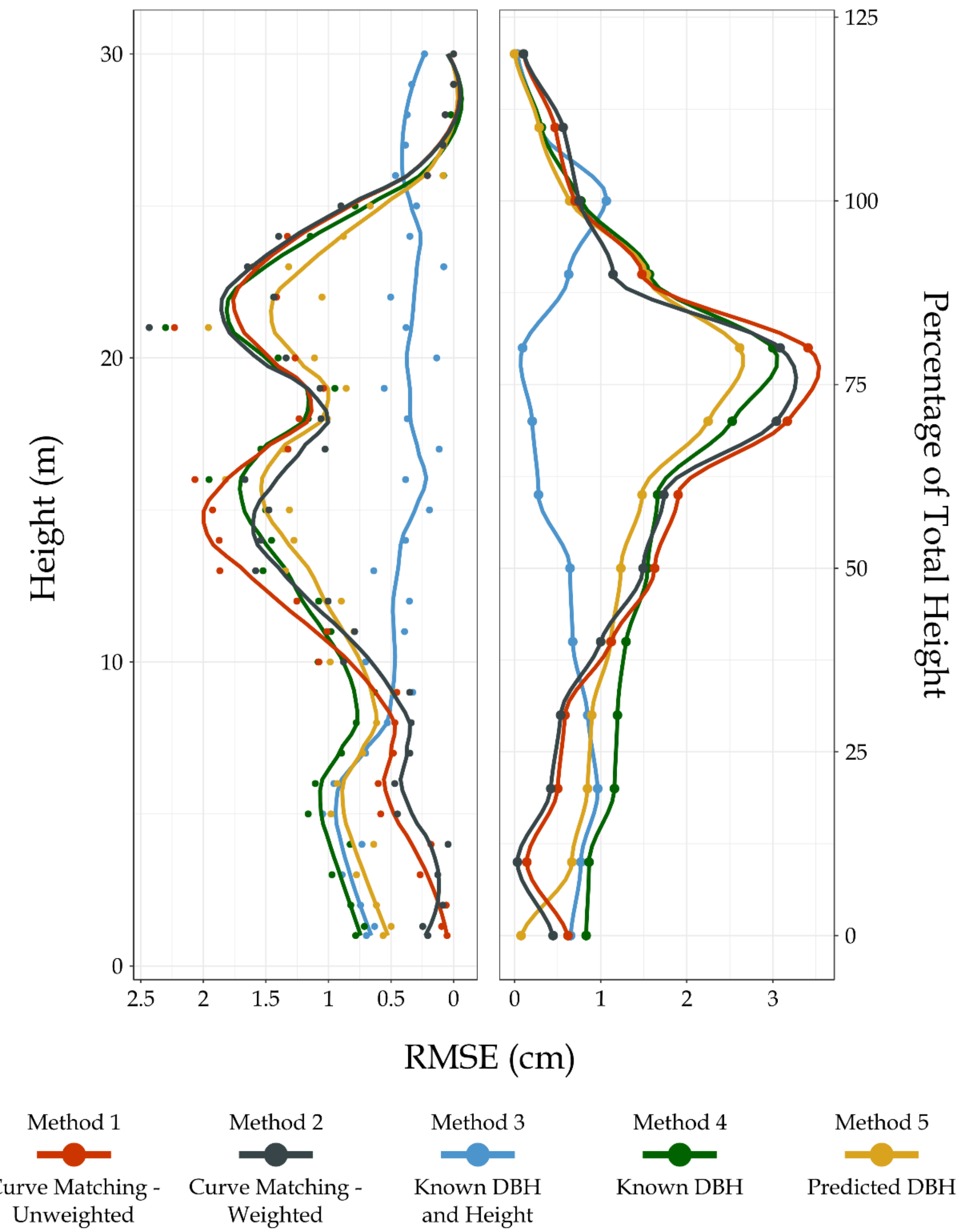

Figure 3.5 - Error (RMSE) of diameter estimates at various heights up the stem, with points indicating RMSE at each measured height and lines showing trend generated by smoothed conditional means. Different colored points and lines refer to the five different estimation approaches. The graph on the left shows the error in terms of the absolute height, while the one on the right shows the error at heights relative to the total tree height in 10% increments. Values over 100% on the y-axis in the right graph indicate an incorrect estimate of total tree height.

3.3.3. – Volume predictions

The relationship between measured and predicted volumes for the different approaches is shown in Figure 3.6. Method 3 (using the field-measured DBH and height) produced the most accurate overall predictions of volume (0.094 m^3 RMSE, 15.5% RMSE). Independent-samples t-tests were conducted to compare mean diameter accuracy. For all techniques, there was no significant difference in the mean accuracy of diameters, suggesting that no one technique performed better or worse than the others. All methods of volume calculation were slightly negatively biased compared to the ground-measured reference. Of the point cloud-based approaches, method 5 (the predicted DBH and allometrically assigned height) yielded the most accurate estimates (0.099 m^3 RMSE, 16.3 RMSE%), but this was only marginally better and not statistically different than the curve matching approaches (methods 1 and 2). Method 1 (unweighted curve matching) produced more accurate volume estimates (.110 m^3 RMSE, 18.1 RMSE%) than method 2 (weighted curve matching; .120 m^3 RMSE, 19.6 RMSE%). However, for all 15 trees, no method performed significantly better or worse than the others.

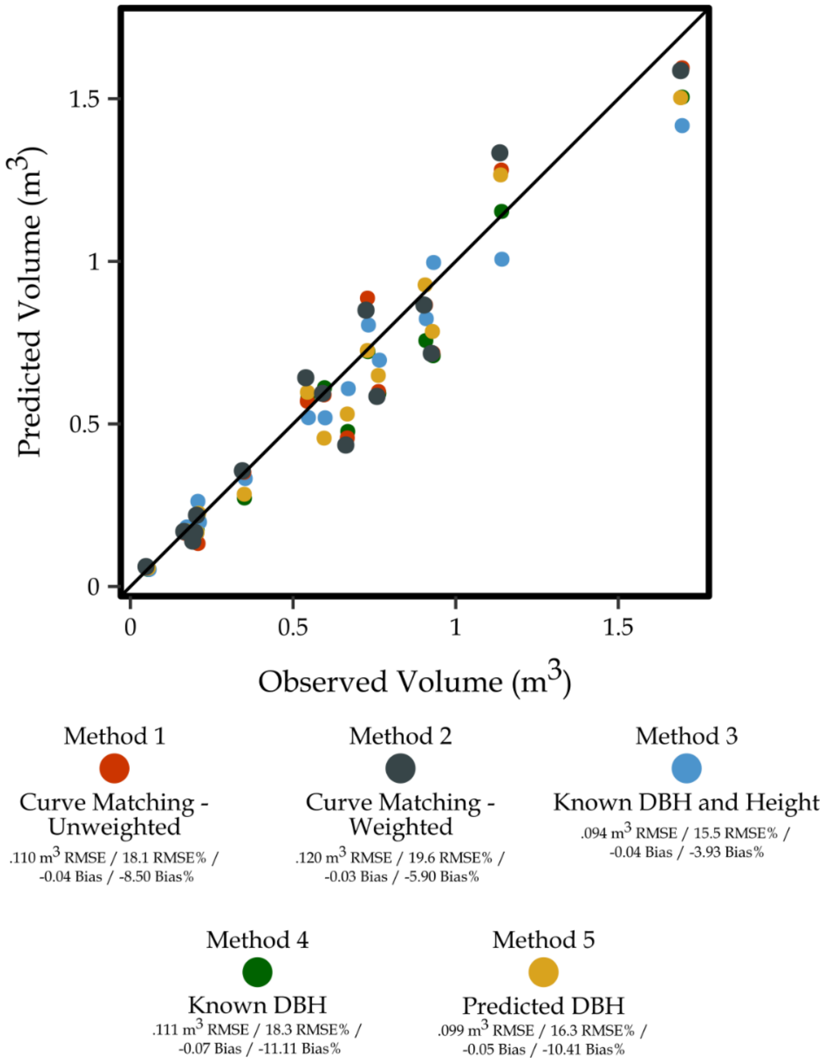

Figure 3.6 - The accuracies of the 5 different methods for volume estimation. Each point represents a tree and is colored according to the method presented.

3.4. - Discussion

3.4.1. – Diameter estimates

Stem diameters at multiple heights were extracted from DTP point clouds. Point clouds produced accurate estimates of DBH (Figure 3.4), showing a RMSE of 1.28 cm and a RMSE% of 5.15. Point cloud-based curve matching approaches (methods 1 and 2) produced the most accurate measurements for the lowest 8 m, or approximately 30% of the stems, while using a known DBH and height (method 3) was the most accurate method for the higher parts of the stem. For trees with irregular allometries, it was possible that the taper models used in this study inaccurately characterized the diameter at different parts of the stem. However, the models were determined to be generally accurate in their characterization of stem taper. In some cases, methods 1, 2, 4, and 5 produced inaccurate estimates of total tree height resulting in inaccurate predictions for volumes and upper stem diameters. This resulted in higher RMSE values for the upper parts of trees (> 50% of total height) in scenarios where the total height was unknown. However, most tree height estimates were within 3 m of the true height (after falling), and all methods produced RMSEs of less than approximately 1.5 cm for diameters in the lowest 50% of the stem. Most tree heights measured in the field by a laser hypsometer were within 1 m of the true height (after falling), but deviated by about 3 m for the tallest two trees. These discrepancies between field-measured (hypsometer) and observed tree height is consistent with findings from Luoma et al. (2017), who determined that the standard deviation of field-measured height was 0.5 m (2.9%), up to a maximum of 4.2 m.

Compared to certain other studies estimating individual tree DBH from DTP point clouds (e.g., Bauwens et al. 2017; Fang and Strimbu 2017; Miller et al. 2015), I used fewer photographs (12) and evaluated more species (6) while achieving similar levels of accuracy (Table 3.2). For example, Fang and Strimbu (2017) reported DBH estimates with an RMSE% of 5 in a monospecific plantation. Similar accuracy with six species indicates that there may not be a strong correlation between tree species and DBH accuracy at least for the species included in this Chapter.

The achieved accuracy with a relatively low number of images may have resulted from the inclusion of six scale bars (i.e. one between each set of adjacent images at three different heights), which was set to the distance between the cameras as they were mounted on the pole. This allowed the point clouds to be scaled more accurately than using the target locations alone. Forsman et al. (2016) also used a camera rig (multiple cameras mounted to a portable device) to scale the images with known distances while using an average of less than 3 images per tree to detect and measure stems on sample plots. Consequently, a rig-based system with known distances between cameras may be helpful in producing accurate estimates of tree dimensions in cases where relatively few images per tree are captured.

3.4.2. – Volume assessment

The photogrammetric point clouds were generally accurate in estimating tree volume. For smaller trees (i.e. volumes less than 0.5 m^3), all methods of volume estimation produced similar accuracies. For the largest two trees, method 3 (using the field-measured DBH and height) produced inaccurate estimates, possibly due to inaccurate height measurements as taken from the ground, which has been shown to be influenced by stand conditions, crown class, and tree species (Wang et al. 2019). Although more accurate diameter measurements at upper parts of the stem came from method 3 (field-measured DBH and height), the majority of a tree's volume is in the lowest portions of the stem, indicating that accurate diameter measurements at the bottom – possibly coming from DTP point clouds – could also result in more accurate volume estimates. For example, the lower 50% of tree stems in the study contained about 80% of the total volume for the trees.

This study addressed the ability of 360˚ cameras to derive detailed tree-level measurements. The cameras' large field of view means that resulting point clouds have a larger coverage area than traditional frame cameras, which are typically employed during field operations. The results of this study indicate the potential of 360˚ cameras to characterize larger areas such as sample plots or stands. Larger coverage from individual images would result in fewer images being required for point cloud generation. As a comparison, the frame cameras used in Liang et al. (2014) and Mokroš et al. (2018) were able to successfully characterize DBH for trees on sample plots, but used up to 973 and 1271 images for 900 and 1225 m^2 plots, respectively. Spherical images could also provide the basis for a combination of terrestrial and aerial photogrammetric point clouds, such as in Mikita et al. (2016), who used terrestrial and aerial images to characterize tree DBHs and volumes in a 0.8 ha stand. However, for individual trees, only a subset of the entire 360˚ field of view was used for tree reconstruction, indicating that similar accuracies may be achieved using a rig-based system of wide-angle or fisheye lens cameras.

Of the related studies listed in Table 3.2, only one estimated volume from DTP point clouds (Mikita et al. 2016). Volume estimates from point clouds in their study (RMSE of 0.082 m^3) were slightly more accurate than those reported here (RMSE of 0.099 m^3). In this study I evaluated the ability to derive individual tree characteristics based on point clouds created from fewer images and tested on more species than presented in Mikita et al. (2016). Additionally, Mikita et al. (2016) combined DTP and DAP point clouds, while my study was limited to ground-based images. More study is needed to determine the relationships, if any, between point cloud accuracy and characteristics such as tree size, branchiness, species, or stand density of the surrounding area. Based on an international benchmarking study of TLS by Liang et al. (2018), stem detection rates decreased with decreasing mean DBHs and stem density, while DBH estimates were stable across stand conditions. Smaller trees will have less surface area for point cloud reconstruction, meaning that there may be a resulting increase in error of DBH estimation with decreasing tree size (Ryding et al. 2015).

3.4.3. – Applications

TLS provides more comprehensive point clouds than DTP that can be used for more detailed study such as wood quality, and has the ability to return points from occluded areas such as in stands with a high stem density or on stems with many branches. However, the results seen in this study indicate the potential for DTP to provide similar levels of accuracy to TLS for DBH and volume estimates. Studies using a single TLS scan reported 1–3 cm RMSE for DBH (Liang and Hyyppä 2013; Maas et al. 2008) and ~10 RMSE% for volume (Liang, Kankare, et al. 2014), similar to the results reported here. Liang et al. (2018), also reported accuracies of 10 and 20 RMSE% for “easy” (low stem density and high mean DBH) and “difficult” (high stem density and low mean DBH) plots, respectively.

While TLS provides attributes such as branching structure and direct measurements of upper stem diameters, the cost of handheld cameras to use for DTP is in the hundreds of dollars, far less than TLS units, which can be 2 orders of magnitude higher. In this Chapter, DTP achieved similar levels of accuracy to TLS for diameter and volume estimates. However, the level of detail from a TLS point cloud can derive more detailed estimates of attributes such as branching patterns or biomass (Liang et al. 2016). Although the focus of this Chapter was on the structural qualities of the point clouds, their spectral attributes could also be used, similar to aerial images, to assess species compositions (e.g. Packalen and Maltamo 2006) and tree condition or quality (e.g. Goodbody et al. 2018). Overall, the low cost and portability of the cameras, in addition to the objectivity and storability of the point clouds, show their value as a tool in forest inventory and modeling.

Chapter 4 – Digital terrestrial photogrammetry to enhance field-based forest inventory across stand conditions

4.1. – Introduction

Individual tree measurements are important for characterizing the structure of trees for applications such as merchantability or carbon storage. Similarly, plot-level structural measurements are used to characterize size variability and past disturbance, or to determine product quality (Landsberg et al. 2005), or predict future growth (García 1992). Airborne remote sensing products such as ALS require manual ground measurements for calibration and validation. As a result, there has been increasing interest in the acquisition of advanced remote sensing information products from within a stand that could be used to augment conventional forest inventory measurements by providing a detailed characterization of the plot at a given point in time for current modeling or retrospective change assessments. Chapter 3 used a smaller image set (n = 12 images per tree) to derive accurate diameter and volume estimates from individual trees that matched or exceeded the accuracies from conventional field-based inventories. Despite these advances in estimating tree-level forest attributes from DTP, less is known about how DTP accuracy is impacted when scaling up from an individual tree point cloud to an individual plot or stand.

At the stand scale, previous DTP applications have shown that tree location, DBH, and stem taper can be derived (Table 4.1); however these studies have utilised more than 1000 images using conventional frame cameras (e.g. Mikita, Janata, and Surovỳ 2016; Mokroš et al. 2018) taken from a variety of positions, increasing the time spent both acquiring and processing images and thereby reducing the cost-effectiveness of DTP for attribute estimation. Furthermore, these studies typically focus on relatively simple forest stands with homogeneous canopy structure and little understory, limiting the understanding of the sensitivity of DTP to different acquisition conditions and stand complexities. This currently limits the widespread adoption of the technology to stands with simple structures, such as those without low-lying branches or those with a sparse understory and using a large image set, potentially discouraging the use of this technology in other forest types. To move towards an operational technology for forest estimation, considerable work needs to be done to scale up from individual trees to plot-level inventory estimates across a range of stand conditions and forest structures. Moving from individual trees to plots requires additional considerations, as stands can be complex, image acquisition conditions such as position and lighting conditions harder to control, and at broader scales more variability exists in stand attributes, including tree size, stem form, branching patterns, and density, and understory and ground cover presence. Methodological developments in the nature of image acquisition focusing on camera rigs and image acquisition patterns can be one way to overcome some of the issues by reducing potential occlusion and minimizing inconsistencies of point cloud generation (Forsman et al. 2016; Mokroš et al. 2018).

*Table 4.1 - A comparison of previous studies using DTP for plot-level tree detection and DBH estimation. * = values calculated based on data in study but not explicitly reported. RMSE% is the RMSE relative to the mean observed diameter value. % Tree Detection is the number of correctly detected stems as a percent of the total number of stems. All studies use conventional frame cameras.*

Study	# of images	Area (m^2)	Images / m^2	# Trees / ha	# of species	Mean DBH (cm)	RMSE of DBH estimate (cm / %)	% Tree Detection
Liang et al. 2014	973	900	1.08	278	2+	31.86	2.39 / 6.6	88
Liang et al. 2015	97 - 1070	900	0.11 - 1.89	278	2	31.86	2.98 - 6.79 / 8.03 – 18.87	60 - 84
Forsman et al 2016	36	1256.6	0.03	95 – 302	3+	21.92*	7.4 / 33.8*	68 - 83
Mokroš et al. 2018	440 - 1271	1225	0.35 - 1.04	547	1	25.3	4.41 - 5.98 / 16.7 – 20.9	49 - 81
Piermattei et al. 2019	338 - 775	706 - 1256	0.42 - 0.70	390 - 875	4	26.83	1.21 - 5.07 / 3.94 – 17.0	65 - 98

In this Chapter, I continued to evaluate the use of DTP for deriving tree form estimates across a range of species, sizes, stem forms, and understory conditions with the aim of furthering the use of this technology as an additional tool for accurate forest inventory collection and update. To do this, I focused on three main components. First, I proposed a methodology aimed at collecting measurements and enhancing traditional field-based forest inventory – that is, to provide information not typically measured from conventional field surveys (e.g., taper). Next, I applied the new methodology across a broader range of forest conditions than most previous studies in order to determine the sensitivity of the detection and DBH estimation accuracy to a set of different acquisition parameters and stand conditions. Finally, I aimed to improve the cost-effectiveness of DTP for plot-level estimates by reducing the number of images taken and therefore lowering processing requirements.

4.2. Methods

4.2.1. – Field inventory

This Chapter used data acquired during the same field season as in Chapter 3, measured in July 2018 (Section 2.2). A summary of the field data for the plots later deemed suitable (see Section 4.2.4) is shown in Table 4.2. In total, the dataset consisted of 653 trees on 12 sample plots, representing one of the largest studies of DTP for tree-level estimates to date and therefore a unique opportunity to explore the patterns of tree detection and estimation accuracy as they relate to either plot or acquisition conditions.

*Table 4.2 - Summary of field data on 12 sample plots used in this Chapter. * indicates the overall DBH range and not the mean. Dominance is based the number of live stems. Aw = Trembling aspen (Populus tremuloides), Pl = Lodgepole pine (Pinus contorta), Sb = Black spruce (Picea mariana), Sw = White spruce (Picea glauca).*

Plot	Density (n/ha)	Mean DBH (SD; cm)	DBH range (cm)	Dominant Species	% Species Dominance	Number of species
1	1750	18.6 (6.8)	7.5 – 30.1	Aw	70.0	2
2	850	27.5 (10.0)	9.5 – 47.6	Sw	82.4	3
3	1475	20.6 (8.0)	7.4 – 39.3	Pl	76.3	3
4	1375	25.2 (6.5)	7.6 – 41.0	Pl	96.4	2
5	1075	24.0 (7.9)	7.5 – 38.8	Pl	81.4	4
6	1100	22.7 (6.7)	8.5 – 34.0	Aw	59.1	2
7	1200	24.7 (8.8)	7.2 – 43.8	Pl	45.8	2
8	2150	18.3 (5.2)	7.9 – 29.8	Sb	45.4	2
9	1625	20.1 (8.9)	8.8 – 43.4	Sw	56.9	4
10	1900	18.6 (6.1)	7.2 – 31.9	Aw	72.4	3
11	750	24.9 (8.5)	10.5 – 38.0	Aw	93.3	2
12	1075	19.4 (9.7)	8.7 – 50.2	Bw	51.2	3
Mean	1360.4	22.0 (7.7)	7.2 – 50.2*	-	69.2	3

4.2.2. – Workflow

The workflow for deriving plot estimates from generated point clouds is summarized in Figure 4.1. First, images were systematically acquired on all plots. Next, images were processed into dense point clouds. Cylinders representing stem diameter at various heights were then fitted to detected and filtered stems. Finally, detected stems seen from multiple camera locations were merged into a final stem map with tree location and DBH, with additional diameter attributes above breast height (1.3 m). These stem maps were evaluated for their accuracy based on measured plot data.

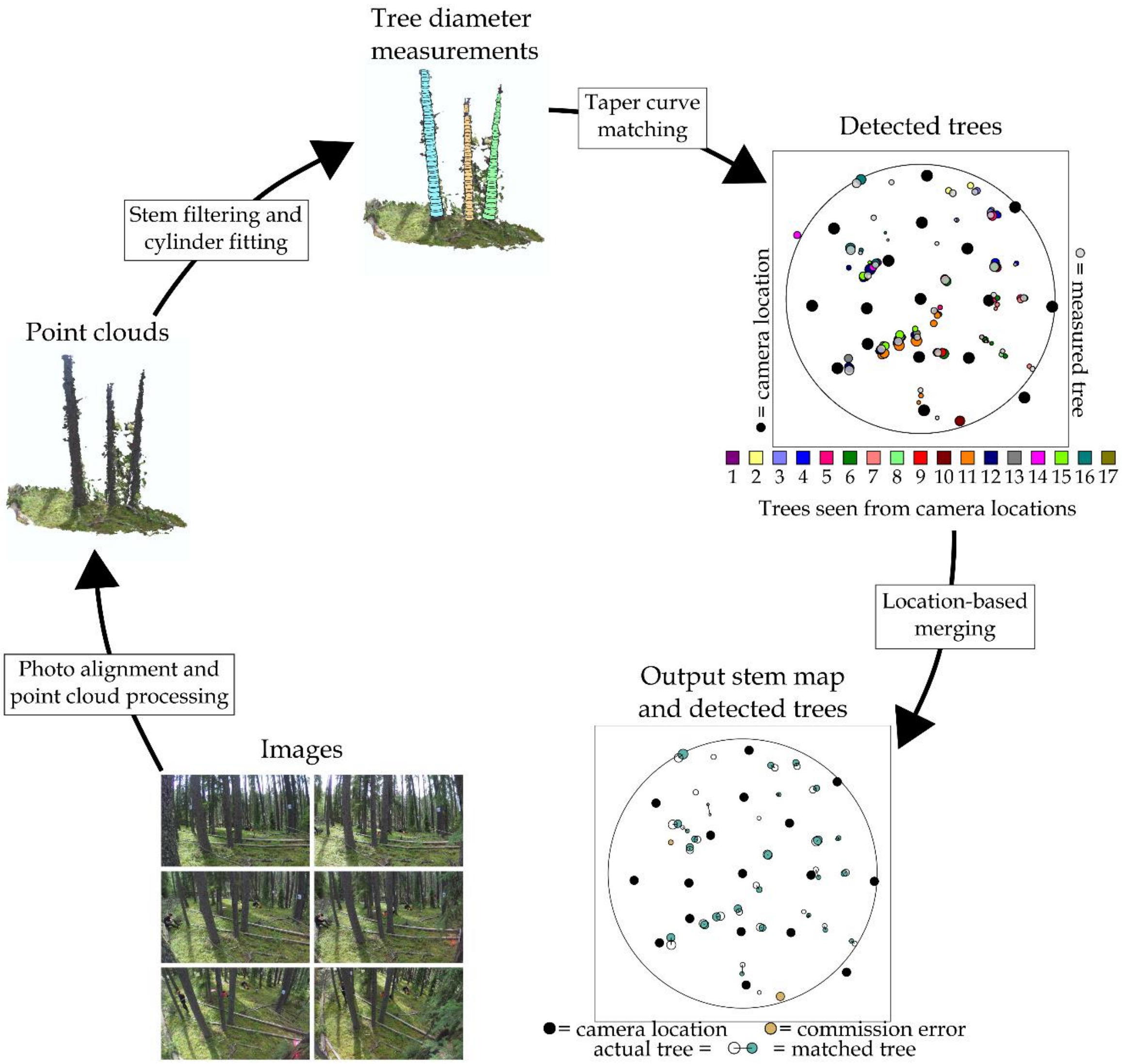

Figure 4.1 - A workflow of the analysis undertaken in this Chapter

4.2.3. – Image acquisition

Sets of spherical images were acquired using a methodology similar to that of Chapter 3. Six images were taken at the same height and configuration as Chapter 3 at each of 17 locations systematically spread around the plot, resulting in a total of 102 images acquired per plot (17 locations x 3 heights x 2 images). Depending on conditions (understory or trees obscuring access to the desired location), image sets were taken at plot center and then at approximately 6 and 12 meters from plot center at 8 cardinal directions (Figure 4.2). These locations of image sets were chosen because they balanced the need to reduce the number of images required to generate the plot-level point clouds, while being able to see most areas of the plot from multiple locations – possibly reducing occlusion of stems from fewer image locations. A combination of the close distance between cameras and spherical nature of the images led to a large image overlap at each location, allowing point clouds to be generated from relatively few images (similar to Chapter 3) which were representative of stems and from which dimensional measurements could be taken.

To spatially register each point cloud within the plot, approximately 20-25 coded targets generated by Agisoft Metashape Professional (Agisoft 2018) were placed in each plot. Each target was printed on a single letter-sized piece of paper (215.9 x 279.4 mm) and the radius of the circular codes was approximately 18 cm. Each code was assigned a number and, when automatically detected in the processing software, could be used to spatially register the resulting point cloud. A total of four targets were put on the ground and the remaining targets were placed at 2 m up tree stems so that at least one target could be seen from each camera location and they did not directly obscure a DBH measurement. The location of each target was recorded by measuring its height above the ground (0 or 2 m) and its distance and azimuth from plot center with the TruPulse 360 laser hypsometer, thereby giving each target a 3D position within the plot.

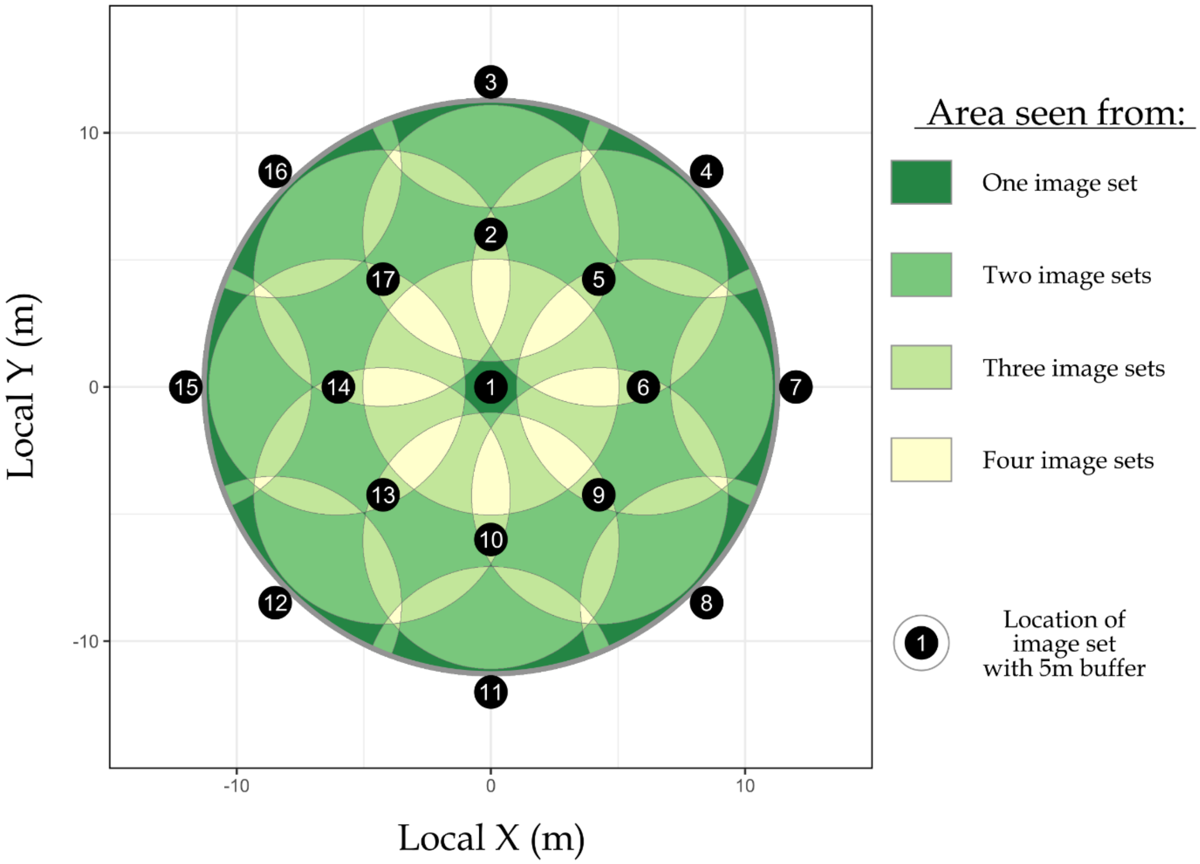

Figure 4.2 - The location of image sets acquired on each sample plot. Image locations are shown with a 5 m radius at which resulting point clouds were generated. Areas of the plot are colored according to the number of image theoretically being able to see that area.

4.2.4. – Point cloud processing and reduction of dataset

Images were processed into point clouds using Agisoft Metashape Professional (Agisoft 2018) using a semiautomated processing approach and a computer with an Intel Xenon E5-2630 (24 cores @ 2.3 GHz), 64 GB of DDR3 RAM, and an NVIDIA Quadro P4000 GPU. First, images were aligned and tie points found using the “highest” accuracy setting. Then, a dense point cloud was generated with depth filtering set to “aggressive” and quality settings set to “high.” Point clouds were translated based on the known camera locations within a local coordinate system using the plot center as origin (X = 0, Y = 0, Z = 0). The targets described in section 4.2.3. were automatically detected and the point cloud was scaled by the known distance between cameras (0.7 m). If an image location did not have an automatically detected target, targets were located on the images manually. This was the only manual intervention in point cloud generation and occurred on approximately <30% of image sets. The representativeness of reconstructed trees would likely decrease with an increasing distance to the spherical camera (Rodríguez-García et al. 2014). Therefore, only resulting points within 5m of the camera location were used. The result was coverage of the plot from one, two, three, and four image locations representing 9.6%, 54.7%, 27.6%, and 8.1% of the total plot ground area, respectively.

4.2.5. – Taper curve matching

A taper curve matching approach was used, based on the weighted approach described in Chapter 3 (Method 2), and using the functions outlined in Huang (1994). Each detected tree with more than 7 derived cylinders was filtered for outliers (cylinders whose diameter measurement was ± 2 standard deviations from the mean of the detected tree) and then matched to a taper function and given an estimate of DBH. The result was, for each camera location, detected stem locations with a fitted taper function.

4.2.6. – Location-based merging

While detecting trees from multiple locations helped to overcome issues with occlusion, this approach also meant that the trees seen from multiple locations needed to be filtered and merged so detected trees would not be counted twice. To do this, similar trees were merged based on the approach of Liang and Hyyppä (2013). Detected trees within a set distance (1 m) of each other were clustered based on those having a similar DBH estimate (within 60% of original DBH). Next, each cluster of similar trees was merged into one output tree and a DBH estimate was calculated as the weighted mean of trees in the cluster, with detected trees closer to an image location having a higher weight. Theoretically, stems closer to a camera location would have more pixels (and therefore points in the resulting point cloud) representing stem points, resulting in a larger number of points with which to fit a cylinder, potentially providing a more accurate estimate of diameter (Liang and Hyyppä 2013). The merging process resulted in information on location, DBH, and taper for all of the detected trees on each plot.

4.2.7. – Accuracy assessment and sensitivity analysis

4.2.7.1. - Tree detection rate and DBH accuracy:

In order to assess the accuracy of the tree detections, I used an approach similar to Liang et al. (2018) who buffered around each measured tree to determine the closest detected tree which had an accurate corresponding diameter to the measured tree (in this Chapter, accuracy was defined as being within 80% of the measured DBH). This tree was selected as the match and removed from the pool of detected trees with which to match to measured trees. Detection accuracy was assessed as the number of matched trees as a percentage of the total number of measured trees. The commission error was also calculated as the number of trees detected with DTP but not corresponding to a field-measured tree, as a percentage of the total number of field-measured trees. The accuracy of estimated DBH was compared to the field-measured DBH using the RMSE and RMSE%. Bias in the DBH estimate was calculated by subtracting DTP estimates of DBH from the measured values, where negative values represent overestimation of DBH and negative values represent underestimation.

4.2.7.2. – Sensitivity analysis:

The sensitivity of the three accuracy measures (% detection, % commission, DBH RMSE) to field and acquisition conditions (Table 4.3) was determined at both the individual tree and plot levels. At both scales, attributes were chosen as representative of the shape, visibility, and variability of the trees and plots. Here, the species of tree and the crown class were used to determine the sensitivity of the accuracy to the shape or form of the target. Species of trees with simpler structures, such as aspen and lodgepole pine are self-pruning, meaning that they generally have fewer low branches and consistently more visible stems (Burns and Honkala 1990). Conversely, species such as black spruce and white spruce have more areas of the stem inconsistently captured or obscured, potentially limiting the ability of the resulting point clouds to be accurately reconstructed. An analysis of field measurements showed that mean live crown ratios (the proportion of the stem having a live crown) for balsam fir, black spruce, and white spruce were approximately 0.25 – 0.30, while those of aspen and lodgepole pine were approximately 0.5 – 0.6. The crown class also represents form, as trees that are intermediate or suppressed typically have different stem forms and branching patterns than those that are dominant or codominant. Any tree that was dead and standing had a species code listed as dead on field forms, resulting in a wide range of possible forms that infrequently resembled live trees of the same species. For this reason, dead trees were used as a separate species class in the sensitivity analysis.

Table 4.3 - A description of variables used in the sensitivity analysis to determine the effect of plot and acquisition conditions on detection and estimation accuracy at the tree and plot scales. For species names, see Section 2.1.1.

Tree-level variable	Plot-level variable	Classes
DBH (cm)	Mean DBH (cm)	-
Mean nearest neighbor distance (n = 5; m)	Standard deviation of DBH (cm)	-
Distance to camera (m)	Stem density (n/ha)	-
Species	Dominant species	Aspen, White birch, Balsam fir, Balsam poplar, Lodgepole pine, Black spruce, White spruce, Dead
Height to live crown (m)	Mean height to live crown (m)	-
Crown class	Most common crown class	Dominant / co-dominant, intermediate / suppressed
-	Minimum DBH	7, 10, and 15 cm

The visibility was represented by the height to live crown, DBH, and distance to camera at the tree scale, and the mean height to live crown and DBH at the plot scale. Trees that are smaller or farther away from the camera have fewer reconstructed 3D points on the stem, potentially reducing their visibility. Lower live crowns would also potentially impact the visibility as they could obscure or occlude the stem. The variability of acquired images was assessed for individual trees by using the mean nearest neighbor (NN) distance (n = 5). The variability of acquired images was tested on plots by using the standard deviation (SD) of DBH and stand density (n/ha). Higher tree densities (smaller NN distance or higher plot density) could increase occlusion or misrepresentation of smaller trees, while highly variable plots (high SD of DBH) could inconsistently detect trees or estimate DBH.

Linear and logistic regression were used on numerical and categorical variables to characterize the influence of the tree-level variables on the estimation error (as a percent of DBH) and detection, respectively. On the plots, linear regression was used to characterize the influence of the acquisition conditions on the RMSE%, percent detection, and percent commission. To do this, the estimation errors (response) were regressed against the acquisition conditions (features). For both individual trees and sample plots, a variable was determined to have a significant effect on the accuracy measure if the p-value of the model was < 0.05 and regression assumptions were met.

The extent to which the minimum DBH influenced the accuracy at the plot level was also determined. While a standard value is generally used, this information could be used to inform expected levels of accuracy on sample plots in different jurisdictions. Three sets of minimum DBH values were tested – using a 7 cm minimum DBH as is standard for Alberta PSPs, using 10 cm minimum DBH which is consistent with inventory in other locations (such as Liang et al. 2014, Liang et al. 2015), and a 15 cm minimum DBH as this is approximately the threshold at which a tree is deemed to be merchantable based on guidelines for forest managers in the study area. However, in assessing the patterns of accuracy, the original dataset (7 cm minimum DBH) was used.

4.3. – Results

4.3.1– Reduction of dataset

After the point clouds were processed for the initial 18 plots, some had large errors, unmatched image sets, or low-quality point clouds. While the majority of the plots had representative point clouds, there were 6 plots that did not, as many trees were either poorly reconstructed or completely missing from the point cloud. These substandard plots shared two conditions unique from the other 12: the mean height to live crown was less than 5 m and over 60% of the measured trees had DBH < 15 cm. Most substandard plots had a dominant species as either black spruce, white spruce, or balsam fir. An analysis of existing diameter distribution and species inventory maps in the study area indicated these conditions only occurred on 5% of the total study area. Based on these conditions, I applied a filter to the original dataset to remove plots where the above conditions were not met. This resulted in a final dataset of 12 plots which were deemed suitable for analysis and therefore used in the remainder of the Chapter.

4.3.2. – Tree-level results

A total of 460 out of 653 trees were detected from the point clouds on 12 sample plots, representing an overall detection rate of 70.4%. Additionally, the DBH was estimated from the detected trees with an RMSE of 4.59 cm or 19.3% (Figure 4.3). The relative DBH estimation error ranged from 0 to 77.0% of DBH; however, only 98 trees (21.3% of detected trees) had errors greater than 25%, and 171 trees (37.2% of detected trees) had estimates within 10% of DBH. The greatest errors generally occurred on medium-sized trees (15 – 30 cm), but the majority of trees fell within this size class (69% of detected trees). There was a slight negative bias to DBH estimates (-0.48 cm, -2.03%), shown by the lines in Figure 4.3 which represent the trend on each plot.

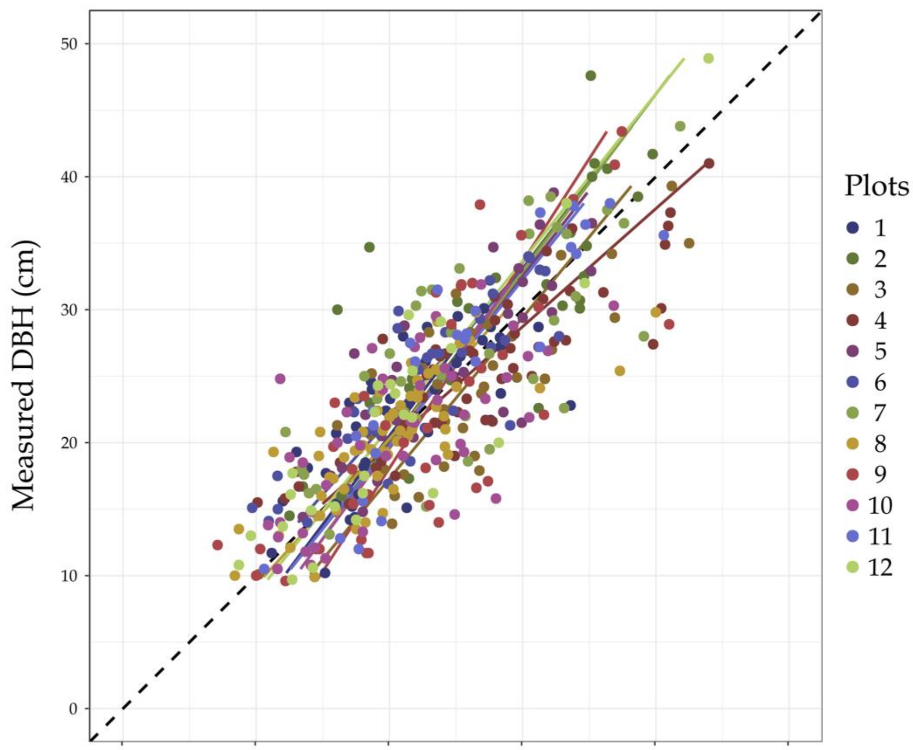

Figure 4.3 - DBH estimation accuracy for all study trees using a minimum DBH of 7 cm (n = 460), with colors corresponding to the 12 sample plots. Lines represent the trend by plot. Plot numbers are the same as in Table 4.2, which includes plot-level summaries.

4.3.3. – Plot-level results

The plot-level results showed a wide range of accuracies for the 12 sample plots (Table 4.4). For example, the detection rate ranged from 60.0% to 90.9%, with a mean value of 72.3%. The commission rates ranged from 8.1% to 26.2% (mean 18.2%). The DBH estimation error stayed fairly consistent, with the RMSE ranging from 3.7 cm to 5.8 cm (mean 4.6 cm) resulting in RMSE% values that ranged from 14.4% to 26.0% (mean 19.0%). With the exception of three plots, the RMSE% of DBH stayed below 20% on each plot.

With increases in the minimum DBH values from 7 to 15 cm, the plot-level results generally showed an increase in the percent detection (from 72.3 to 79.3%), an increase in the percent commission (from 18.2 to 20.0%), a slight decrease in the RMSE of DBH (4.6 to 4.5

cm), and a decrease in the RMSE% (from 19.0 to 17.5%). There was a wide range of results within each scheme (Table 4.4) with, for example, the detection accuracy ranging from 60 to 90% and the RMSE% ranging from 14.4 to 26.5% at the 7 cm minimum DBH.

Table 4.4 - Plot-level results, showing the percent detection, percent commission, and DBH estimation accuracy for all plots at each of three minimum DBH schemes.

Plot Number	Percent Detection			Percent Commission			DBH RMSE (cm)			DBH RMSE%		
Min. DBH (cm)	7	10	15	7	10	15	7	10	15	7	10	15
1	61.4	71.7	80.4	10.0	11.7	13.0	3.9	3.9	4.0	17.8	17.8	17.5
2	82.4	81.8	86.2	14.7	15.2	10.3	5.8	5.4	5.5	19.4	17.7	17.8
3	62.7	71.2	75.0	23.7	21.2	22.7	4.6	4.3	4.4	19.0	18.1	17.3
4	90.9	90.7	87.0	12.7	11.1	13.0	4.2	4.2	4.0	16.4	16.4	15.6
5	69.8	73.2	77.8	14.0	14.6	16.7	4.1	4.1	4.0	15.8	15.8	15.1
6	84.1	86.1	92.1	25.0	18.6	10.5	4.0	3.8	3.9	16.3	15.8	15.5
7	77.1	82.2	78.6	20.8	17.8	14.3	5.7	5.2	4.8	21.2	19.3	17.5
8	69.8	70.4	83.3	8.1	9.9	15.0	3.7	3.6	3.8	18.1	17.3	17.4
9	60.0	61.3	69.1	26.2	29.0	47.6	5.8	5.9	6.1	26.0	25.9	23.3
10	60.5	65.7	70.8	13.2	12.9	20.8	5.0	5.0	5.4	24.5	24.5	23.1
11	83.3	83.3	80.8	20.0	10.0	19.2	3.8	3.5	3.6	14.4	13.2	12.5
12	65.1	68.4	70.4	30.2	34.2	37.0	4.2	4.3	4.7	18.8	18.3	17.5
Mean	72.3	75.5	79.3	18.2	17.2	20.0	4.6	4.4	4.5	19.0	18.3	17.5

4.3.4. – Accuracy and sensitivity analysis

Six variables for both individual trees and on sample plots were tested for their effects on the accuracy of resulting estimates (Table 4.5). Linear and logistic regression were used to characterize the influence of these variables on the accuracy metrics (detection, commission, and DBH error), with significant impacts representing variables in the regression with $p < 0.05$. Generally, the accuracy on the tree scale was more sensitive to the variables tested than at the plot scale; however, there were far more samples for the trees ($n = 460$) than the plots ($n = 12$). At the tree level, significantly affecting the detection of individual trees was the DBH, distance to camera, certain species of tree, height to live crown, and crown class, while only DBH, mean nearest neighbor distance, distance to camera, and one species affected the error of DBH estimation (Figure 4.4). At the plot level, mean DBH and stand density significantly ($p < 0.05$) affected the detection rate, while the standard deviation of DBH and the most common crown class significantly affected the percent commission (Figure 4.5). Of the variables tested, none had a statistically significant impact on the DBH RMSE% at the plot level. Furthermore, the dominant species and mean height to live crown had no significant effect on the accuracy of plot-level estimates.

*Table 4.5 - The sensitivity of the detection, commission, and percent error to different plot and acquisition conditions. Listed numbers are p-values, with * indicating that the variable significantly impacts the results (α = 0.05) and the assumptions of linear regression are met. The species listed are those having a significant impact on the results, with Bw = White birch, Sw = White spruce, and Dd = dead trees. At the tree level, % error refers to the error as a percentage of the DBH, while representing the RMSE% at the plot level. Commission rate is only assessed at the plot level due to only plot-level variables having a potential effect. I/S = Intermediate/Suppressed*

	Tree-level variable	Detection rate	Commission	% error (DBH)
Tree scale (n = 460)	DBH (cm)	<0.01*	-	<0.01*
	Mean nearest neighbor distance (k = 5; m)	0.50	-	0.01*
	Distance to camera (m)	<0.01*	-	<0.01*
	Species	Bw (<0.01), Sw (<0.01), Dd (0.01)*	-	Sw (0.02)
	Height to live crown	<0.01*	-	0.07
	Crown class	All <0.01*	-	I/S (<0.01)*
Plot scale (n = 12)	Mean DBH (cm)	<0.01*	0.98	0.21
	Standard deviation of DBH (cm)	0.94	0.03*	0.66
	Stand density (n/ha)	0.05*	0.15	0.13
	Dominant species	0.67-0.90	0.28	0.21-0.97
	Mean height to live crown	0.98	0.70	0.49
	Most common crown class	0.17	0.02*	0.13

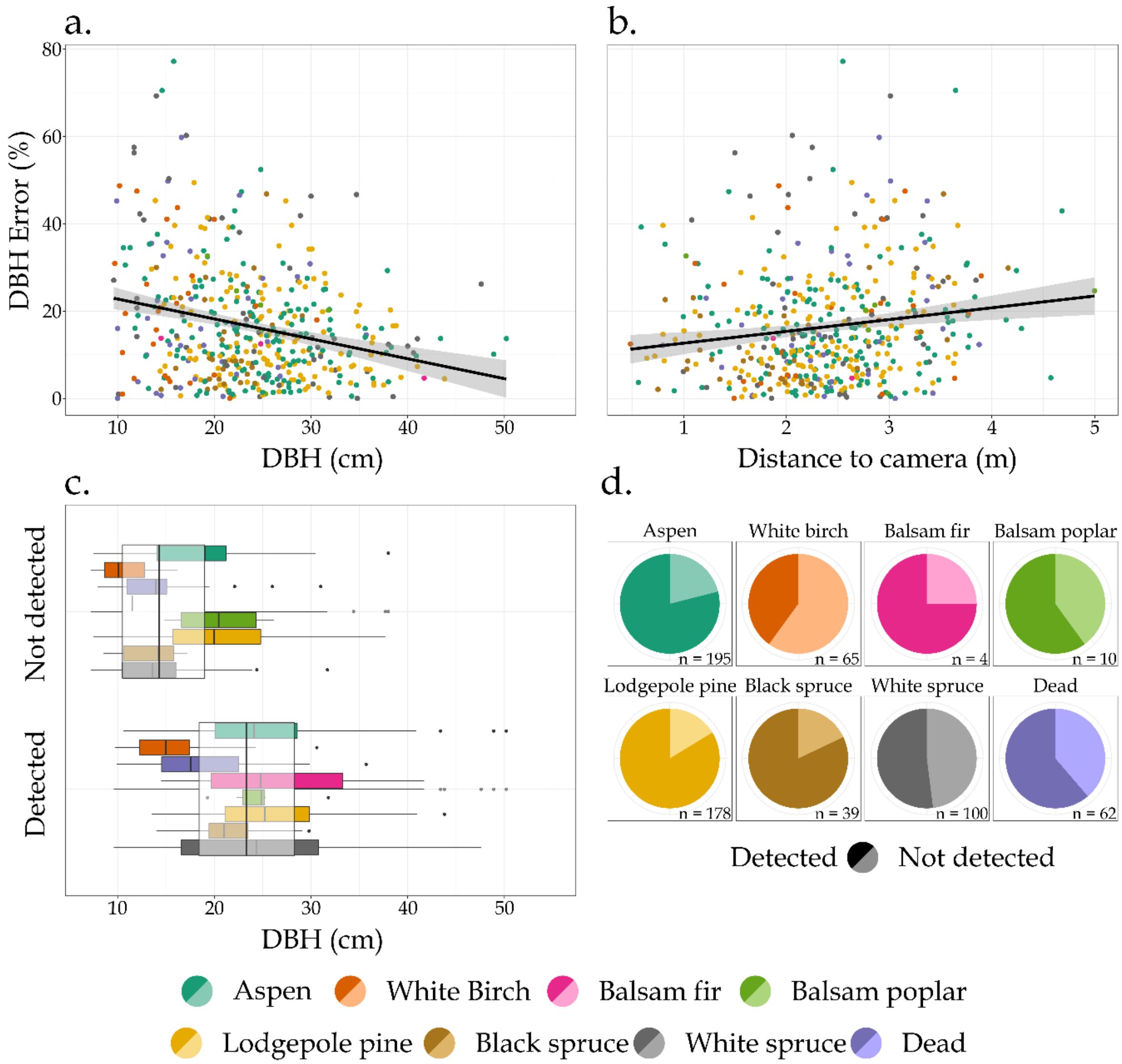

Figure 4.4 – The influence on accuracy at the individual tree level (n = 460). The DBH (a) and distance (b) from the tree to the camera detecting it on the accuracy of the DBH estimate, with the colors of the points corresponding to the tree species. DBH error on the top row is the difference in the DBH estimate from measured DBH, expressed as a percentage of the measured value. The black line represents a linear model to predict the percent error, with shaded area being the standard error of the model. The bottom row shows the influence of species (c, d) and DBH (d) on the detection accuracy of individual trees.

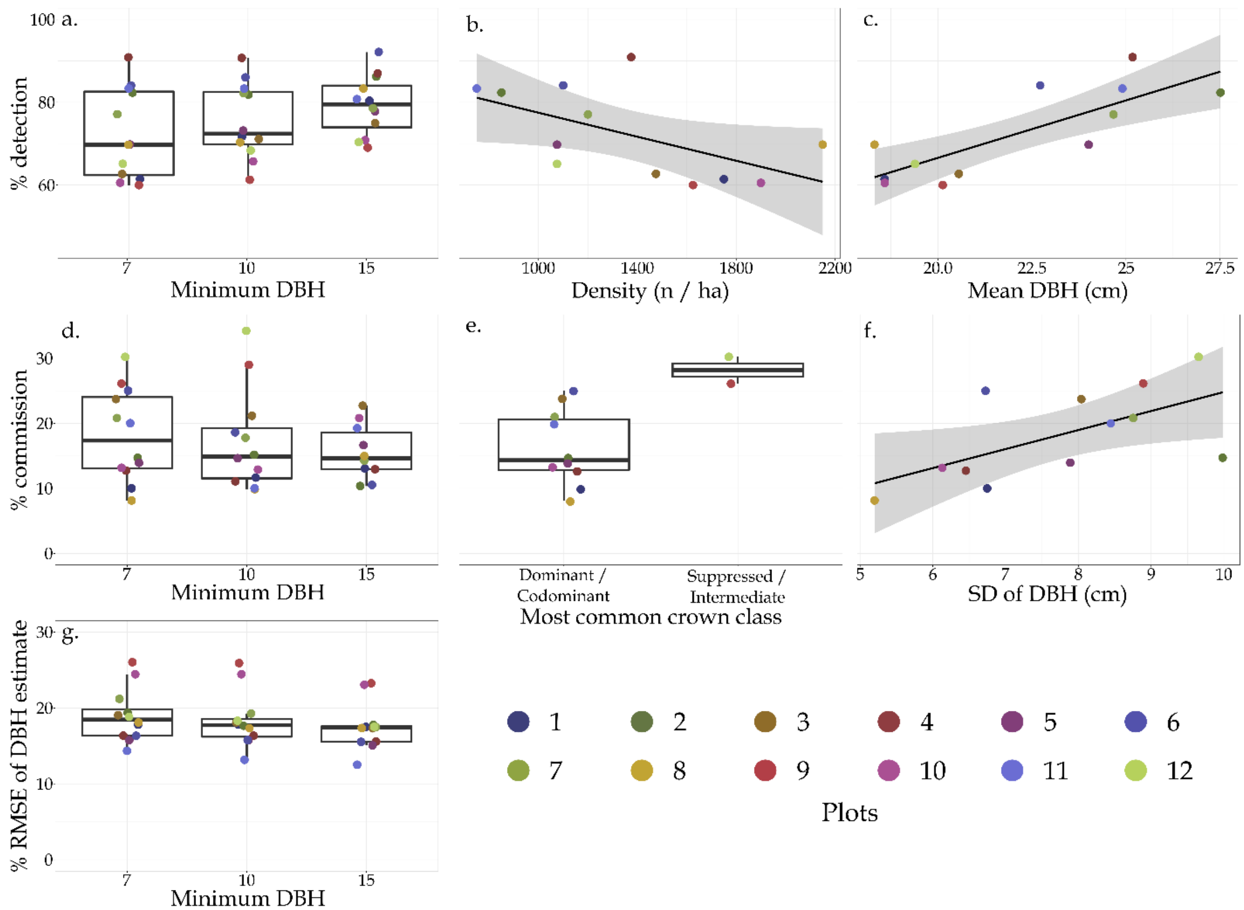

Figure 4.5 - Patterns of accuracy at the plot level (n = 12). The top row shows the effects of minimum DBH measurement (a), stem density (b) and mean DBH (c) on detection accuracy. The middle row shows the effect of minimum DBH (d), crown class (e), and the standard deviation of DBH (f) on percent commission. Finally, the bottom plot shows the effect of minimum DBH (g) on percent detection. On scatterplots, the black line represents the linear relationship between the variables and the percent detection or commission, with the grey area being the standard error. On boxplots, a black line connects the means for each group of minimum DBH values. Plot numbers are the same as in Table 4.2, which includes plot-level summaries.

4.4. – Discussion

4.4.1. – Tree-level accuracy

In general, the overall detection rate and estimation accuracy from this Chapter is comparable to other studies (~70% detection and ~4 cm RMSE; Table 4.1). However, the results were able to demonstrate the use of DTP in forest types that were more heterogeneous and had a wider range of understory conditions and branching patterns than in previous studies. Trees with larger DBHs and those closer to image sets had significantly lower error in DBH estimation from DTP (Table 4.5, Figure 4.4a-b). While there may be a compounding effect of variables such as tree size and distance to camera, these variables were not correlated to one another. If a tree is larger or closer to a camera, it will take up more pixels in the image, resulting in more matched points in the output point cloud. Likewise, tree size also had a significant impact on detection (Table 4.5, Figure 4.4c). Only a few species – white spruce, white birch, and dead trees – were significantly less likely to be detected, while white spruce was the only species with significantly higher error in tree-level DBH estimates. The bark of white birch is thin and can flake off, thereby resulting in a wide range of stem forms that may not represent the true size, while standing dead trees have a wide range of potential forms (leaning, rotting, etc.), possibly resulting in their lower likelihood of detection (Burns and Honkala 1990). White spruce, conversely, is shade-tolerant and retains its branches, even those lower on the tree (Bergeron et al. 2014). The shade tolerance of white spruce means that they may grow in the understory and develop higher densities than that of other species in the study area, likely increasing occlusion of other stems. Another possible reason for lower detection rates and estimation accuracies for white spruce may be that portions of the stem containing branches increase the possibility of occlusion in the images, especially when images were taken from greater heights or trees had larger distances to the camera. Patterns of DBH estimation accuracy in this Chapter were similar to that of Chapter 3, in which black spruce and white spruce trees with low branches had only partial reconstructions of the stem and larger error of diameter estimates farther up the stem.

4.4.2. – Plot-level accuracy

With a 7 cm minimum DBH, the results showed a mean plot-level stem detection rate of 72.3%. Although slightly lower in some cases, the accuracy and detection rates reported were comparable to that of others (Table 4.1) despite using a smaller set of images (102) in plot conditions that were denser (750-2150 stems/ha) and more variable (mean DBH 22.0 cm, SD 7.7 cm; Table 4.2). For example, Liang et al. (2014) achieved a detection rate of 88%, using 973 images on a 900 m^2 sample plot that had a stem density of 278 stems/ha. On the best plot in their study area, Piermattei et al. (2019) achieved a detection rate of 98%, using 338 images on a 707 m^2 sample plot with a density of 651 stems/ha. The mean RMSE of DBH estimation on all plots – 4.6 cm or 19.0% – was also comparable to other studies. For four methods tested by Mokroš et al. (2018), the DBH RMSE% ranged from approximately 16 to 20, which was similar to results seen in this chapter. Forsman et al. (2016) had higher errors for DBH estimates (approximately 30% RMSE) than those of the present work, but took fewer pictures that were generally farther away from sample trees, suggesting that there may be a balance of the number of images and the resulting accuracy when using DTP at the plot scale.

Despite the similar accuracies, forest types in other studies were markedly different than that of the Slave Lake study area. For example, the studies described in Table 4.1 had far lower densities and generally larger and less variable mean DBH values, likely indicating more even-aged stands with limited understory. These studies provided important context and methodological recommendations to that of the current Chapter, but direct applications of past methods may not be sufficient in more complex habitats. The current Chapter provides recommendations for future study, but more research is needed to apply these methods for deriving operational inventory estimates in heterogeneous forest types such as the boreal mixedwood.

Results from other studies follow the general trend seen here, that detection rate tends to increase with larger tree sizes and lower stem densities. Although using fewer images, my results are comparable to those from similar plot conditions in previous studies, likely due to the use of high image overlap at each camera location and a spherical camera for point cloud generation. In all previous studies using DTP at a plot scale, a conventional frame camera was used. While spherical cameras have a wider field of view, there are also issues and considerations to be made with the geometric distortion of objects in the view (Barazzetti, Previtali, and Roncoroni 2017). In order to overcome these issues, high overlap from six cameras in an image set and also close ranges used (5m radius) seemed to reduce these issues. Although not investigated in the current work, future work investigating the effect of camera types and image specifications on the accuracy of resulting point clouds is needed. Additionally, the small number of plots used in the study may limit some of the takeaways from the error analysis.

Other studies have investigated the use of stereoscopic hemispherical images for forest attribute estimation. Stereoscopic hemispherical images have great potential to benefit forest inventory as they can substantially reduce the number of required images and therefore the amount of time spent on the sample plot. For example, Rodríguez-García et al. (2014) used pairs of images in a Eucalyptus plantation to derive accurate measurements of stem position and diameter at different heights up the stem. Additionally, results showed that measurement precision was stable up to distances of 8 m from the camera setup. Some studies have used methods for automated detection and segmentation of tree stems before estimating attributes such as diameter or basal area (Herrera et al. 2011; Sánchez-González et al. 2016). This Chapter used multiple filtering steps to reduce error in generated point clouds, but automated detection and segmentation of tree stems may generate point clouds which require less filtering. Despite the advances of studies using stereoscopic hemispherical photos, many of them use proprietary algorithms to derive information from the photographs. To develop the operational capacity for these technologies for estimation of forest inventory attributes, either standardizing existing algorithms or open processing pipelines will be required.

As the minimum DBH changed for the different estimation schemes (7, 10, and 15 cm), the detection rate also changed from 72.3% to 75.5% to 79.3%. Additionally, as the minimum size changed, the absolute RMSE for DBH was stable (around 4.5 cm), indicating that the DBH error was more inherent to the acquisition and merging parameters than the tree size. This could imply that DTP is more accurate when estimating groups of larger trees or that the smallest trees had low detection rates and inaccurate DBH estimates, so excluding them from the dataset increased the overall accuracy in terms of the % detection and RMSE%. This could also imply that tree size had no influence on error from 7 to 15 cm DBH, seen in Figure 4.5g, showing a wide range of accuracies for trees in this DBH range, while that of larger diameters is generally more accurate and less variable. This analysis also showed that the mean height to live crown had no significant influence on the DTP accuracy. The original dataset of 18 plots was reduced to a set of 12 plots suitable for analysis. This was due to unsuitable plot conditions (e.g. mean height to live crown < 5 m and mean DBH < 15 cm) which caused the resulting point clouds to be unrepresentative and difficult from which to take detailed measurements. As plots with low stem visibility were removed from the analysis, this result may suggest that after a certain threshold of visibility (here, a mean height to live crown of 5 m), the height to live crown no longer influences the accuracy of the results at the plot scale. These conditions were likely a key factor in the misregistration of the DTP point clouds because 5 m was also the greatest height at which an image was acquired, meaning that trees with partially occluded stems may not be fully reconstructed in a resulting point cloud. Additionally, smaller trees (diameter < 15 cm) have fewer reconstructed 3D points on the stem due to the smaller tree size and therefore fewer matched points in the point cloud, especially for trees further away from camera locations. A critical component of this methodology at the plot scale is the consideration of the conditions in which DTP is to be used. For example, limitations may exist on the species (those without many branches low on the stem) and tree sizes (> 60% over 15 cm) for which DTP is successful. While this may represent a limitation of the technology, the determination that only a small proportion of the study area contains these conditions (~5%) is encouraging to the wider adoption of the technology to different forest types. Furthermore, the results from this Chapter may show patterns of accuracy expected under different conditions to those wanting to undertake their own research using DTP.

4.4.3. – Comparison to TLS

An international benchmarking study using TLS by Liang et al. (2018) first classified stands into categories of complexity and then tested the outcomes of different algorithms for tree detection and estimation. The study described general tree detection rates for single-scan TLS of 70% and 60%, while multi-scan results showed 90% and 80% detection for easy and medium stands, respectively. Furthermore, the RMSE% of DBH estimation was approximately 10% for easy and 15% for medium stands. “Medium” difficulty plots in the study had a density around 1000 stems per ha and some understory vegetation, meaning this category may be closest to the plots used in this Chapter. Therefore, the detection rate and DBH estimation accuracy achieved using the DTP methodology in this Chapter could be comparable to TLS, albeit with slightly lower accuracy.

Ultimately, the costs and complexity of TLS should be weighed with their accuracy. TLS units often cost in the tens of thousands of dollars or more (Eitel et al. 2013). To compare, the cameras, mount, and pole used in this work cost less than CAD$700 in total. Depending on the forest type and the variable of interest, point clouds generated from TLS units could potentially have more accurate results than those of DTP. Additionally, point clouds derived from TLS have more detail in characterizing attributes such as branching patterns or providing direct measurements of upper portions of stems (Liang et al. 2016). However, results from this Chapter and others (Table 4.2) have shown that DTP could present a viable alternative to detection and DBH estimation when tree, stand, or acquisition conditions are suitable and costs need to be minimized.

4.4.4. – Applications and context

Deriving plot attributes using DTP has associated costs, such as the cost of cameras and computing resources to generate point clouds. However, the resulting estimates and point clouds could provide vital information to a variety of forest inventory applications. First, point clouds represent objective and methodologically consistent estimates across acquisitions. Point clouds are also storable, meaning that they can be used to track changes over time (for example, to derive changes in tree size or stem form over time, including for biomass allocation or carbon storage) or be used to derive. Furthermore, they can be used to derive additional information not taken on traditional field inventory, or those taken using destructive sampling methods. Such estimates could be taper or merchantable volume, which require diameters of upper parts of the stem, such as in Chapter 3, where it was determined that DTP-based estimates of taper were more accurate than conventional approaches for the lowest parts of the stem. Finally, plot-level estimates could be used as inputs to aerial inventories or used as field data to support area-based estimates. Future studies could include DTP-based estimates of plot attributes to either validate aerial models or update existing area-wide inventory estimates.

Chapter 5 - Enhancing the estimation of stem-size distributions for unimodal and bimodal stands in a boreal mixedwood forest with airborne laser scanning data

5.1. – Introduction

Chapters 3 and 4 demonstrated the importance of ground-based structural measurements in forest inventory. These measures are important for intensive inventories at small spatial scales and for providing calibration and validation for airborne surveys. The next scale at which forest inventory information is required is the stand or landscape (Figure 1.2), in which measures of structure and composition are used to characterize the forest at broader spatial scales such as a forest management unit or region. While these measurements can include information such as the species mixtures or disturbance history, attributes such as SSDs provide robust structural information which benefit a range of timber production and ecological monitoring purposes. To support these information needs, there is increasing interest in the capacity to estimate stand-level SSDs over large areas, and to understand patterns of their variance – particularly across the diverse species and age gradients that exist in mixedwood stands.

SSDs of homogenous stands are typically unimodal, while two or more maxima are often observed in heterogeneous stands with more complex structure. Various statistics, such as the bimodality coefficient or Hartigan's dip statistic (Freeman and Dale 2012), can be used to assess multimodality of SSD. However, it can also be characterized using the ecological characteristics of the stand, including if stands are multilayered (Podlaski 2010), have high variance in diameters (Maltamo and Gobakken 2014), ages (Zhang et al. 2001), or number of species (Liu et al. 2002), or by more complex metrics such as the ratio of stem density to top height (D/H; Thomas et al. 2008). As stands mature, they do not follow a linear pattern of structural development, making the prediction of mature stand structures difficult (Kane, McGaughey, Lutz, et al. 2010). Heterogeneity, typically associated with multimodal stands, results from ecological legacies and disturbance histories specific to individual areas (Franklin et al. 2002).

In addition to size class frequencies, SSDs can be summarized using a variety of statistical models or probability density functions (PDFs). The most common PDF for characterizing SSDs is the Weibull distribution because of its flexibility with a limited number (two) of parameters to predict or impute (Bailey and Dell 1972). Fitting PDF parameters to measured diameter at breast height (DBH) values relies on optimization techniques such as maximum likelihood estimation (MLE; Myung 2003). Despite the flexibility of the Weibull distribution, it is limited to characterization of stands with unimodal SSD (Packalen and Maltamo 2008). If an SSD of a stand is not unimodal, it should be characterized by a more complex distribution or use a nonparametric estimation method such as a Finite Mixture Model (FMM; Thomas et al. 2008) or k-NN (Penner et al. 2015).

For complete characterization of forest structure, the SSD of all stands in the area of interest need to be estimated or measured. SSDs derived from field measurements are spatially constrained, time consuming and expensive to acquire. Hence, field-based estimates of SSDs alone cannot provide the large-area spatial coverage required in a forest management context. A common inventory approach to address the limitation in spatial coverage is to use air-photo interpretation, which can provide complete spatial coverage of an area. However, this approach is limited to the scale of the aerial photography and the expertise of the interpreter, and as a result it is difficult to provide the detailed tree-level information required for an SSD. Eid et al. (2004), for a spruce/pine forest in Norway, determined that photo interpretation provided poorer estimates of stand inventory attributes, such as basal area, height, and number of trees, than estimation by other remote sensing methods. They found, for example, deviations of 20% for photo-interpreted height, compared to deviations of 12% for laser scanning estimates. Inaccurate photo-interpreted estimates were projected to have more than three times the loss in the value of a stand than ALS-based estimates.

These limitations in spatial coverage and accuracy, coupled with increasing financial pressures and needs for highly detailed data, are resulting in the increased use of active remote sensing technologies for informing forest inventories. Airborne laser scanning (ALS) has been incorporated into forest inventories because it provides very detailed information on forest structure over large spatial extents (White et al. 2016). It has been demonstrated (Næsset 2002) that attributes such as dominant height, mean diameter, stem number, basal area, and volume can be adequately estimated using ALS data in combination with a sample of ground plots (van Leeuwen and Nieuwenhuis 2010; Næsset 2007). ALS also has been used to characterize SSDs in unimodal stands requiring relatively simple estimation techniques (Maltamo et al. 2005) and in multimodal stands with more complex procedures (Penner et al. 2015). However, less has been done to estimate SSDs of boreal mixedwood forests, which can have both simple and irregular distributions in neighboring stands, making them more difficult to predict (Liu et al. 2002), and estimation of stand modality with ALS has been limited to vertical forest structure (e.g. Kao et al. 2005; Maltamo, Suvanto, and Packalén 2007). In the case of forests varying between unimodal and multimodal SSDs, the thresholds for applying different fitting techniques is also poorly understood. Landscape-scale evaluation of modality in predicting SSD in mixedwood stands can provide valuable insights into the complexity of these forests.

In this chapter, I evaluate the efficacy of ALS metrics to first differentiate plots with unimodal and multimodal SSDs and then to predict parameters of those distributions. Using both ground plot measurements and ALS estimates of plot structural characteristics (e.g. height or age), I investigate the capacity of ALS metrics to distinguish between areas with single or multimodal distributions and then apply ALS to predict SSDs with the distribution most appropriate to the characterized distribution type. I then compare ALS parameter estimates to fitted parameters and ground measured SSDs. Finally, I discuss the applications of this methodology and explain how estimates could be predicted across an entire area of interest.

5.2. – Methods

5.2.1. – Modality

The bimodality coefficient (Pfister et al. 2013) is a statistical approach to assessing a stand's modality. It has also been used in botany (Ellison 1987) and psychology (Freeman and Dale 2012) and provides a measure from 0 (perfect unimodality) to 1 (perfect bimodality). A critical value of 5/9 (~ 0.5556) is used to distinguish bimodal (> 5/9) from unimodal (< 5/9) distributions (Freeman and Dale 2012). The bimodality coefficient was applied to 71 PSPs and identified 23 (32%) as bimodal and 48 as unimodal with respect to SSD.

5.2.2. – ALS data processing

ALS data processing began with separating point clouds into ground and non-ground returns based on adaptive TIN models (Axelsson 2000). Next, point clouds were normalized to heights above the ground surface before being clipped to the extent of sample plots. Metrics describing the vertical distribution of returns in each plot were calculated based on normalized ALS point clouds using FUSION (McGaughey 2008), as well as the statistical software R (R Core Team 2018) with the lidR package (Roussel and Auty 2019). A suite of these metrics was selected to fully characterize the height, variability, cover, and structure of the area corresponding to each PSP (Table 5.1). ALS metrics were separated into categories of similar types: height (e.g., height of 50th percentile), cover (e.g., percent above 2m), standard deviation, and canopy structure (e.g., rumple).

Table 5.1 – ALS metrics used to predict PDF parameters

Metric	Description	Source	Category
P05	Height of the 5th percentile of returns	McGaughey 2008	Height
P25	Height of the 25th percentile of returns	McGaughey 2008	Height
P50	Height of the 50th percentile of returns	McGaughey 2008	Height
P75	Height of the 75th percentile of returns	McGaughey 2008	Height
P95	Height of the 95th percentile of returns	McGaughey 2008	Height
Std.Dev.	Standard deviation of return heights	McGaughey 2008	Variability of Heights
Variance	Variance of return heights	McGaughey 2008	Variability of Heights
IQ	Interquartile range of return heights	McGaughey 2008	Variability of Heights
Skewness	Skewness of return heights	McGaughey 2008	Variability of Heights
Kurtosis	Kurtosis of return heights	McGaughey 2008	Variability of Heights
AAD	Average absolute deviation of return heights	McGaughey 2008	Variability of Heights
Median	Median of return heights	McGaughey 2008	Variability of Heights
% First Returns Above 2m	Percent of first returns above 2 meters	McGaughey 2008	Cover
% All Returns Above 2m	Percent of all returns above 2 meters	McGaughey 2008	Cover
0.5 m – 2 m Return Proportion	Proportion of returns between 0.5 and 2 m	McGaughey 2008	Cover
2 m – 5 m Return Proportion	Proportion of returns between 2 and 5 m	McGaughey 2008	Cover
5 m – 10 m Return Proportion	Proportion of returns between 5 and 10 m	McGaughey 2008	Cover
10 m – 20 m Return Proportion	Proportion of returns between 10 and 20 m	McGaughey 2008	Cover
Rumple	Ratio of canopy surface area to plot area	Kane, McGaughey, Bakker, et al. 2010	Structure
Filling Ratio	Proportion of returns in voxels under the canopy	Tompalski 2012	Structure
VCI	Vertical complexity index – distribution of abundance of returns in specified height bins	van Ewijk, Treitz, and Scott 2011	Structure
Vertical Rumple	Measure of variance of vertical structure as a function of filled voxels in point cloud	Tompalski et al. 2015	Structure
LAD CV	Coefficient of variation of leaf area density – vertical dispersion of foliage density through the canopy	Bouvier et al. 2015	Structure

Filling ratio (FR) is a proportion of filled voxels under the canopy (Tompalski 2012). Voxels are volumetric pixels—cubic bins of a pre-defined size (e.g., 1m x 1m x 1m), which, when stacked, cover the entire 3-dimensional extent of the ALS point cloud (Popescu and Zhao 2008).

$$FR = \frac{V_{VEG}}{\sum_{i=1}^{i_{max}} \sum_{j=1}^{j_{max}} H_{MAX_{ij}} - H_{G_{ij}}}, \tag{1}$$

where V_{VEG} is the volume of vegetation (represented as the volume of voxels with returns), $H_{MAX_{ij}}$ is the maximum voxel height for ij, and $H_{G_{ij}}$ is the ground height of point ij (a value of 0 in normalized point clouds).

5.2.3. – Analysis approach

Figure 5.1 summarizes the workflow applied. The measured trees within each ground plot were first combined into of 2-cm diameter classes and classified as either unimodal or bimodal using the bimodality coefficient. Then, various stand characteristics, measured on plots and predicted using ALS, were assessed for their ability to identify the plots as either unimodal or bimodal. Once the best ALS metric for identification was determined, it was used to categorize plots for estimation of SSD parameters by ALS. Field-based SSD on classified plots were used as response data for prediction with ALS metrics. Each of these steps is described in further detail below.

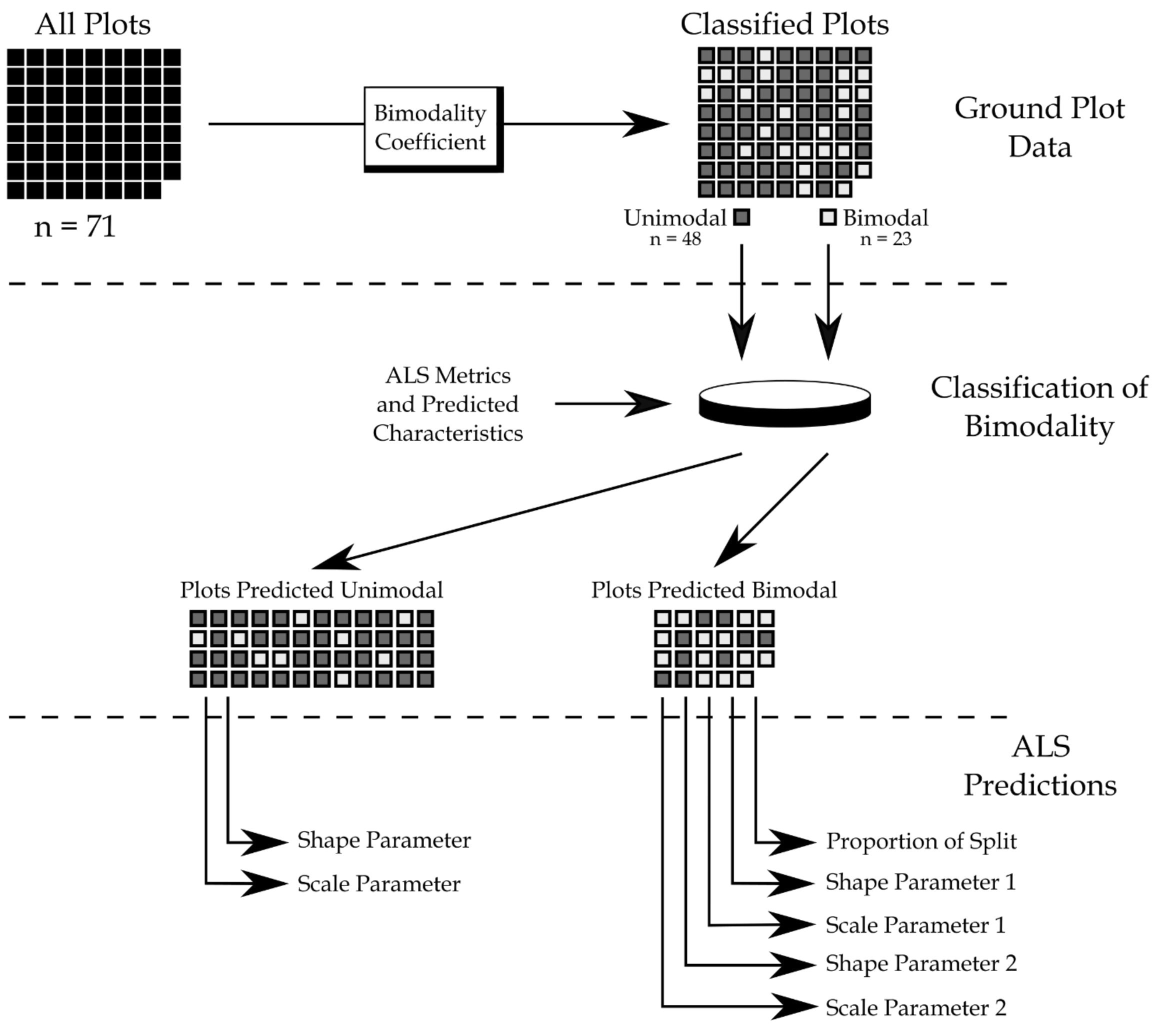

Figure 5.1 - Workflow for differentiating bimodal plots and estimating SSD parameters with ALS.

5.2.4. – Differentiation of modality in stem size distributions

Stands classified as multimodal are thought to be highly variable and structurally heterogeneous, and this heterogeneity has been quantified in different ways (Table 5.2). I examined how effective each of the characteristics identified in Table 5.2 were for differentiating between unimodal and bimodal SSD using both ground measurements and ALS-derived predictions of the five characteristics for differentiation. In an operational context, the use of a single ALS metric would be advantageous if it could be used as an effective heuristic to identify unimodal and bimodal grid cells, because a single metric would be available wall-to-wall (wherever ALS data is acquired), would be generated as a standard preliminary processing step for an area-based approach (described below), and would require no ground samples or additional modelling.

Table 5.2 – Published predictors of multimodal diameter distributions and how they are used to classify bimodal plots.

Differentiation	Source	Quantified as
Uneven-aged stands	Zhang et al. 2001	Std. dev. of ages
Mixed-species stands	Liu et al. 2002	% Dominant species
Density / Height Ratio	Thomas et al. 2008	N / top height
Multilayered	Podlaski 2010	Std. dev. of heights
Varied diameters	Maltamo and Gobakken 2014	Std. dev. of DBHs

First, as a baseline, five ground-measured characteristics were assessed for their ability to discriminate unimodal and bimodal plots. Next, using an area-based approach, predictive models were developed to estimate each of the five ground-measured characteristics in Table 5.2 using ALS metrics (Table 5.1) as predictors and the ground-measured characteristics as response variables. Models were built using stepwise linear regression, and final models were selected based on combinations of up to 3 metrics (to avoid overfitting) that captured the most variation in the sample population. Predictor variables were selected so that those showing a strong correlation ($r > 0.8$; van Aardt, Wynne, and Oderwald 2006)) with each other or coming from the same category of descriptors were not included in the same model. The accuracy of area-based models for each of the aforementioned characteristics was assessed in terms of an adjusted r^2 and relative RMSE for all sample plots. Finally, individual ALS metrics were used to differentiate SSD modality.

5.2.5. – Accuracy of modality differentiation

Modality differentiation was assessed by determining the overall accuracy of the classification that each measure produced. The classification accuracy was defined as the percentage of all PSPs which were correctly classified as either unimodal or bimodal. This was assessed for each characteristic and ALS metric, and allowed for consistent comparison between structural characteristics and individual metrics. A successful classification was defined as a statistically significant improvement from no classification (i.e. if I assume all plots are unimodal). The exact binomial test was used to assess the statistical difference between each classification method and the classification of all plots as unimodal (Aronoff 1982).

5.2.6. – Predictive modeling of SSD parameters using ALS metrics

Once an SSD of a plot was classified as either unimodal or bimodal using the most accurate ALS model, a structurally appropriate distribution function was fit to the ground-measured SSD (Figure 5.2). As complete data in the study area exists for trees > 7 cm DBH, a truncated Weibull distribution was used for describing the SSD in unimodal stands, with the truncation point set at 7 cm (McGarrigle et al. 2011). While nonparametric imputation such as k-NN and Random Forest have been used to predict SSDs (Bollandsås et al. 2013), these typically require large amounts of samples to be taken (Maltamo et al. 2009). Instead, a Finite Mixture Model (FMM), which applies *k* separate distributions to *k* components of data which are split at statistical breakpoints, where *k* is the number of modes in the data (Liu et al. 2002), was used for the bimodal distributions (i.e., k = 2). Similar to Thomas et al. (2008), separate Weibull distributions were fit using MLE. Once the parameters of the appropriate distributions were estimated from the measured DBHs, the parameters were used to develop area-based models from the ALS metrics in order to estimate the PDF parameters and the SSD across the management area.

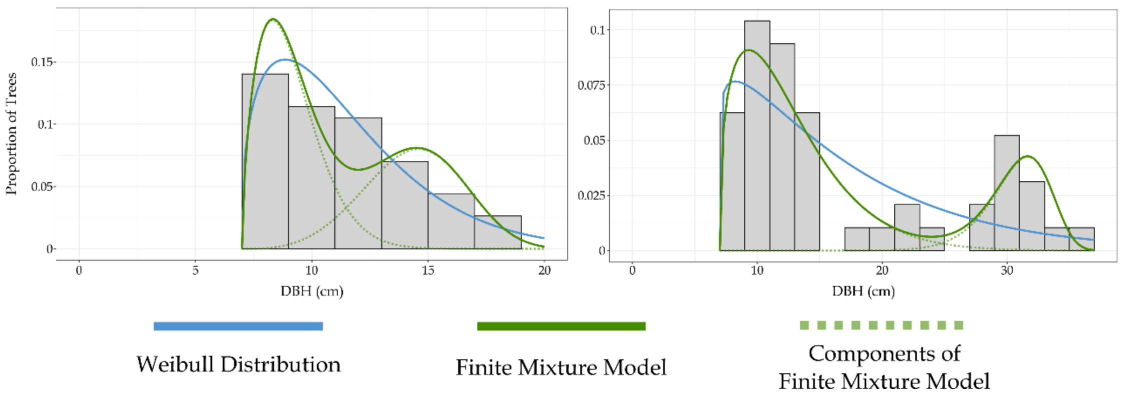

Figure 5.2 – Weibull distributions (blue) best fit unimodal stands (left), while more complex distributions such as a Finite Mixture Model (green) best fit multimodal stands (right).

5.2.7. – Evaluation of SSD parameters using the error index (EI)

To examine the fit of the ALS-predicted SSD to the original measured tree stem DBHs, the Error Index (EI) proposed by Reynolds et al. (1988) was used. The EI reports the sum of observed differences in each class as a proportion of the number of trees at a site. The EI is a frequently used method of evaluating SSD functions, as it allows for comparison across different fitting techniques (e.g., Palahí, Pukkala, and Trasobares 2006) or PDFs (e.g. Zhang et al. 2003). Two different EI calculations were used – one to compare fits of ground-measured distributions (EI_G, Equation 2) and one to compare fits of ALS-estimated distributions (EI_{ALS}, Equation 3):

$$EI_G = \sum_{i=1}^{m} 100 \left| \frac{f_{REF\,i} - f_{PDF\,i}}{n_{REF\,i}} \right|, \tag{2}$$

$$EI_{ALS} = \sum_{i=1}^{m} 100 \left| \frac{f_{REF\,i}}{n_{REF\,i}} - \frac{f_{ALS\,i}}{n_{ALS\,i}} \right|, \tag{3}$$

where f_{REFi} is the measured frequency in DBH class i, f_{PDFi} is the PDF-derived frequency in DBH class i, f_{ALSi} is the estimated frequency in DBH class *i*, n_{REFi} is the total number of measured stems in class *i*, and n_{ALS} is the total number of estimated stems in class *i*. EI_{ALS} was determined following Packalén and Maltamo (2008), with n_{ALS} determined using an area-based approach and the same variables used for the PDF parameter estimation. Both error indices range from 0, indicating a perfect fit, to 200, indicating non-overlapping distributions.

5.3. – Results

5.3.1. – Differentiation of modality in stem size distributions

Most of the metrics and models were successful in differentiating plots into either unimodal or bimodal distributions (Table 5.3). SD_{DBH} and the SD_H had the highest overall classification accuracy (70.4% and 67.6%, respectively) of the ground-measured metrics, while the SD of ages and % dominant species had the lowest accuracy (both 59.2%).

*Table 5.3 – Accuracy of bimodal plots classification using ground measurements, ALS predictions, and corresponding ALS metrics. * indicates a significant improvement from no classification (i.e. assuming all plots are unimodal).*

	Differentiation	Overall Accuracy	ALS Prediction Accuracy	
			Adj. r^2	RMSE%
Plot Data	SD_A	59.2	-	-
	% dominant species	59.2	-	-
	D/H	64.8	-	-
	SD_H	67.6	-	-
	SD_{DBH}	70.4	-	-
ALS Predictions	SD_A	66.2	.059	88.4
	% dominant species	63.4	.155	27.3
	D/H	74.7*	.600	43.8
	SD_H	67.6	.694	25.7
	SD_{DBH}	74.7*	.640	31.2
ALS Metrics	Variance	77.5*	-	-
	Kurtosis	46.5	-	-
	Canopy Relief Ratio	57.8	-	-
	% All Returns > 2m.	63.4	-	-
	Filling Ratio	66.2	-	-
	Rumple	74.7*	-	-

Characteristics related to tree size variability (SD_H, SD_{DBH}, D/H) were most accurately predicted by ALS (Adj. $r^2 > 0.6$), while as expected, characteristics not related to tree dimensions (SD_A, % dominant species) had poorest predictions (Adj. $r^2 < 0.2$). In terms of their capacity to discriminate modality, the best ALS-predicted characteristic was SD_{DBH} (74.7%), while the poorest was % dominant species (63.4%). Of the individual ALS metrics used to differentiate modality, the variance of ALS return heights was the most accurate (77.5%) and provided the most accurate differentiation overall. The variance of ALS return heights was therefore selected for differentiating modality for the remainder of this Chapter.

5.3.2. – Predictive modeling of SSD parameters using ALS metrics

The adjusted r^2 values for the predicted Weibull and FMM parameters were similar (0.5 – 0.6) with the exception of the unimodal shape parameter and the shape parameter for the second group of the FMM (0.3925 and 0.2019, respectively; Table 5.4). Although each of the metrics in Table 5.1 was used in at least one predictive model, some appeared more frequently than others. The most frequently used metrics were P95, Kurtosis, % All Returns Above 2 m, and the Filling Ratio.

Table 5.4 – Prediction accuracy of SSD parameters for unimodal (n = 48) and bimodal (n = 23) plots as differentiated by ALS.

	Parameter	Prediction Accuracy	
		Adj. r^2	RMSE%
Unimodal	Shape	.3925	23.26
	Scale	.6271	30.39
Bimodal	$Shape_1$	.5497	30.25
	$Scale_1$	.5898	32.86
	$Shape_2$	.2019	33.93
	$Scale_2$	.5203	29.81
	% over breakpoint	.5389	42.91

5.3.3. – Accuracy of predicted distributions

Using a mixture model on bimodal plots resulted in a higher accuracy than using a unimodal distribution on all plots for both ground-measured and ALS-predicted parameters (Table 5.5; Figure 5.3). For ground-measured plots, the mean EI_G was 28.20 using mixture models and unimodal distributions when appropriate, while only using a unimodal distribution would have resulted in an EI_G value of 31.24. Similarly the mean EI_{ALS} was 49.13 after differentiating modality, while predicting only a unimodal distribution on all plots would have resulted in a mean EI_{ALS} value of 51.31. Plots deemed bimodal based on ground measurements and ALS predictions had higher mean error values than unimodal plots, with a difference of 9.01 between EI_G values and 19.35 between EI_{ALS} values.

Table 5.5 – Measured (EI_G) and predicted (EI_{ALS}) values on sample plots, showing differences in unimodal and bimodal plots.

	Ground estimates (EI_G)	ALS predictions (EI_{ALS})
Mean *EI* (unimodal plots)	25.29	42.86
Mean *EI* (bimodal plots)	34.30	62.21
Mean *EI* (all plots)	28.20	49.13
Mean *EI* (Unimodal Weibull on all plots)	31.24	51.31

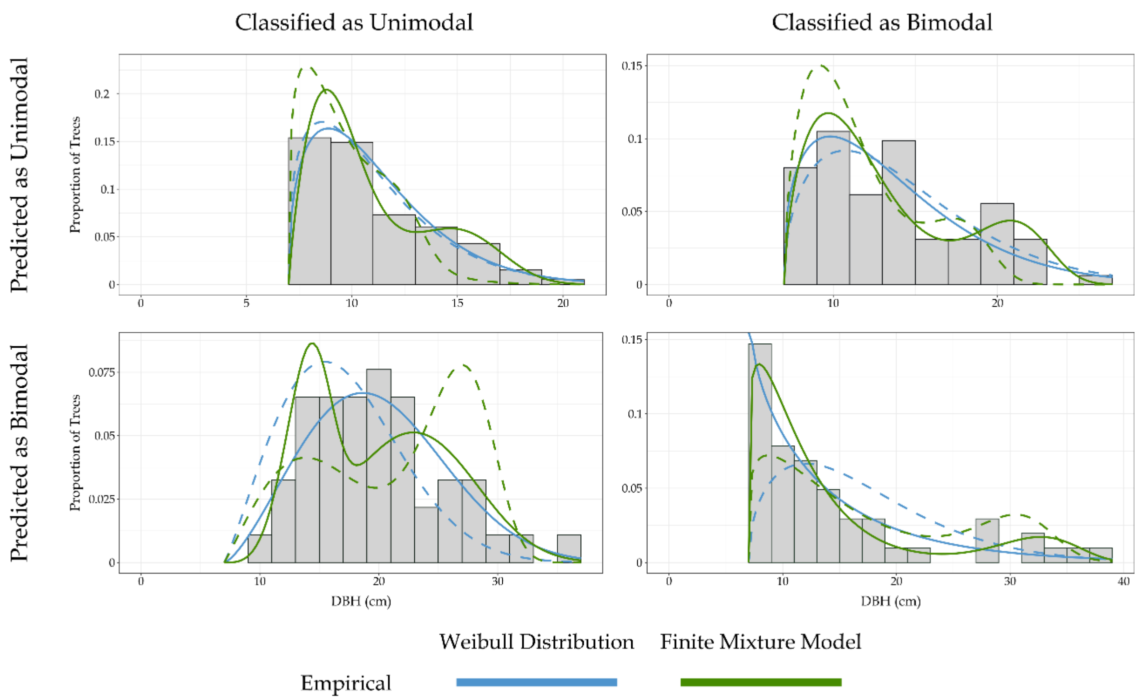

Figure 5.3 – Examples of measured and predicted curves following correct and incorrect differentiation on four plots.

5.4. – Discussion

5.4.1. – Differentiation of modality in stem size distributions

The fact that neighboring stands in the boreal mixedwood forest can have vastly different structures requires flexible and spatially detailed approaches to SSD estimation. Field campaigns to measure SSD across large, diverse, and often remote areas are not feasible given constraints on time and resources. In addition, a priori knowledge of an appropriate PDF to use for fitting the SSD would be valuable when operating in structurally diverse areas. The methodology outlined in this Chapter provides the ability to quickly and effectively characterize diverse forests over large spatial extents by providing detailed measures of the vertical distribution of vegetation over large areas using ALS data.

The ground-measured variables best able to differentiate bimodal distributions were those relating to tree sizes, such as SD_H and SD_{DBH}. This is consistent with estimating SSD, which represents the variation in tree DBH. If a stand has highly variable tree sizes, there will be a correspondingly large variance in DBHs and heights, likely reflecting in a multimodal SSD. Age variability and species mixtures provided less accurate differentiations, as maturing stand structure depends more on disturbance trends and ecological legacies than species or age differences (Franklin et al. 2002; Kane, McGaughey, Lutz, et al. 2010).

Likewise, the most accurate ALS predictions of plot characteristics came from those related to tree size. This was expected, as ALS metrics best characterize physical structure and have more difficulty in estimating intrinsic characteristics such as the age or species of a tree. While attributes such as the percent dominant species and the SD of ages can be used to classify bimodal plots at the ground level, they are not predicted very accurately with ALS, which limits their use at an operational capacity. The variance of ALS heights performed the best in classifying bimodal plots, and was chosen as the preferred determinant of modality in this Chapter. This metric is commonly calculated as part of the standard suite of ALS metrics generated from software packages such as LAStools (Isenburg 2014) and FUSION (McGaughey 2008). Consequently, it is easily generated, accessible, and readily interpretable as a heuristic for distinguishing modality. While alternative approaches to modality characterization could include logistic regression or other modeling techniques, the parsimony, consistency, and transferability of a single metric makes this approach more applicable in other study areas and research. Further work could investigate more detailed ALS-based stratification of the study area to appropriately model other forest characteristics in addition to SSD.

5.4.2. – Predictive modeling of SSD parameters using ALS metrics

The parameters of the Weibull and FMM distributions were predicted well using ALS-derived metrics. Thomas et al. (2008) predicted Weibull and FMM parameters using ALS in a similar study area and achieved similar or slightly more accurate results for parameter predictions. However, their study first stratified by species and structural groups and predictive models included up to 7 variables, whereas I used no more than 3 input variables in each model and did not stratify by species groups. Applying predictions across the landscape using the approach of Thomas et al. (2008) would require the availability of reliable species information at the same spatial resolution as the ALS data, which can be difficult or expensive to acquire. Likewise, the current capacity of ALS does not allow for accurate and spatially detailed species characterization, making stratification by species often not feasible.

The density of ALS data used in this Chapter was around the minimum required for regression using an area-based approach (generally around 1 pt/m^2; White, Wulder, Vastaranta, et al. 2013). However, a study by Cao et al. (2016) using multiple point densities determined that density did not significantly impact the prediction accuracy, suggesting that lower point density data may still successfully characterize forest structure when used in an area-based approach. The plots used in this study had an area of 400 m^2, which may be considered small when compared to those of other studies. However, Ruiz et al. (2014) found that larger plot sizes do not significantly increase the accuracy of models, but contributed to larger costs of measurement. Using the provincial network of 400 m^2 plots seemed to balance the need for large plots with the need for many plots over a large area and therefore was determined to be an appropriate size for this Chapter.

5.4.3. – Accuracy of predicted SSDs

The aforementioned discrepancies in prediction accuracy of SSD parameters likely compounded the errors of distributions fitted to ALS data. Thus, the mean EI_{ALS} value for bimodal plots was slightly higher than that for unimodal plots. However, the methodology used in this Chapter produced more accurate results in terms of both EI_G and EI_{ALS} than if all plots had been classified as unimodal. The difference in EI_{ALS} values was relatively low for predicted distributions and slightly higher for measured distributions; this suggests that the accuracy of a predicted SSD decreases with decreasing parameter prediction accuracy. Thomas et al. (2008) did not report EI values; however, a study by Tompalski et al. (2015) reported similar EI_{ALS} values to those reported herein when predicting SSD for unimodal distributions. Tompalski et al.

(2015) scaled EI values by 0.5 while I used 100 (Equation 3). When correcting for this difference in scale, my mean EI_{ALS} values were slightly more accurate than those reported by Tompalski et al. (2015), whose mean value was 71.6.

5.4.4. – Model application

Unless a stand is small or completely homogeneous, a single plot-level SSD will likely not be representative of SSD for the stand (Borders, Wang, and Zhao 2008). Therefore, techniques for aggregation of predictions from cell-level SSD are necessary to generate a stand-level SSD. One such approach involves summing predicted SSDs from each grid cell composing a delineated stand (Siipilehto et al. 2016). More complex approaches involve multidimensional scaling (Magnussen and Renaud 2016), in which an estimator can be used for extrapolation to larger units, or segmenting areas into smaller units such as microstands, which are areas grouped by similar ALS-predicted attributes such as volume and height (Lundholm 2018). If stand-level predictions are the desired result, a final aggregation step should be used to scale up from cell-level predictions; however, this was beyond the scope of the Chapter and SSD predictions remained at the cell level.

Chapter 6 – Structural development following stand-replacing disturbance in a boreal mixedwood forest

6.1. – Introduction

The structure of a forest stand can be used to directly characterize the state of the forest at a given point in time, but it also represents a key tool to understanding past, present, and future stand dynamics. Although dependent on localized factors such as disturbance, stand structures change relatively predictably with increasing time since disturbance (Enquist and Niklas 2001). Based on a review of studies in the boreal mixedwood forest, Chen and Popadiouk (2002) define four main structural phases, which include (with increasing structural complexity): stand initiation, stem exclusion, canopy transition, and gap dynamics. Understanding the structural differences between these phases and the resulting ecological implications is critical for a variety of applications. For example, stand structure is helpful in understanding future biomass accumulation (Brown, Schroeder, and Birdsey 1997) and identifying areas of old growth which provide valuable services such as harboring biodiversity (Lindenmayer and Franklin 2002) and improving water quality (Wirth 2009). Furthermore, knowing the general structures of existing forests helps to predict what structures might be present under future climate scenarios (Toledo et al. 2013).

Passive, optical, remotely sensed imagery can provide useful insights on the return of vegetation following disturbance (Griffiths et al. 2014; Hansen et al. 2013; Kennedy et al. 2012). Spectral recovery refers to the identification of relevant image-based metrics that characterize the spectral return of vegetation and forest post-disturbance (Broadbent et al. 2006; Chu and Guo 2013; Frolking et al. 2009). Linkages between spectral measures of recovery derived from remotely sensed data and measures of forest structure and composition derived from ALS (White et al. 2018) and field plots (White et al. 2019) are nascent. Depending on the information need, measures of forest recovery can be structural, compositional, or functional. ALS has been used to classify areas based on the structural complexity of stands (Kane, McGaughey, Lutz, et al. 2010); however, study of post-disturbance forest structure across species and disturbance types has been limited. Whereas the fine spatial and temporal resolutions of Landsat time series are critical in studying spectral recovery trends (Pickell et al. 2015; White et al. 2017), ALS's ability to provide detailed three-dimensional metrics makes it a key tool for the study of structural recovery following disturbance (White et al. 2018). For example, Bolton et al. (2015) used ALS metrics as a means of determining changes in forest structure in the first 25 years following fire in the boreal forest of Canada. However, spatially extensive studies such as this typically use only individual metrics and not more detailed indicators of forest structure such as SSDs.

There are a variety of different ways to quantify a forest's response to disturbance. As forest stands develop following a stand-replacing disturbance, attributes such as aboveground biomass and species richness may reach values comparable to late seral stands in as few as 30 years for tropical forests (Letcher and Chazdon 2009). Depending on the disturbance regime and stand conditions, however, a boreal stand may take a few hundred years to reach its pre-disturbance SSD. Despite this, SSDs are an information-rich asset to determining or quantifying structural phases. For example, Zenner (2005) used a > 400–year chronosequence of SSDs to model structural development in Douglas-fir forests. Furthermore, SSDs have been used to understand mechanisms underlying structural changes. Toledo, Magnusson, and Castilho (2013) studied the abiotic factors which change tropical forest SSDs and determined that smaller trees (≤ 22 cm DBH) were more susceptible to competition-based disturbance, while exogenous disturbances and senescence primarily affected larger stems ($\geq$ 45 cm DBH). Despite knowledge of the mechanisms of change and the general dynamics of SSDs, more research is needed to examine how developing SSDs differ between and within both species groups and disturbance types. Doing so can further ecological understanding of the expected developmental pathways across these attributes.

In this analysis, ALS-derived SSDs are used to characterize the patterns of structural development across species and disturbance type in a boreal mixedwood forest. Using these SSDs and photo-interpreted stand polygons of similar species, age, and disturbance, a chronosequence representing over 50 years of forest structural development was developed to determine the patterns of structural development following stand-replacing disturbances.

First, I will investigate the differences in structural development phases based on the type of disturbance. Although having initially different rates of regeneration, harvested and burned stands are thought to eventually reach the same structure (Brassard and Chen 2010). However, the pathways that both disturbances take to this eventual structure are not well known. Stands regenerating after fires are understood to generally have more rapid rates of initial growth and structural development, but quantification of structural development is limited (Bartels et al. 2016). An enhanced understanding of structural development following fire could enable insights on disturbance legacies resulting from different disturbance types.

Next, development will be characterized by species. There are a variety of possible structural pathways that a stand could take following disturbance, depending on qualities such as the pre-fire composition or productivity (Bergeron et al. 2014; Taylor and Chen 2011). Time since disturbance alone is not sufficient to predict structure, as stand development is known to be a nonlinear process (Kane, McGaughey, Lutz, et al. 2010; Taylor and Chen 2011). Stands with a high compositional diversity, such as those in the boreal mixedwood, will have different growth patterns than pure stands due to interspecific competition for resources (del Río et al. 2016). A species-level understanding of the initial structural pathways of these stands following disturbance will help to inform their management and understand their development, particularly under future climate scenarios.

Finally, structural development will be characterized by both species and the disturbance type. Structural gains from species-specific adaptations to post-fire establishment and growth in the boreal forest, such as cone serotiny in lodgepole pine (*Pinus contorta*) or root suckering in aspen (*Populus tremuloides*), have been previously studied (Bergeron et al. 2014). However, an understanding of differences in species-level regeneration is needed to determine how dynamics differ between stands originating from fire and from harvest. While knowledge of stand structural dynamics in the boreal forest is well-documented (Angelstam and Kuuluvainen 2004; Bergeron et al. 2014; Oliver 1981), there has been limited work in quantifying development with broad-scale and detailed data such as an SSD.

In addressing these questions, I aim to characterize SSDs for different species and disturbance types at three different structural phases in order to better understand structural development from stand-replacing disturbances in the boreal mixedwood forest.

6.2. Methods

6.2.1. – Workflow

Wall-to-wall diameter distributions produced in Chapter 5 were initially summarized for all delineated stand polygons. Then, based on the mean SSD for each stand, stands were clustered into structural development phases based on species and disturbance. Finally, stands in each cluster were summarized using generalized additive models (Figure 6.1).

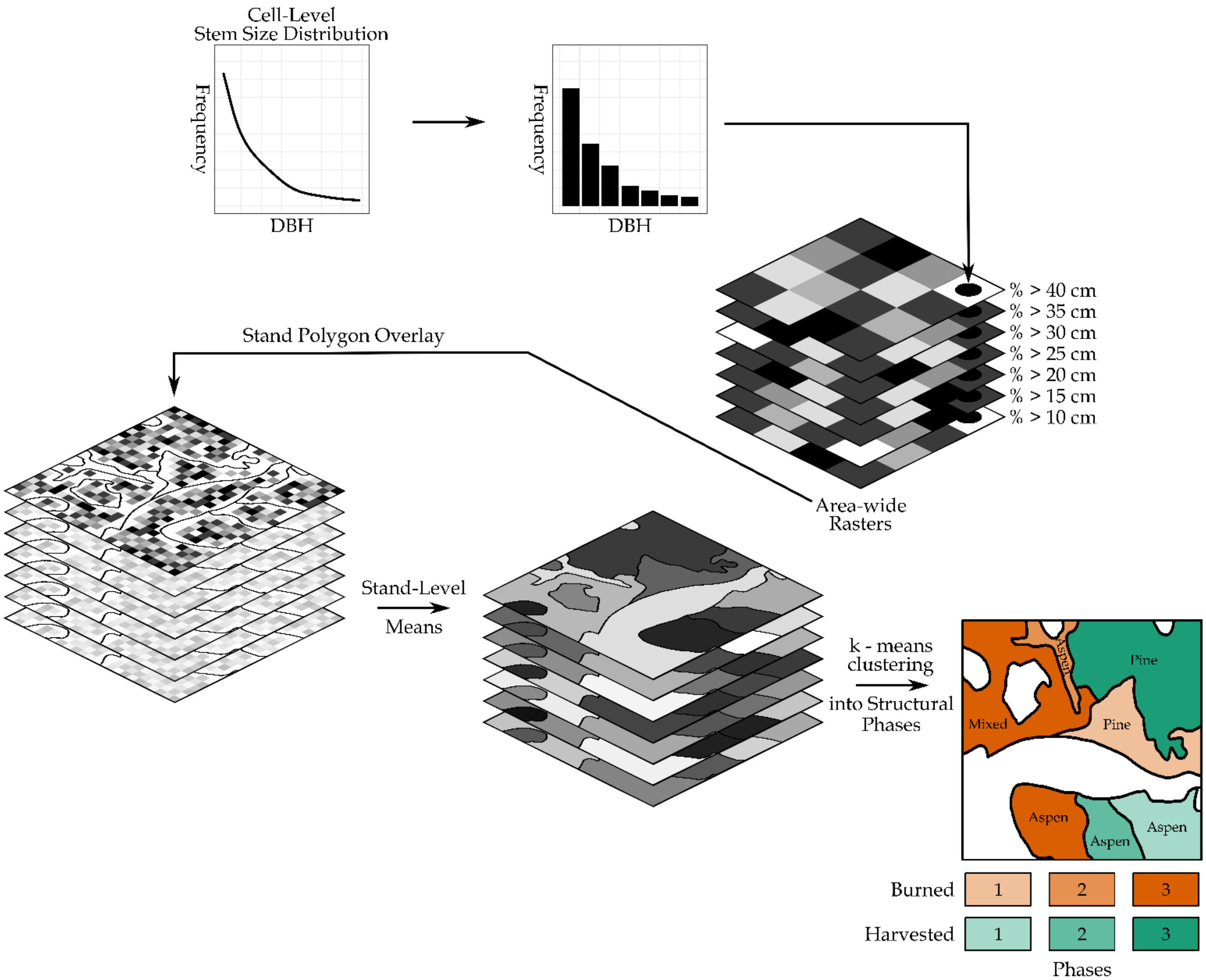

Figure 6.1 – A workflow detailing the structural classification approach. "Stand-Level Means" refers to the averaging of SSD cell values for each raster for each individual stand polygon.

6.2.2. – Alberta vegetation inventory (AVI) data

The stand polygons used were a part of the AVI and were photo-interpreted by professional interpreters based on 1:60,000 or 1:40,000 air photos (Government of Alberta 2005). To distinguish stand-level disturbances, only stands with a single, stand-replacing disturbance were used. This resulted in 7,087 stands being used for analysis – 6,180 disturbed by fire and 907 disturbed by harvesting. Although photo-interpretation may only be able to directly identify the species of upper canopy vegetation (Wulder and Franklin 2003), this was deemed to be suitable for this study as the young stands used for analysis would likely have limited, if any, understory vegetation of significance. AVI polygons have an estimate of stand age, but there may be difficulties in correctly estimating stand age, especially for complex stands. Additionally, stand structure does not linearly develop in relation to the time since disturbance, as stands may reach different structural phases at far different times, dependent upon the different successional pathways present for each stand. For these reasons, the time since disturbance was not considered for this study.

6.2.3. – Stem size distributions

This Chapter uses SSD models developed in Chapter 5. The derived models were applied across the entire study area, giving each 20 x 20-meter grid cell an estimate of SSD parameters. Only forested areas – those meeting the common definition of at least 10% canopy cover (FAO 2005) – were included in the predictions by removing cells whose percentage of ALS first returns over 2 m was less than 10% (similar to Bolton et al. 2018). For each cell with SSD parameters, the proportion of trees within bins of 5 cm increments were calculated (similar to Zenner 2005). This meant that, regardless of the modality, each cell had a comparable set of values representing the proportion of stems greater than the lower bound of each size class (10, 15, 20, 25, 30, 35, and 40 cm). In order to mitigate any effect from neighboring stands, cells within 20 m (the size of a single cell) of a stand border were removed. For each disturbed polygon, the mean of these proportions were used to represent the mean SSD of the stand (Figure 6.2).

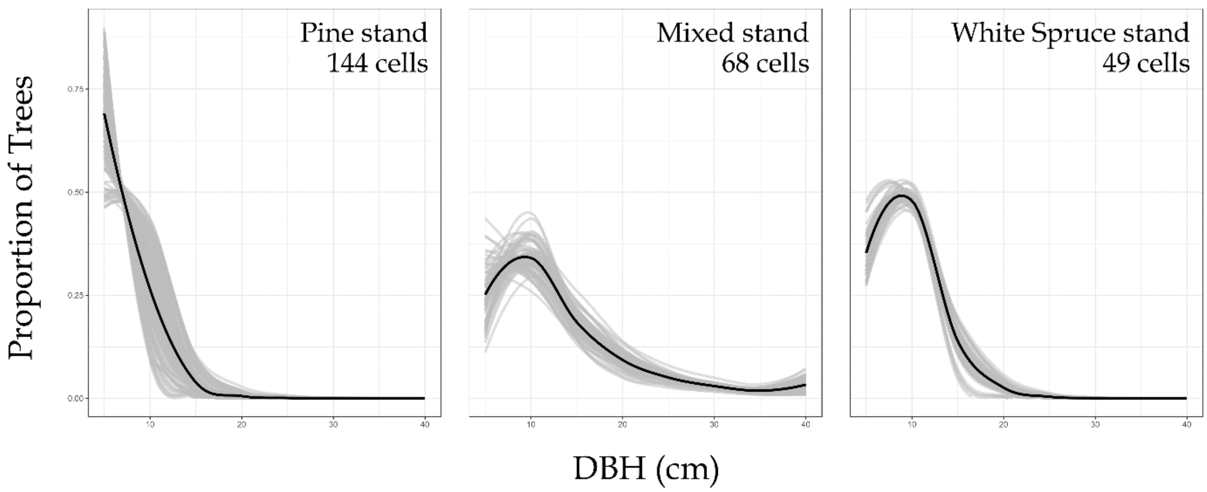

Figure 6.2 – Three examples of summarizing the individual SSDs in a stand into one representative curve

6.2.4. – Chronosequence of forest stands disturbed by wildfire and harvest

Species proportions in AVI polygons were used to assign species groups to each stand. If a species was estimated to represent at least 80% of trees in that stand, it was assigned to one of four species groups according to provincial classifications, listed in Table 6.1 (Huang, Meng, and Yang 2009). If no species formed at least 80% of the stand, then the stand was added to a fifth "mixed" group (Smith 1996). The number of stands by species and disturbance type is shown in Table 6.2.

Table 6.1 - Species and their resulting groups occurring as dominant within AVI polygons

Species	Group
balsam poplar (*Populus balsimifera*) trembling aspen (*Populus tremuloides*) paper birch (*Betula papyrifera*)	aspen
black spruce (*Picea mariana*)	black spruce
lodgepole pine (*Pinus contorta*)	pine
balsam fir (*Abies lasiocarpa*) white spruce (*Picea glauca*)	white spruce

Table 6.2 – Number of stands by species and disturbance type.

	Aspen	Black	Mixed	Pine	White	Total
Burned	1,814	986	1,817	1,307	256	6,180
Harvested	320	9	222	268	88	907
Total	2,134	995	2,039	1,575	344	7,087

6.2.5. – Identifying structural phases

To understand differences in structure across the study area, each stand was clustered into distinct phases of structural development based on the species, disturbance type, and SSD proportions outlined in Section 6.2.3. Of the four structural phases named by Chen and Popadiouk (2002), only the first three (stand initiation, stem exclusion, canopy transition) would be expected given the 50-year chronosequence. While approximately 50 years could correspond to the early stages of the canopy transition phase in shade tolerant and mixed-species stands, pure stands of shade intolerant species such as aspen and pine may not have had sufficient time to reach this phase. However, SSDs of aspen and pine stands in a third phase of development could still be different from those in the stem exclusion phase. Therefore, SSDs were grouped based on a k-means clustering approach with *k* equal to 3 clusters and limited to a minimum of 10 stands in each cluster. It was determined that using three clusters for the dataset instead of another value highlighted the differences between structural phases while minimizing the variation within each cluster. Clusters were sorted in terms of increasing structural development (e.g. fewer small stems and more large stems) and named “Phase 1”, “Phase 2”, and “Phase 3”, which approximated to the three structural phases outlined above. Clustering was based on the SSDs for each combination of species and disturbance type. In other words, stands were first separated by species and disturbance type and then clustered based on the SSDs in each stand. For example, there were 3 phases each for harvested aspen, burned aspen, harvested pine, burned pine, etc. In total, this resulted in 30 phases – 3 structural development phases for each of 5 species groups and 2 disturbance types. The result was a dataset that had, for each disturbed stand polygon, attributes of the species group, disturbance type, structural development phase, and SSD proportions.

6.2.6. – Summary with generalized additive mixed models

Generalized Additive Mixed Models (GAMMs) were used to model SSDs and their variation for each species and disturbance type. GAMMS were chosen to model nonlinear trends between multiple variables (here, SSD proportions) while also accounting for over-dispersion in data which was often highly variable within species or disturbance groupings. GAMMs use cubic regression splines to estimate nonlinear relationships between the explanatory and response variables (Wood 2017), and have been used to model nonlinear trends in fields such as movement ecology (Rickbeil et al. 2017) and photogrammetric error modeling (Goodbody, Coops, Hermosilla, Tompalski, and Pelletier 2018). SSD proportions by species or disturbance were related to the SSD proportions using negative binomial GAMMs in order to model the distribution of SSD values within each structural phase (Zuur et al. 2009). GAMM predictions and their standard error were used to assess significance between species groups and disturbance types. For all curves, 95% confidence intervals were constructed around the predicted value. If two or more confidence intervals did not overlap on an SSD for a given diameter, the curves were characterized as being significantly distinct from one another at this diameter. All analysis was carried out in R using the “mgcv” package (R Core Team 2018; Wood 2001).

6.3. Results

6.3.1. – Wall-to-wall SSD predictions

The variance of ALS return heights identified approximately 30.43% of forested cells in the study area to be bimodal, which corresponded well with the proportion of bimodal sample plots used in the analysis (32.39%; Table 6.3). Stand boundaries generally followed homogenous areas of modality (Figure 6.3c), but developing stands were typically heterogeneous in terms of their modality (Figure 6.3a and 6.3b).

Table 6.3 – Counts of areas determined unimodal and bimodal in sample plots and those predicted by ALS

	Unimodal	Bimodal	Total
Sample Plots	48 (67.61%)	23 (32.39%)	71
Wall-to-Wall Cells	10,222,949 (69.57%)	4,473,115 (30.43%)	14,696,069

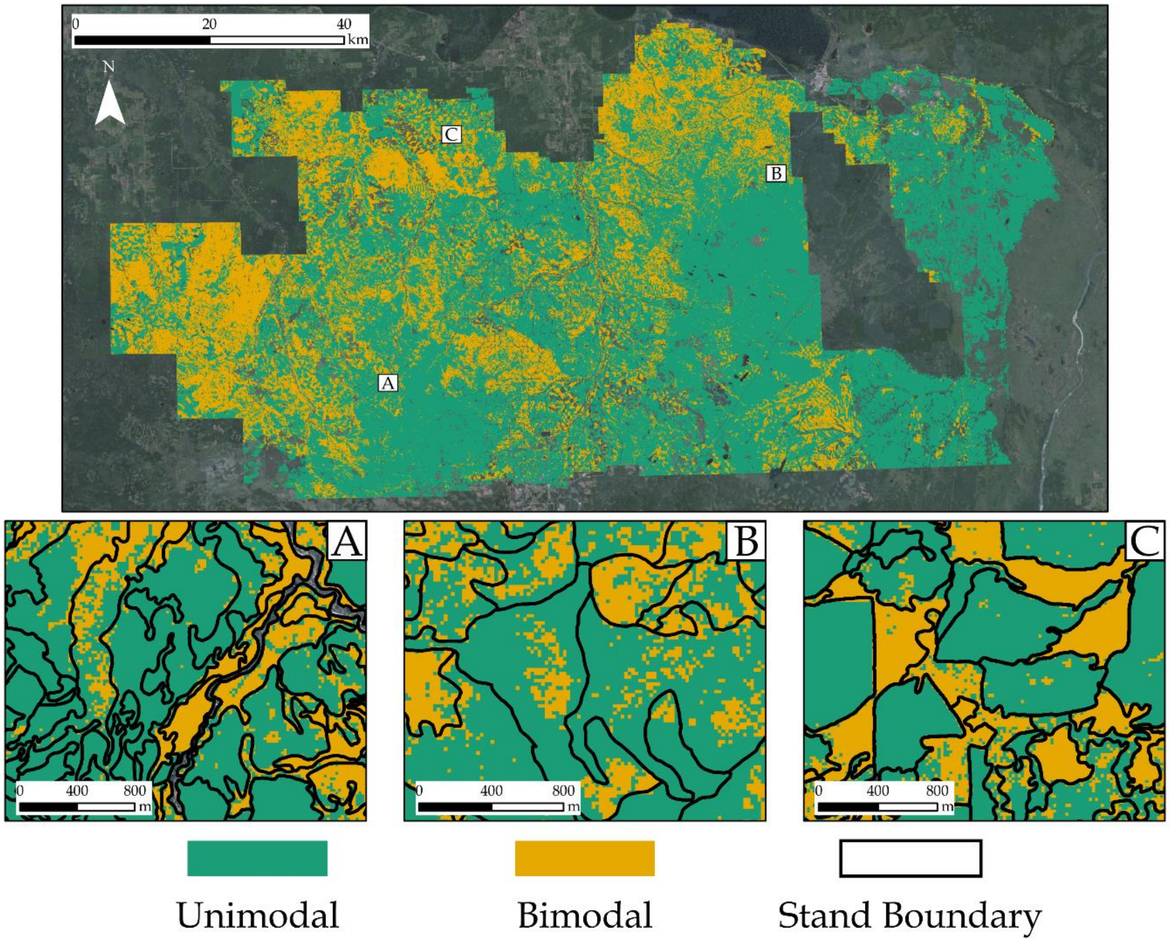

Figure 6.3 – Map outlining cells predicted to be unimodal or bimodal, and their position in the study area and within stand boundaries.

For the entire study area, GAMMs were used to summarize the SSDs of all stands belonging to each species group (Figure 6.4). Stands in the aspen and pine groups had slightly fewer small stems (less than 10 cm DBH), while those in the mixed and black spruce groups had slightly more stems in this size class. However, none of the differences among different species groups were significant. Furthermore, for much of the modeled SSDs, GAMMs of all species groups showed almost no difference.

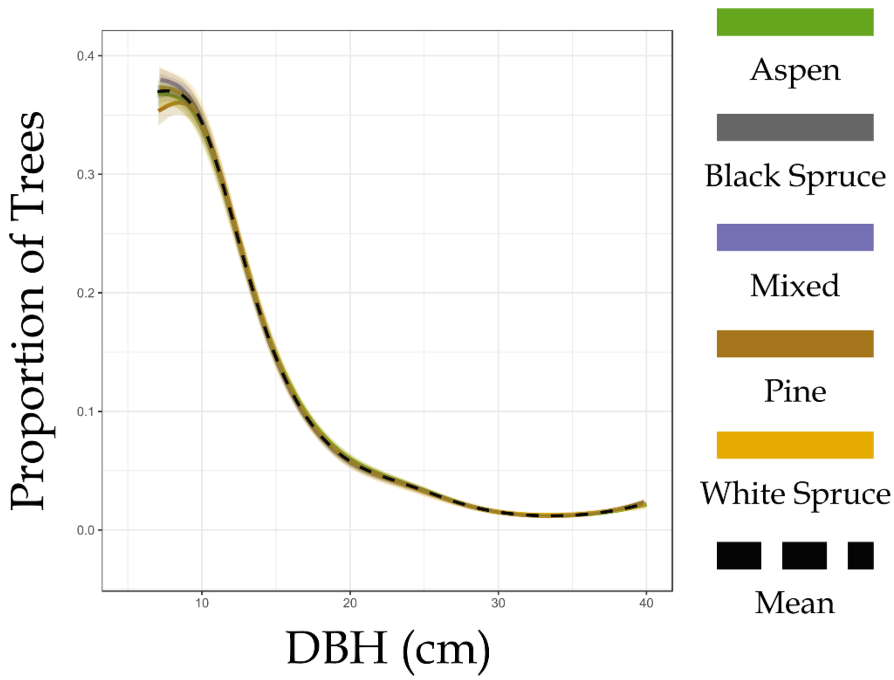

Figure 6.4 – Stem size distribution estimates for all cells in the study area, summarized with GAMMS by species. Colored lines represent the means by species, and the dashed black line represents the global mean. Shading indicates a 95% confidence interval.

6.3.2. – Overall structural development phases

Cell-level SSD predictions were then summarized into stands and clustered into structural development phases based on species and disturbance type (Table 6.4). Phases were sorted based on increasing structural development (fewer small stems and more large stems). For most species and disturbance types, the highest proportion of stands fell within Phase 2. The only exception was harvested stands in the black spruce group. The low sample size (n = 9) for this group was determined to be insufficient for comparison with the other groups and it was therefore removed from further analysis.

*Table 6.4 – Counts of the number of stands in each Phase. *Due to a low sample size, harvested black spruce stands were removed from further analysis*

	Phase 1		Phase 2		Phase 3	
	Burned	Harvested	Burned	Harvested	Burned	Harvested
Aspen	510	109	714	143	590	68
Black Spruce	378	4*	500	2*	108	3*
Mixed	560	102	886	110	371	10
Pine	530	64	567	109	210	95
White Spruce	58	24	134	54	64	10

GAMMS were constructed to compare burned and harvested stands within each structural phase (Figure 6.5). The SSDs of Phase 1 for both disturbance types were similar to one another and showed no significant difference. In Phase 2, burned stands had slightly more trees in larger diameter classes (up to ~ 25 cm), but these differences were not significant. However, Phase 3 burned stands showed an SSD with significantly fewer trees from approximately 7 – 9 cm DBH and more trees from approximately 14 – 23 cm DBH than harvested stands.

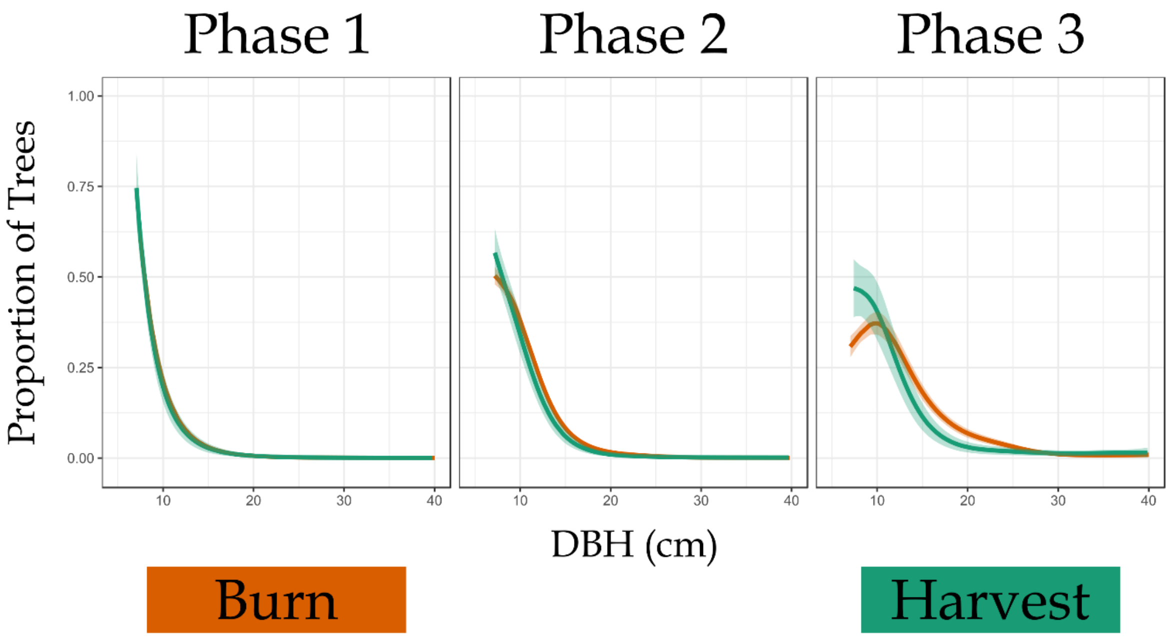

Figure 6.5 – SSD for overall structural development phases by disturbance type. Shading indicates a 95% confidence interval around GAMM estimates (solid line), with significant differences in SSD as non-overlapping confidence intervals. Phases represent general structural pathways of development, similar to stand initiation, stem exclusion, and canopy transition.

6.3.3. - Structural development phases following disturbance

Structural phases for both disturbance types were generally the same among the different species groups (Figure 6.6). The only exception was burned stands in the black spruce group, which showed significantly fewer stems in lower diameter classes in Phase 1. However, there were no significant differences between the SSDs of species for the other phases. The variability in SSDs for each phase, shown by the 95% confidence interval (shaded areas in Figure 6.6) increased as the phases increased in development. Additionally, harvested stands generally had more variability in the SSDs for each phase.

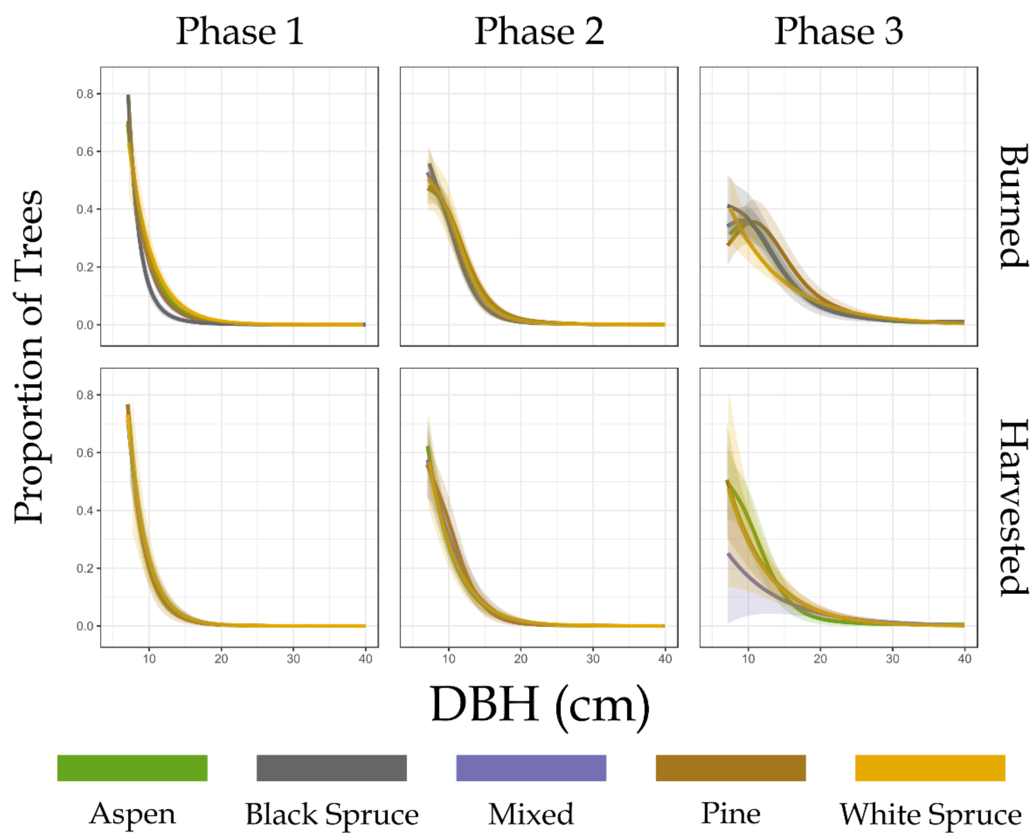

Figure 6.6 – Stands clustered on structural development phases within species and disturbance types. Harvested black spruce stands had insufficient sample size for analysis (n = 9) and are not shown. Shading represents a 95% confidence interval around each GAMM prediction.

6.3.4. – Species-level responses to disturbance

Similar trends in SSDs for each structural phase were seen in aspen and pine dominated stands (Figure 6.7). For both species groups, there was no difference in SSDs of burned and harvested stands for Phase 1. Phase 2 showed slight but significant differences between disturbance types for some diameter classes – significantly more trees in burned stands for approximately 11 – 13 cm and 10 – 13 cm DBH for aspen and pine stands, respectively. The greatest differences between the SSDs of the disturbance types was seen in Phase 3 for both species, where both aspen and pine stands had significantly fewer trees in small diameter classes (~ 7 – 9 cm), and pine stands also had significantly more trees in the ~ 14 – 22 cm DBH classes.

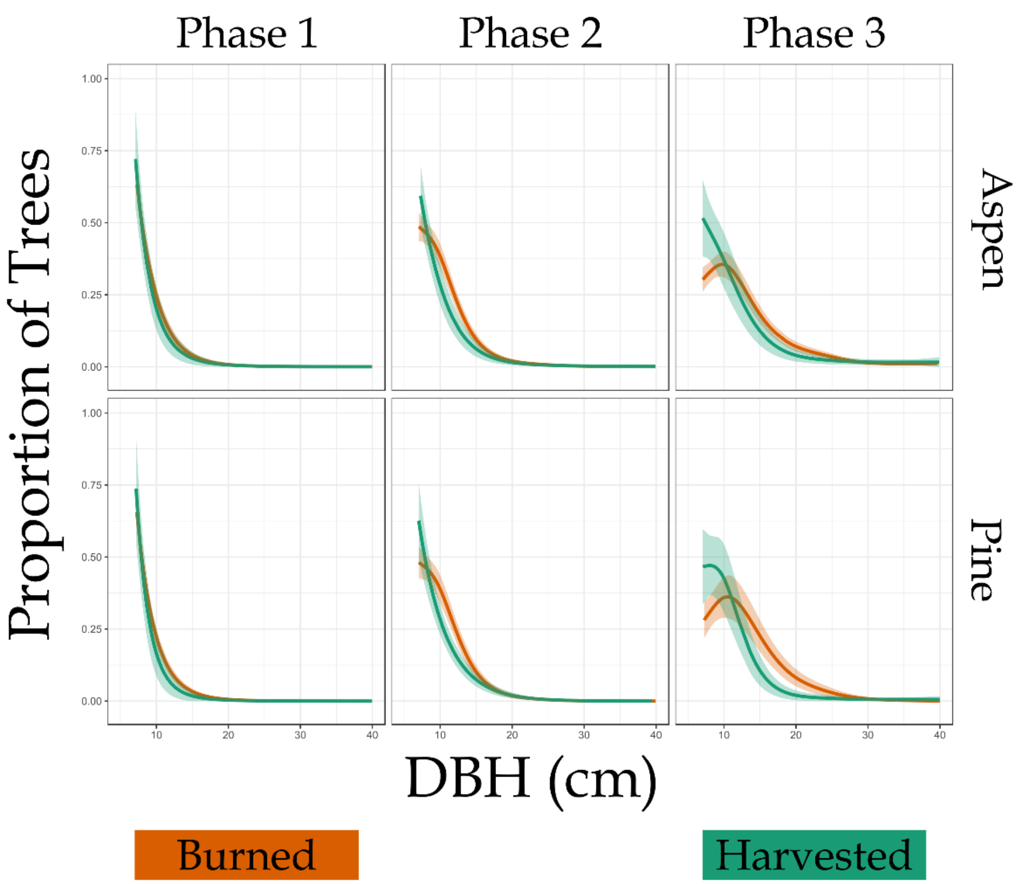

Figure 6.7 – Differences between structural clusters for aspen and pine stands following disturbance. Shading represents a 95% confidence interval around each GAMM prediction.

The mixed and white spruce species groups had similar SSDs for each structural phase and disturbance type (Figure 6.8). In fact, for both species types, there were no significant differences between burned and harvested SSDs in all phases for all diameter classes. In some cases, SSDs of burned and harvested stands showed slight differences – for example from 10 –

15 cm DBH in Phase 2 for both mixed and white spruce stands – but these differences were not significant. Additionally, the highest variances seen in any phase for all species groups occurred in Phase 3 for both harvested mixed and white spruce stands.

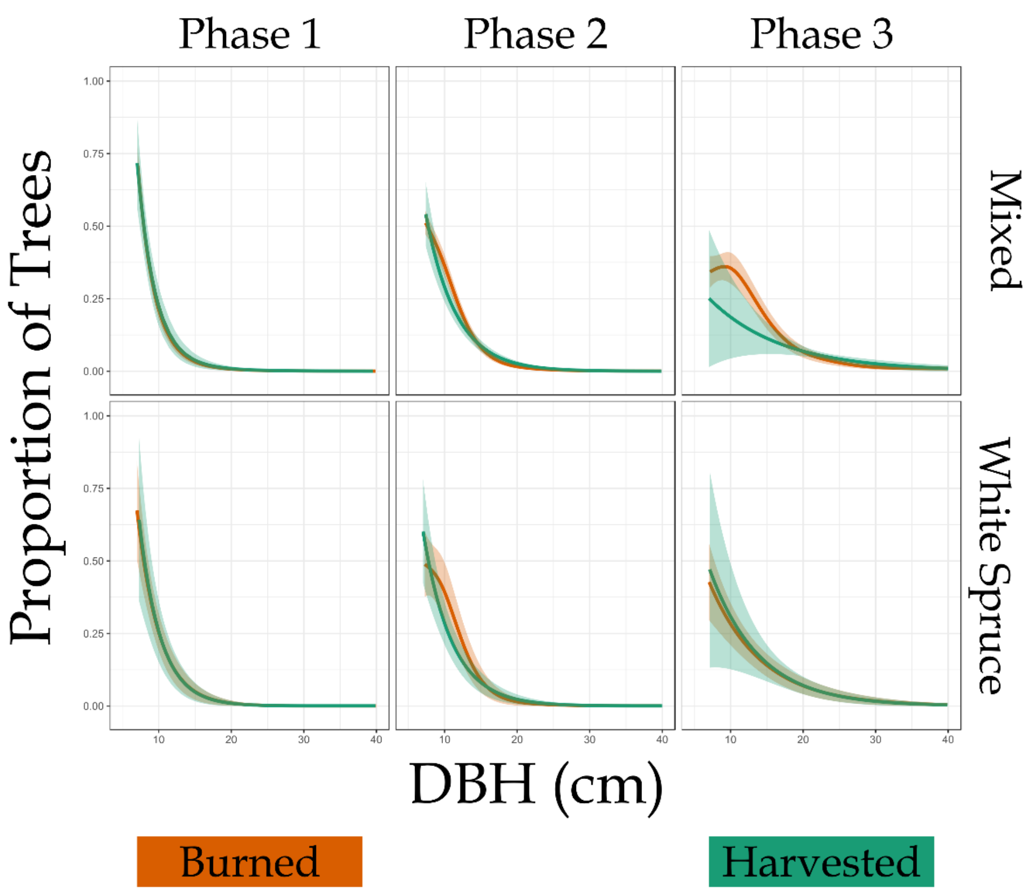

Figure 6.8 – Differences between structural phases for mixed and white spruce stands following disturbance.

6.4. – Discussion

6.4.1. – Wall-to-wall SSD predictions

SSD parameters were predicted using an area-based approach in order to provide estimates of SSD for all forested cells. SSD curves, separated by species, were not significantly different from one another (Figure 6.4). The most difference (although not significant at α = 0.05) was for the proportions of trees in the smallest DBH class (7-10 cm). Stands in the pine and aspen groups had slightly lower proportions of trees in this class, while stands in the mixed and black spruce groups had slightly higher proportions. This may be due to different growth rates. For example, pine and aspen stands are primarily comprised of shade intolerant trees with fast initial growth rates, while black spruce stands are comparatively slower growing (Bergeron et al. 2014; Chen and Popadiouk 2002). On the other hand, inter-specific competition in mixed species stands is known to significantly alter growth rates of trees compared to pure stands, which may be a reason for the mixed group having higher proportions in the smallest DBH class (Brassard and Chen 2010; del Río et al. 2016).

Any errors in the predictive models for SSD parameters would have been passed along to the area-wide SSD estimates. However, an ALS-derived area-based approach is the principal method for area-wide SSD estimation, and was therefore seen to be the best approach to use in this study (Maltamo et al. 2007; Xu et al. 2014). Two averaging steps (cells into stands and stands into phases) were taken to reduce the effect that any error may have on conclusions from the analysis. Conversely, the opposite may have also occurred – that is, over-generalization of the variation in the SSD curves. However, confidence intervals from the GAMMS in the analysis were useful in assessing both inter-phase differences and intra-phase variability of the SSDs. Lastly, the focus of this study was to compare the shapes of predicted SSDs to one another, and not necessarily to construct highly accurate SSD models. Therefore, if there was a prediction error, it would likely be found in all curves and any comparisons between curves would still be valid. There was no significant bias in either the parameter predictions or the estimates of proportions in each DBH class, confirming the use of the SSD models as developed in Chapter 5 for this research.

6.4.2. – Structural development phases

My results showed that there was no significant difference between SSDs of burned and harvested stands for Phase 1 or Phase 2. However, burned stands had significantly more large trees and significantly fewer small trees than harvested stands in Phase 3. This indicates that there may be more structural development within the chronosequence for burned stands, or that there are conditions which give burned stands different pathways to future development (Brassard and Chen 2010). For example, there is generally more residual vertical structure in stands following a fire than following a harvest, which could provide seed, nutrients, or an older age cohort to encourage structural development in these stands (Brassard and Chen 2010). A key influence on future structure and growth of naturally regenerating stands is initial stand development, which could be described with attributes such as stand density and composition. For example, the findings of Johnstone et al. (2004) showed that patterns of stand structure initiated within a few years after fire are maintained through subsequent decades of stand development.

6.4.3. – Structural development phases by disturbance type

All species groups had similar SSDs across all structural phases for both disturbance types (Figure 6.6). The only significant differences between curves were for stands in the black spruce group, which had fewer trees in the smaller diameter classes than the other species groups in Phase 1. This may be due to the relatively slower growth rate of black spruce, as trees of this species may not have had sufficient time during the chronosequence (~ 50 years) to develop a more heterogeneous structure (Chen and Popadiouk 2002). Species groups showed similar SSDs for the all structural phases. In other words, the SSD of a stand in the stem exclusion phase following a fire will look generally the same regardless of the species present. Stands take different amounts of time to reach certain structural phases depending on factors such as productivity (Bergeron et al. 2014). However, from the perspective of the SSD, all species had the same general structures in each phase of stand development.

Phase 3 in burned and harvested stands had the highest intra-phase variability for all phases (Figure 6.6). Phase 3 often had the smallest sample for each species (Table 6.4), so it is possible that Phase 3 was the most variable and, as such, SSD curves in this cluster could have been more variable than in clusters with larger and more homogeneous samples. Additionally, intra-phase variability increased with increasing structural development (Figure 6.6). A variety of successional pathways dependent on external factors may lead stands to a specific development phase (Taylor and Chen 2011), meaning that there may be a variety of shapes to an SSD depending on, for example, smaller disturbance sizes (Coomes et al. 2003).

For both disturbance types, stands in the white spruce group had more trees in the smaller diameter classes, possibly as a result of the slow growth rate in this group compared to that of the others (Chen and Popadiouk 2002). In harvested stands, the mixed group had significantly more structural development than the other species groups. Heterogeneous stands contain trees with different growth rates, patterns of regeneration, and levels of shade tolerance (Chen and Popadiouk 2002), leading to a higher likelihood of achieving a more complex structure (Taylor and Chen 2011).

6.4.4. – Structural development phases within species groups

Stands in the aspen and pine groups showed similar patterns of development between disturbance types (Figure 6.7). Both species groups showed initial structural similarity between burned and harvested stands (Phase 1), but more structural development in burned stands in Phases 2 and 3. Fast-growing and fire-adapted species such as these (e.g. root suckering in aspen and cone serotiny in lodgepole pine) have a more developed structure following fires than following harvesting (Bergeron et al. 2014; Frey et al. 2003). Additionally, the high shade intolerance of aspen means that trees of this species will be among the quickest to display initial structure because of their capacity for rapid initial establishment after disturbance (Bergeron et al. 2014). Also, burned stands typically have higher initial stem densities, leading to more self-thinning and stem exclusion and therefore a quicker reduction in the proportion of trees in smaller diameter classes than in harvested stands.

It is possible that pure stands of shade-intolerant species may not have secondary cohorts of regenerating trees, meaning that there will be lower proportions of smaller trees in later development phases. This is seen in Phase 3 of Figure 6.7 as there being comparatively fewer trees in the smallest diameter classes than the initial cohort of regenerating trees. Conversely, the white spruce and mixed groups did not have this decrease in the proportion of small trees in Phase 3, as the presence of shade tolerant species meant that a secondary cohort of trees could establish. This phenomenon is seen in Figure 6.8 as there being higher proportions of smaller trees in Phase 3 of the white spruce and mixed species groups.

The mixed species and white spruce groups also showed similar patterns of structural development to one another (Figure 6.8). These species groups differed from stands in the aspen and pine groups in that burned and harvested stands had very similar SSDs for Phases 1 and 2.

One reason for the mixed group showing such similarities would be the variety of possible species compositions present in this group. This variety would lead to a corresponding variety of growth rates and different post-disturbance adaptation strategies. Thus, the patterns of structural development may resemble one another, as the initial regeneration would follow similar patterns of growth and competition (Taylor and Chen 2011). Additionally, shade tolerance and slow growth rates of species in the white spruce group mean that these stands would have similar structural development to one another (Phases 1 and 2), as they may not have had time during these earlier phases to develop heterogeneous structures (Chen and Popadiouk 2002).

Chapter 7 - Three-dimensional remote sensing for augmentation of next-generation forest inventories

7.1. – Context of dissertation

The accuracies attained in Chapter 3 indicate the potential for DTP for supporting forest inventories. National Forest Inventories (NFIs) have typical accuracy requirements of 0–2 cm for DBH, 10–20% for volume, and 1-3 cm for upper stem diameters (Liang et al. 2016). Each of these accuracy requirements was met using DTP point clouds techniques in this Chapter. Other potential applications of raw images and resulting point clouds include the estimation of canopy leaf area (Bréda 2003) or as inputs to centroid sampling of tree volume (Wiant, Wood, and Gregoire 1992). Additionally, point clouds provide measurements which can be stored as an objective, 3D record of tree or forest condition at a given point in time. This indicates the potential for use of DTP in calibrating or validating models of forest growth. If images of the same tree are acquired at multiple times, a time series of point clouds could be generated and analyzed to monitor tree growth or change either at an individual tree or at stand level (Liang et al. 2012; Sheppard et al. 2016).

Across all sample plots, results from Chapter 4 showed a wide range of accuracies which may influence the applications of the work. For example, performing the methods presented in this Chapter in a high-value timber stand to achieve a low accuracy of detection and DBH estimation may not have substantial value to forest managers. In this example, however, timber value is often positively correlated with tree size, and results from this Chapter showed higher accuracies on large trees (Figure 4) and plots with larger mean DBH values (Figure 5). The patterns of accuracy seen in this Chapter can also be used to leverage expectations of accuracies in future work. Other value in the work could come with the objectivity and permanence of raw images and resulting point clouds, having inherent value for forest inventory applications by providing a potential for assessment of plot attributes not typically measured during a forest inventory (e.g., understory condition, stem form) and can be stored for retrospective analysis.

The difference in structures among stands requires detailed, landscape-level information to guide the fitting and modeling process. In order to meet the scope and detail needed for accurate forest management decisions, Chapter 5 used ALS as a means of differentiating and predicting SSD parameters in a boreal mixedwood forest. The differentiation step allowed me to fit structurally appropriate SSDs to respective stands and allowed for more robust characterizations of SSD than using a single model for the entire study area. The structural heterogeneity of the boreal mixedwood may have led to lower parameter prediction accuracies and error index values in this Chapter when compared to those of other studies (Packalen and Maltamo 2008; Tompalski et al. 2015). However, differentiating bimodal areas and their subsequent characterization by FMMs should provide insights into stand characteristics that would lead to more informed decisions and more accurate understanding of stand structure in complex forest types.

Chapter 6 demonstrated the ability of wall-to-wall, ALS-derived SSDs to capture differences in structural development following stand-replacing disturbance. Understanding forest structural development is critical to interpreting past changes and predicting future conditions. For example, this knowledge can be used by forest managers to prescribe silvicultural treatments under ecosystem-based management techniques. These techniques aim to mimic natural stand dynamics using management interventions such as thinning or prescribed burns. Therefore, they rely on detailed knowledge of the development of natural stands under post-fire scenarios. This work could also be used as a benchmark as the patterns of development following a disturbance under current ecological conditions for comparison to past or future patterns of development.

7.2. – Forest inventories – current status and challenges

Regardless of the level of application, forest inventories have basic data acquisition requirements (based on recommendations for Canada; Gillis 2001). First, inventories need to be representative; that is, to provide a detailed and complete or near-complete perspective of the forest. With increasing economic and ecological pressures on forest managers, the need for enhancing the capacity of forest information is also increasing (Smith 2002). Inventories also need to be consistent (McRoberts et al. 2005). For example, managers operating in heterogeneous forests or across large extents need to know that the data were collected using methods that are reliable and unbiased across all sites. When considering inventories across large spatial extents, this is especially important, as inventory measurements across a range of forest types, stand conditions, and acquisition methods will likely increase the disparity of data acquisition. Next, the data needs to be timely, representing a detailed snapshot of the forest at a given point in time and put into a database which can be used for future monitoring (Gillis 2001). The timeliness of the inventory demonstrates the temporal reliability of the information. Finally, the inventory needs to be effective (Kangas 2010). This relates to both the accuracy of the measurements undertaken as well as the cost-effectiveness of the data acquisition approach. Having accurate information is crucial for management, as subsequent decisions can influence the resulting economic or ecological value of forest stands (Bergseng et al. 2015). Cost-effectiveness is of particular importance when access to field sites is difficult or the number of required field plots is high (Andersen et al. 2009; Wulder et al. 2012).

The intensity and scale of measured attributes may depend on the information need and the scale at which the inventory is carried out. For example, operational inventories are typically localized to stands of interest for wood procurement and generally include intensive dimensional measurements of trees or plots of interest (Laamanen and Kangas 2011). Strategic inventories generally include a network of sample plots measured at regular intervals (Gillis et al. 2005). On the plots, typical measurements include the height, DBH, species, and condition (Smith 2002; White, Wulder, Varhola, et al. 2013). These inventory measurements are then scaled up to larger areas using aerial data or existing maps (White et al. 2016). Stand polygons delineated from vertical aerial photographs are a common source of airborne data and include photo-interpreted attributes such as species composition, age, size (e.g. stand height, basal area, or mean diameter), and condition (Leckie and Gillis 1995). Satellite imagery can be used as an alternative source of aerial information, but in Canada this is generally limited to northern regions with difficult accessibility and high costs for fieldwork (Falkowski et al. 2009; Gillis et al. 2005).

There are challenges with the collection and assessment of data acquired for forest inventories across all of these information needs (Table 7.1). Table 7.1 describes four important characteristics of forest inventory; representativeness, consistency, timeliness, and effectiveness. Representative information in forest inventory is data that provide robust detail about the structure and composition of the forest. In the case of operational inventories in particular, more representative information may be required for important attributes such as diameters above or below breast height, stem size distributions, detailed volume estimates, understory condition, or the quantity of coarse woody debris on the ground. Consistency in forest inventory measurements is important in diverse forests or broad spatial extents. While some inventory measurements such as diameter or species are generally consistent, attributes that require subjective interpretation such as stand or tree condition may differ across different individuals. Additionally, the measured height of trees may differ more than other attributes such as DBH (Luoma et al. 2017; Wang et al. 2019) and may vary by location, as trees in denser stands are more difficult to accurately measure from the ground due to occlusion from other stems (Andersen, Reutebuch, and McGaughey 2006). When combining inventory information across different areas or that was collected with different purposes in mind, issues can arise due to inconsistencies across acquisitions. Different measurement methods, training, and tools, such as minimum DBH thresholds or height sampling approaches, can impact the compatibility of data from different field campaigns. Inventory standards are often implemented to ensure consistent field protocols are implemented within jurisdictions. For example, the minimum DBH measured differs between the neighboring provinces of British Columbia (4 cm for living trees and 10 cm for dead trees) and Alberta (7 cm) in Canada, meaning that merging inventory measurements from these two areas is challenging (Alberta Sustainable Resource Management 2005; Ministry of Sustainable Resource Management 2003).

Timeliness in forest inventories refer to the near-complete snapshot that the information demonstrates at a given point in time. In field-based forest inventory measurements, the ability of the field data to provide a complete perspective of the stand at a point in time may be insufficient, as recorded dimensional measurements may not provide sufficient insight to allow for a detailed retrospective analysis of stand condition. Finally, the effectiveness of an inventory means that the acquired information is accurate and justified by the costs. In ground-based forest inventory, the cost may come into question when the required number of field plots is high, access to remote areas is challenging, or the application of the data is narrow (Kangas 2010). Field campaigns can cost an average of CAD$400 or more per plot measured (Bourgeois et al. 2018), and as high as several thousands of dollars in remote locations (Wulder et al. 2012). Increasing the costs of transportation to remote sites or the salaries of individuals spending more time on a site will likely result in greater costs per plot. For areas with lower values (e.g. low timber values in an operational inventory), high costs may not be justified. Due to limitations regarding the representativeness, consistency, timeliness, and effectiveness of conventional data acquisition, there is a need to augment these inventories with other methods in order to address these limitations and improve characterizations of the forest across all scales of inventory.

Table 7.1 – An assessment of the advantages and disadvantages for data requirements of conventional field-based forest inventories

	Conventional field-based inventory	
	Advantages	Disadvantages
Representativeness	Standard measurements strong in describing overall stand characteristics	Usually no direct measurements of taper or form of stems
Consistency	Usually consistent for attributes such as species or DBH	Not always consistent for attributes such as condition or height in dense stands
Timeliness	Ability to directly measure and capture detail in stands	Limited physical record to determine changes other than explicit measurements
Effectiveness	Accurate and generally cost-effective in simple forests	Likely less cost-effective in areas of lower timber value or poor accessibility

7.3. – Three-dimensional remote sensing for enhanced forest inventory

Both ALS and DAP have seen success in representative, consistent, timely, and effective wall-to-wall estimates of inventory attributes such as height, volume, or diameter (Table 1.1; Næsset 2002), and have begun to be integrated into data acquisition for operational inventories (Kangas, Astrup, et al. 2018a). In addition, more robust predictions can be made for attributes such as crown dimensions or leaf area (Roberts et al. 2005). Spectral properties of DAP point clouds have been shown to estimate properties such as insect defoliation (Goodbody et al. 2018), although the utility DAP spectral information for estimation of forest inventory attributes is yet to be demonstrated (Tompalski, White, et al. 2019). ALS estimates of forest properties are consistent across acquisitions, particularly due to the predictable nature of the interaction between laser pulses and canopy layers and the ground (Baltsavias 1999). Image acquisitions and processing algorithms may differ between DAP acquisitions, potentially limiting the consistency of resulting point clouds. These potential inconsistencies have been alleviated with methods such as normalizing the DAP point cloud with ALS-derived elevation models or using point-matching procedures such as iterative closest point to align point clouds (Gressin et al. 2013; Zhang, Glennie, and Kusari 2015). Both ALS and DAP point clouds represent a permanent three-dimensional record of an area, and the gridded nature of resulting products (e.g. rasters of area-based predictions) allow for consistent summary of information when compiling data across spatial and temporal extents (Holopainen, Vastaranta, and Hyyppä 2014). Integral to the effectiveness of ALS and DAP is the procurement of wall-to-wall coverage, meaning that spatially-explicit maps of forest attributes can be made at the tree, grid-cell, or stand level for an entire area. This represents a substantial advantage over purely ground-based methods, which often have extents limited by access or costs, and costs of area-based approaches for ALS are less than those of conventional field-based inventory methods (Andersen et al. 2006; Vastaranta 2012). Furthermore, when trees are properly identified, ALS may be more accurate in height measurement of taller trees than ground-based methods (Wang et al. 2019).

TLS and DTP have been able to meet information needs and achieve the precision required for inventory estimates (Liang et al. 2015, Liang et al. 2018). Point clouds from terrestrial data sources are more spatially constrained than those from airborne data, but provide a much higher level of localized detail. In addition to standard inventory measurements such as DBH or basal area, representative dimensional measurements such as taper, volume, and stem form can be derived with TLS or DTP (Liang et al. 2016; Piermattei et al. 2019). While species identification is critical in inventories, it remains a challenge to accurately classify species with three-dimensional remote sensing data, demonstrating the need for developing research or using field crews to augment remote sensing data collection (Lin and Herold 2016; White et al. 2016). TLS estimates typically are more consistent in different forest types than those of DTP (Liang et al. 2015, Liang et al. 2018) because of properties of the laser pulses (e.g., ability to penetrate vegetation). DTP measures are generally consistent, but the accuracies have been shown to differ among forest types (Chapter 4). The data storage capacity is an important consideration to make, as terrestrial point clouds can require large computing resources to process and store. However, the complete perspective of a given stand at a point in time is critical to understanding forest condition (e.g. understory condition, tree form), and the storability of these point clouds becomes a great asset to their use in forest inventories. Moreover, ground-based point clouds allow non-destructive estimates that match or exceed the level of accuracy of destructive manual sampling (Chapter 3). Liang et al. (2015) showed that TLS may provide slightly more accurate estimates of forest inventory attributes than DTP, with 100% detection and 4% RMSE of DBH measurements of TLS data when compared to values of 84% detection and 10% RMSE for DTP. However, the initial costs of TLS devices are tens to hundreds of times higher. Despite these costs, the value of ground-based characterizations remains high and they represent an invaluable source of information for forest inventory. A summary of the representativeness, consistency, storability and effectiveness of three-dimensional remote sensing data sources is shown in Table 7.2.

Table 7.2 - A comparison of conventional field-based inventory with airborne and terrestrial three-dimensional remote sensing methods for data acquisition

	Airborne – 3D point clouds from ALS / DAP		Terrestrial 3D point clouds from TLS / DTP	
	Advantages	Disadvantages	Advantages	Disadvantages
Representative	Structural characteristics (e.g. crown dimensions) or spectral properties (e.g. defoliation from DAP) can be derived	Tree-level detail such as species is difficult to derive	Capable of providing detailed dimensional measurements (e.g. diameters up the stem)	Characteristics such as species are more difficult to derive
Consistent	Both sources have consistent heights, especially when using previous ALS acquisitions to normalize or register DAP point clouds	DAP only captures outer canopy points and generally shows less variation in height	Generally consistent, and measurements are unbiased	Accuracies may vary depending on stand condition, especially with DTP
Timely	Spatially complete coverage provides complete aerial perspective at a given time	Processing and additional estimation required for attributes such as DBH or volume	Near-complete perspective of the area at a given point in time aids in current and retrospective monitoring	Measurements aren't direct and require instrument calibration and processing
Effective	Cost-effective surveying of complete area with very accurate heights	Inability of DAP to penetrate into the canopy limits its abilities to characterize vertical structure	Able to provide accurate and non-destructive estimates, particularly for attributes that are difficult to measure from the ground	High cost of equipment (TLS) and processing requirements

7.4. – Next-generation forest inventories

Next-generation forest inventories at all scales should integrate the strengths of a range of different types of measurements. This would include field-based assessment of attributes difficult to derive using remote sensing technologies (e.g. species mix and health condition). These field data would be augmented by an array of point cloud datasets acquired from the ground to provide an accurate assessment of tree and stand structure at ground level, ensuring attributes like DBH, number of stems and taper are accurately assessed. As well, aerially-derived point cloud information would be incorporated to provide an opportunity to map and extend these fine plot scale measurements over larger areas in a cost-effective way. Data collection on harvesters can also be implemented, allowing for detailed stem characterizations or summaries of standing timber to calibrate or validate existing models (Holopainen et al. 2014; Saukkola et al. 2019). Using these inputs would enhance the capabilities of forest inventory and move towards providing a complete, accurate, unbiased, and detailed snapshot of the forest at a given point in time. A visual example of a next-generation forest inventory is shown in Figure 1 and described in Sections 7.4.1 and 7.4.2. These examples primarily focus on enhancing operational forest inventories (Stinson and White 2018); however, strategic forest inventories may also benefit from the data acquisition examples below.

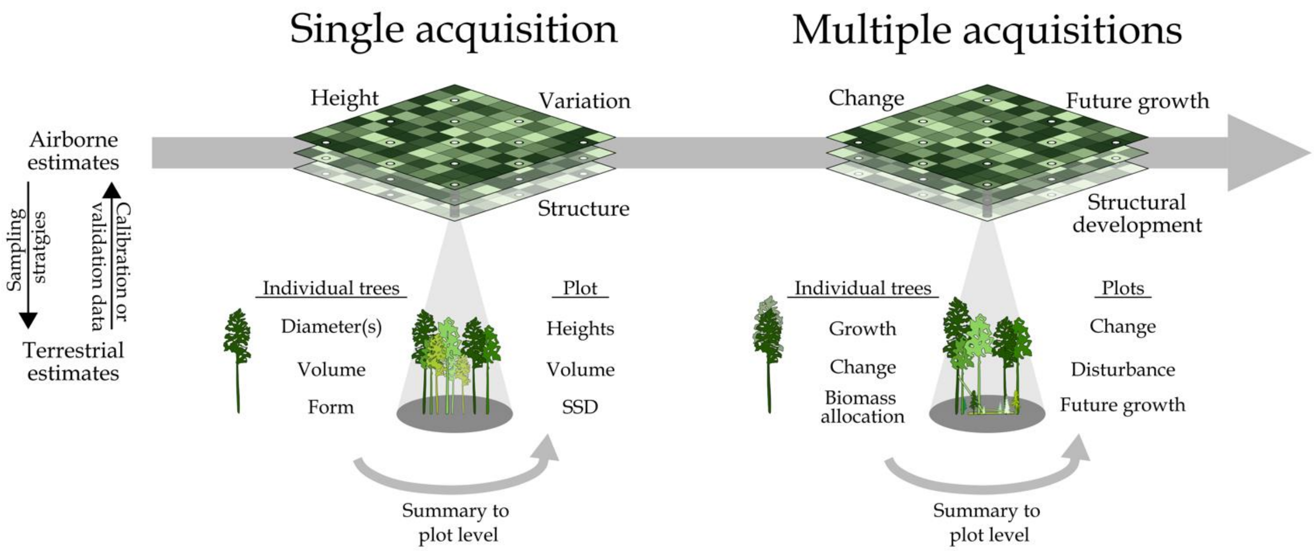

Figure 7.1 - An example of next-generation forest inventory using single or multiple acquisitions of three-dimensional remote sensing data

7.4.1. – Sample design and field measurements

Sampling design is critical to accurate and representative forest inventory. When accounting for the input costs of inventory and the subsequent loss due to suboptimal or inaccurate information, Holmström, Kallur, and Ståhl (2003) found that proper planning of sampling locations had the potential to reduce overall costs of an inventory by as much as 50%. Additionally, if ground samples are not representative of the range of forest conditions, resulting models may not perform consistently across all forest types (White, Wulder, Varhola, et al. 2013). Airborne remote sensing data can be processed and used to inform the location of sample plots using structurally guided sampling, which uses metrics such as height percentiles, cover, or variability to design a sampling strategy motivated by forest structure. Groupings can be defined by principal component analysis (PCA), in which many highly correlated structural metrics are summarized into a set of fewer uncorrelated metrics. The PCA feature space can then be stratified into classes representing different structural conditions (Kane, McGaughey, Lutz, et al. 2010). More simply, structural groups can be defined by stratifying individual airborne metrics or combinations of uncorrelated metrics. After groups or strata are defined and located, sample plots can be randomly placed in each group.

Next, the field component of the inventory would occur. While the measured attributes may change depending on the goal of the inventory, common attributes include the location, height, DBH, species, and condition of trees on sample plots (Smith 2002; White, Wulder, Varhola, et al. 2013). Concurrent with the manual inventory should be ground based three-dimensional data acquisition. Regardless of the technology (DTP or TLS), the resulting point cloud should provide complete coverage of the plot and be georeferenced to supply the locations of the detected trees. The point cloud should be able to detect all or most trees, or at least come with an understanding of the trees expected to be missed with the technology (for example small, suppressed trees as in Chapter 4). Finally, the resulting dataset should provide sufficiently detailed measurements of the resulting stems, to derive tree attributes such as taper, volume, lean, or shape. These measurements should meet approximately similar accuracy requirements as NFIs – for example, within 2 cm of DBH, 10-20% of volume, and 1-3 cm of upper stem diameters (Liang et al. 2016).

7.4.2. – Implementation and outcomes

7.4.2.1. – Single date

Single data acquisitions for a next-generation forest inventory could be used to generate wall-to-wall predictions from an area-based modeling approach (Næsset 2002). Inputs to these models can be derived from the terrestrial point clouds, which would provide estimates of attributes such as DBH or volume. Furthermore, the detailed nature of the point clouds could provide insight into output from the predictive models where conventional inventories may not. For example, where predictions have large deviations from the measured values, users could look to stand characteristics such as the species or age to support hypotheses explaining such deviations and to evaluate the consistency of the predictions across the range of conditions seen in the area of interest.

7.4.2.2. – Multiple acquisitions

While acquisition of three-dimensional data at a single point in time can provide a detailed perspective of the forest at that time, the acquisition of multitemporal data provides an opportunity to investigate changes in tree size and condition across spatial scales. At fine scales, changes in individual trees could be seen in both aerial and terrestrial point clouds, particularly those geolocated in terrestrial point clouds. For example, multitemporal terrestrial acquisitions can be used to show differences in DBH leading to a non-destructive estimate of the annual increment of trees (Mokroš et al. 2020). Across broader spatial scales, multitemporal airborne acquisitions can be combined to assess stand differences between acquisitions (Tompalski, Rakofsky, et al. 2019) or to predict future stand growth (Tompalski et al. 2018). Just as with single-date acquisitions, the combination of airborne and terrestrial data can provide information about the condition of the forest or why the changes may have taken place (e.g. assessing disturbance or irregular growth).

7.5. – Impediments to implementation

Despite the extent to which three-dimensional remote sensing technologies have been used for augmenting conventional forest inventories, more work needs to be done in developing their use for widespread adoption. For example, the cost (approximately CAD$5 per ha for ALS) of data acquisition can be prohibitive, particularly across very broad scales (Wulder et al. 2008). However, research has shown that costs can be alleviated by using ALS transects or strip sampling with satellite data to interpolate metrics and estimates across broad extents (Babcock et al. 2018; Hilker, Wulder, and Coops 2008). Recent years have seen the development of new ALS technologies and methods for forest attribute estimation, such as multispectral (Wallace et al. 2014) and single-photon LiDAR (Swatantran et al. 2016). While these technologies have shown promise in generating high-quality point clouds, more needs to be known before their widespread adoption, including their utility in different forest types and cost-effectiveness when compared to standard ALS, which uses near-infrared wavelengths. In addition, multispectral imagery has enhanced the spectral capabilities of DAP (Goodbody et al. 2018; Shen et al. 2019); however, increases in the number of image bands will likely lead to an increase in the time required to generate point clouds. These technologies are still in development but could be promising additions to available methods for providing airborne three-dimensional data for forest inventory.

TLS data acquisition also has seen rapid expansion in recent years, but still requires methodological and technological development before widespread implementation into forest inventories can be achieved. First, TLS units are generally expensive, costing as much as $40,000 or more (Eitel et al. 2013). While the potential value for data products is very high, the initial cost of the units may be prohibitive to some operators. However, the use of low-cost and low-resolution systems have been shown to produce similar data at a lower initial cost to the user, while also reducing processing time and storage requirements (Hilker et al. 2012; Kelbe et al. 2015). Ground-based forest attribute estimation with TLS is generally more accurate than DTP (15-20% higher detection rate and >5% lower DBH RMSE; Liang et al. 2015), but accuracies also decrease with increasing stand homogeneity or density (Liang et al. 2018). While DTP has recently emerged as a potential cost-effective alternative to TLS, methodological and technological developments are still required to make this technology operational for larger areas and to have accuracies of resulting point clouds match those of TLS.

To encourage widespread adoption of the technologies, steps should also be made in sharing and communicating methods, data, and resources. Many levels of government around the world have made three-dimensional remote sensing data freely available to the public (Kangas, Astrup, et al. 2018b). As an additional tool to forest managers and scientists, a central repository of data processing methods or easily replicable steps would help to ensure the consistency of processed data, especially across broad spatial or temporal extents. As the cost of ALS data acquisition can be prohibitive to some stakeholders, either centralized or localized cost sharing agreements could be used to provide data to meet an array of needs (Reutebuch, Andersen, and McGaughey 2005).

7.6. – Context of this dissertation

7.6.1. – Limitations

While the approaches developed in this research are valuable for deriving forest inventory attributes across a range of spatial and temporal scales, they have some limitations. First, DTP can produce accurate estimates of dimensional measurements such as DBH or taper, but the stand conditions are an important consideration when undertaking such an analysis. As shown in Chapter 4, tree detection and DBH estimates are more accurate when the trees are larger and closer to the camera, while plot-level estimates are more accurate in less dense stands, with less occlusion with larger trees. Additionally, the processing and storage of the point clouds should be considered when undertaking this analysis. While some standard processing pipelines are in place to go from raw images to forest inventory data, there may be some manual intervention required in, e.g., aligning the images or deriving measurements from the point clouds. These interventions may be minor but would require additional training and knowledge from the user.

Components of this thesis have demonstrated the capacity for three-dimensional remote sensing to provide detailed estimates at each spatial scale of a forest inventory. However, a sufficient quantity of terrestrial and airborne data were not acquired concurrently in the study area, so a complete end-to-end next generation forest inventory using three-dimensional point clouds could not be undertaken. Additionally, the results reported in Chapter 4 indicate that more work needs to be done to improve the consistency and accuracy of DTP methods across a range of forest types such as those found in a boreal mixedwood forest.

Limitations around the airborne datasets used in this thesis also exist. Predicted SSDs in Chapter 5 were classified as either unimodal or bimodal, whereas more complex structures and modality may have existed. In this case, nonparametric means of SSD estimation may have been more appropriate, but the estimation of such detail may have been inaccurate or inconsistent with low point densities of the ALS data used in this study (~1.5 points/m^2 in the study area). Furthermore, SSD predictions were made at the cell level, while management may be done at the stand level, meaning that an additional scaling step would be needed to derive stand-level predictions. Just as with any forest inventory attribute estimate from ALS, errors in SSD prediction are passed on to other modeling steps. In the case of Chapter 6, these were structural development phases following disturbance. This was addressed by using a large number of samples (>7,000 disturbances) to characterize structural development phases, but any errors would have been propagated to the estimated SSD for each phase.

7.6.2. – Innovations

Chapter 3 and 4 developed novel methods for improving the cost-effectiveness of DTP at the individual tree and plot level, respectively. In Chapter 3, spherical cameras and known scaling distances were used to model the taper and volume of sample trees with a relatively small number of photographs and a low processing time. Chapter 4 applied similar techniques to the plot level to show the utility of DTP for assessing plot-level forest inventory attributes, in addition to demonstrating the influence of different acquisition and field conditions on the accuracy of point clouds.

Widening the scope of inventory to Chapters 5 and 6 require the use of ALS to generate area-based estimates of forest structure. Boreal mixedwood forests exhibit a wide range of forest conditions, meaning that structural complexity may exhibit large variation in adjacent areas. Chapter 5 developed a novel method for estimation of stem size distributions (SSD) in these forest types which used the potential variation to contextualize the complexity of the estimated SSD. Chapter 6 investigated temporal components of forest inventory by incorporated these SSD estimates with photo-interpreted stand polygons of disturbance. While previous studies have used optical imagery or single ALS metrics to characterize the patterns of development following stand-replacing disturbance, I used a robust measure of forest structure (SSD) to characterize different structural phases across a wide range of species.

While the use of DTP for generating terrestrial estimates and ALS for estimating wall-to-wall attributes have been previously demonstrated in other studies, they generally focus on simple or homogeneous forests. The utility of these technologies as they pertain to more complex forests is critical for their widespread applications in forest inventory. Refining these methods for use in heterogeneous forests is of particular importance to Canada, where mixedwood stands are a dominant component of the boreal forest which makes up 78% of the nation's total forested area (Brandt et al. 2013). Additionally, this thesis grew knowledge around patterns of accuracy of DTP, underscoring the importance of stem visibility in terms of the mean DBH (> 15 cm), stand density (lower densities are more accurately detected), and the species of trees (those without low branches) which allow for more accurate detection and DBH estimation. This knowledge could be used to develop expectations and baselines for those looking to use similar methods in future work.

7.6.3. – Future work

Future work should also focus on automation of point cloud processing for DTP and approaches to enable the integration of data sources (e.g. ALS and DAP, ALS and TLS, DAP and DTP, etc.). When doing this, the cost-effectiveness and accuracy of using TLS or DTP when compared to conventional field-based estimates should be considered. Advancements in DTP could also determine the effectiveness of different image acquisition methods such as using video, drone imagery from above and below the canopy, or single pairs of stereo images.

This dissertation was able to derive forest inventory estimates using DTP in a variety of forest types. However, work using this technology is still developing and more study is needed before it can be used in a fully operational context. Based on the methods and results from this dissertation, the following methodological recommendations and considerations are presented to those wanting to undertake future study using DTP for forest attribute estimation:

1. Consideration of field conditions
    a. Conditions such as the stem density (lower densities are more accurate), tree size (generally a mean DBH below 15 cm), and species (those without branches obscuring the lower portions of the stem) should be taken into consideration, with an expected range of accuracy associated with each
2. Camera setup
    a. Spherical cameras such as those used in this work increase the field of view and allow for fewer images to be taken, but have greater distortion, especially as the distance from the image increases.
    b. Reduces the number of required images (about 0.26 per m^2 of plot area) and allows for a potentially faster processing scheme as only a small set of images need to be matched at each time
3. Taper curve matching
    a. Allows for estimation of DBH without needing to see stem at breast height
    b. Reducing possible error of cylinder fitting by matching a smoothed taper curve through potentially erroneous diameter measurements

While nonparametric methods to SSD estimation have previously been used, these typically rely on more complex estimation techniques and may not generalize well to new areas (Bollandsås et al. 2013). Future work can be done in order to compare the conditions under which different estimation techniques are more accurate. This would be useful to understand the forest types or airborne datasets that are more conducive to different estimation techniques such as ABA or nonparametric methods.

Applications of wall-to-wall predictions of SSD could continue to be used in understanding patterns of structural development. While this dissertation did not make use of explicit age or non-stand replacing disturbance, future work could use finer temporal or disturbance information to understand more detailed patterns of development or dynamics following non-stand replacing disturbance. Bergeron et al. (2014) describe the different pathways that mixedwood stands may take in structural development, but more explicit quantification of these pathways would be useful to forest managers in order to understand the trajectories of stands as they develop and respond to non-stand replacing disturbance such as insect damage or drought (Coops et al. 2020).

7.7. – Conclusions

The importance of forests continues to increase with global ecological and economic changes. Dealing with these changes will require innovations in the means in which they are inventoried. Gains from the augmentation of conventional forest inventories with three-dimensional remotely sensed data can be seen at all spatial scales of inventory. For tactical inventories, the information gained from detailed stem reconstructions could yield an increase in resources or a better perspective of possible timber procurement. Operational forest inventories could incorporate detailed wall-to-wall estimates of current forest attributes or monitor these attributes through time, including the projection of future forest resources. Finally, strategic inventories would benefit from the spatially consistent nature of the data collected to allow for direct comparisons across sites with scalable estimates for regional or national forest inventories.

Changing resource demands and climatic conditions require cost-effective means of deriving robust and accurate forest inventory measurements. DTP is one such tool that could be used to enhance traditional forest inventories. This dissertation showed that accurate estimates of tree location and DBH can be obtained with DTP under certain forest conditions, with a variety of possible applications such as updating existing forest inventories or determining merchantability. However, requirements of stem visibility and data storage and processing requirements may be potential drawbacks, with more study required to advance the operational capacity of the technology. Nevertheless, results from this dissertation showed promise in the use of DTP in a range of forest types, demonstrating its potential future use as an effective technology in forest inventory when conditions are appropriate.

The structurally complex SSDs that exist in the boreal mixedwood forest should be fit with correspondingly complex distribution models. The difference in structures among stands requires detailed, landscape-level information to guide the fitting and modeling process. Using a differentiation step allowed me to fit structurally appropriate SSDs to respective stands and allowed for more robust characterizations of SSD than using a single model for the entire study area.

This dissertation also demonstrated the ability of wall-to-wall, ALS-derived SSDs to capture differences in structural development following stand-replacing disturbance. Understanding forest structural development is critical to interpreting past changes and predicting future scenarios. Information on the general structure of stands at different developmental stages can be used by forest managers to help prescribe silvicultural treatments, by ecologists to understand differences in development between stands, or by governments to help inform policy on management of forests.

Uncertain future environmental conditions underscore the need to continue the development of methods for representative, consistent, timely, and effective monitoring of the world’s forests. Three-dimensional remote sensing technologies have the capacity to fill in critical data and knowledge gaps currently seen in some forest inventories. If used successfully, these technologies can be used to augment conventional inventories to inform sustainable and effective management and monitoring of the world’s 4 billion hectares of forest (FAO 2010).

References

van Aardt, Jan A. N., Randolph H. Wynne, and Richard G. Oderwald. 2006. "Forest Volume and Biomass Estimation Using Small-Footprint Lidar-Distributional Parameters on a per-Segment Basis." *Forest Science* 52(6):636–49.

Agisoft. 2018. "Agisoft Metashape Professional."

Alberta Sustainable Resource Management. 2005. *Permanent Sample Plot (PSP) Field Procedures Manual*. Edmonton.

Andersen, Hans-Erik, Tara Barrett, Ken Winterberger, Jacob Strunk, and Hailemariam Temesgen. 2009. "Estimating Forest Biomass on the Western Lowlands of the Kenai Peninsula of Alaska Using Airborne Lidar and Field Plot Data in a Model-Assisted Sampling Design." Pp. 19–22 in *Proceedings of the IUFRO Division 4 Conference:"Extending Forest Inventory and Monitoring over Space and Time*.

Andersen, Hans-Erik, Stephen E. Reutebuch, and Robert J. McGaughey. 2006. "A Rigorous Assessment of Tree Height Measurements Obtained Using Airborne Lidar and Conventional Field Methods." *Canadian Journal of Remote Sensing*.

Angelstam, P. and – T Kuuluvainen. 2004. "Boreal Forest Disturbance Regimes, Successional Dynamics and Landscape Structures – a European Perspective." *Ecological Bulletins* 51(September 2014):117–36.

Aronoff, S. 1982. "Classification Accuracy: A User Approach." *Photogrammetric Engineering and Remote Sensing* 48(8):1299–1307.

Axelsson, Peter. 2000. "DEM Generation from Laser Scanner Data Using Adaptive TIN Models." Pp. 110–17 in *International Archives of the Photogrammetry, Remote Sensing and Spatial Information Sciences*.

Babcock, Chad, Andrew O. Finley, Hans-Erik Andersen, Robert Pattison, Bruce D. Cook, Douglas C. Morton, Michael Alonzo, Ross Nelson, Timothy Gregoire, and Liviu Ene. 2018. "Geostatistical Estimation of Forest Biomass in Interior Alaska Combining Landsat-Derived Tree Cover, Sampled Airborne Lidar and Field Observations." *Remote Sensing of Environment* 212:212–30.

Bailey, Robert L. and R. Dell. 1972. "Quantifying Diameter Distributions with the Weibull Function." *Forest Sciences* 19(2):97–104.

Baltsavias, E. P. 1999. "Airborne Laser Scanning : Basic Relations and Formulas." 199–214.

Barazzetti, L., M. Previtali, and F. Roncoroni. 2017. "Fisheye Lenses for 3D Modeling: Evaluations and Considerations." Pp. 79–84 in *2017 TC II and CIPA-3D Virtual Reconstruction and Visualization of Complex Architectures*. Vol. 42. International Society for Photogrammetry and Remote Sensing.

Barrett, Frank, Ronald E. McRoberts, Erkki Tomppo, Emil Cienciala, and Lars T. Waser. 2016. "A Questionnaire-Based Review of the Operational Use of Remotely Sensed Data by National Forest Inventories." *Remote Sensing of Environment*.

Bartels, Samuel F., Han Y. H. Chen, Michael A. Wulder, and Joanne C. White. 2016. "Trends in Post-Disturbance Recovery Rates of Canada's Forests Following Wildfire and Harvest." *Forest Ecology and Management* 361:194–207.

Bauwens, Sébastien, Adeline Fayolle, Sylvie Gourlet-Fleury, Leopold Mianda Ndjele, Coralie Mengal, and Philippe Lejeune. 2017. "Terrestrial Photogrammetry: A Non-Destructive Method for Modelling Irregularly Shaped Tropical Tree Trunks." *Methods in Ecology and Evolution* 8(4):460–71.

Belton, David, Simon Moncrieff, and Jane Chapman. 2013. "Processing Tree Point Clouds

Using Gaussian Mixture Models." *Proceedings of the ISPRS Annals of the Photogrammetry, Remote Sensing and Spatial Information Sciences, Antalya, Turkey* 11–13.

Bergeron, Yves, Han Y. H. Chen, Norman C. Kenkel, Albanie L. Leduc, and S. Ellen Macdonald. 2014. "Boreal Mixedwood Stand Dynamics: Ecological Processes Underlying Multiple Pathways." *Forestry Chronicle* 90(2):202–13.

Bergeron, Yves and Nicole J. Fenton. 2012. "Boreal Forests of Eastern Canada Revisited: Old Growth, Nonfire Disturbances, Forest Succession, and Biodiversity." *Botany* 90(6):509–23.

Bergseng, Even, Hans Ole Ørka, Erik Næsset, and Terje Gobakken. 2015. "Assessing Forest Inventory Information Obtained from Different Inventory Approaches and Remote Sensing Data Sources." *Annals of Forest Science* 72(1):33–45.

Berveglieri, Adilson, R. O. Oliveira, and A. M. G. Tommaselli. 2014. "A Feasibility Study on the Measurement of Tree Trunks in Forests Using Multi-Scale Vertical Images." *ISPRS - International Archives of the Photogrammetry, Remote Sensing and Spatial Information Sciences* 40(5):87–92.

Berveglieri, Adilson, Antonio Tommaselli, Xinlian Liang, and Eija Honkavaara. 2017. "Photogrammetric Measurement of Tree Stems from Vertical Fisheye Images." *Scandinavian Journal of Forest Research* 32(8):743–47.

Bohlin, Jonas, Jörgen Wallerman, and Johan E. S. Fransson. 2012. "Forest Variable Estimation Using Photogrammetric Matching of Digital Aerial Images in Combination with a High-Resolution DEM." *Scandinavian Journal of Forest Research* 27(7):692–99.

Bollandsås, Ole Martin, Matti Maltamo, Terje Gobakken, and Erik Naesset. 2013. "Comparing Parametric and Non-Parametric Modelling of Diameter Distributions on Independent Data

Using Airborne Laser Scanning in a Boreal Conifer Forest." *Forestry* 86:493–501.

Bolton, Douglas K., Nicholas C. Coops, Txomin Hermosilla, Michael A. Wulder, and Joanne C. White. 2018. "Evidence of Vegetation Greening at Alpine Treeline Ecotones: Three Decades of Landsat Spectral Trends Informed by Lidar-Derived Vertical Structure." *Environmental Research Letters* 13(8):84022.

Bolton, Douglas K., Nicholas C. Coops, and Michael A. Wulder. 2015. "Characterizing Residual Structure and Forest Recovery Following High-Severity Fire in the Western Boreal of Canada Using Landsat Time-Series and Airborne Lidar Data." *Remote Sensing of Environment* 163:48–60.

Borders, Bruce E., Mingliang Wang, and Dehai Zhao. 2008. "Problems of Scaling Plantation Plot Diameter Distributions to Stand Level." *Forest Science* 54(3):349–55.

Bourgeois, W., C. Binkley, V. LeMay, I. Moss, and N. Reynolds. 2018. "British Columbia Forest Inventory Review Panel Technical Background Report. Prepared for the Office of the Chief Forester Division, British Columbia Ministry of Forests, Lands." *Natural Resource Operations and Rural Development*.

Bouvier, Marc, Sylvie Durrieu, Richard A. Fournier, and Jean-Pierre Renaud. 2015. "Generalizing Predictive Models of Forest Inventory Attributes Using an Area-Based Approach with Airborne LiDAR Data." *Remote Sensing of Environment* 156:322–34.

Brandt, James P. 2009. "The Extent of the North American Boreal Zone." *Environmental Reviews* 17(NA):101–61.

Brandt, James P., M. D. Flannigan, D. G. Maynard, I. D. Thompson, and W. J. A. Volney. 2013. "An Introduction to Canada's Boreal Zone: Ecosystem Processes, Health, Sustainability, and Environmental Issues." *Environmental Reviews* 21(4):207–26.

Brassard, Brian W. and Han Y. H. Chen. 2010. *Stand Structure and Composition Dynamics of Boreal Mixedwood Forest: Implications for Forest Management*. Edmonton, Alberta: Sustainable Forest Management Network.

Bréda, N. J. J. 2003. "Ground-Based Measurements of Leaf Area Index: A Review of Methods, Instruments and Current Controversies." *Journal of Experimental Botany* 54(392):2403–17.

Broadbent, Eben N., Daniel J. Zarin, Gregory P. Asner, Marielos Penña-Claros, Amanda Cooper, and Ramon Littell. 2006. "Recovery of Forest Structure and Spectral Properties after Selective Logging in Lowland Bolivia." *Ecological Applications* 16(3):1148–63.

Brown, Sandra, Paul Schroeder, and Richard Birdsey. 1997. "Aboveground Biomass Distribution of US Eastern Hardwood Forests and the Use of Large Trees as an Indicator of Forest Development." *Forest Ecology and Management* 96(1–2):37–47.

Burns, Russell M. and Barbara H. Honkala. 1990. *Silvics of North America*. Vol. 2. United States Department of Agriculture Washington, DC.

Cao, Lin, Nicholas C. Coops, John L. Innes, Stephen R. J. Sheppard, Liyong Fu, Honghua Ruan, and Guanghui She. 2016. "Estimation of Forest Biomass Dynamics in Subtropical Forests Using Multi-Temporal Airborne LiDAR Data." *Remote Sensing of Environment* 178:158–71.

Cavard, Xavier, S. Ellen Macdonald, Yves Bergeron, and Han Y. H. Chen. 2011. "Importance of Mixedwoods for Biodiversity Conservation: Evidence for Understory Plants, Songbirds, Soil Fauna, and Ectomycorrhizae in Northern Forests." *Environmental Reviews* 19:142–61.

Chen, Han Y. H. and Roman V Popadiouk. 2002. "Dynamics of North American Boreal Mixedwoods." *Environ. Rev* 10(3):137–66.

Chu, Thuan and Xulin Guo. 2013. "Remote Sensing Techniques in Monitoring Post-Fire Effects and Patterns of Forest Recovery in Boreal Forest Regions: A Review." *Remote Sensing* 6(1):470–520.

Coomes, David A., Richard P. Duncan, Robert B. Allen, and James Truscott. 2003. "Disturbances Prevent Stem Size-Density Distributions in Natural Forests from Following Scaling Relationships." *Ecology Letters* 6(11):980–89.

Coops, Nicholas C., Thomas Hilker, Michael A. Wulder, Benoît St-Onge, Glenn Newnham, Anders Siggins, and J. A. Trofymow. 2007. "Estimating Canopy Structure of Douglas-Fir Forest Stands from Discrete-Return LiDAR." *Trees - Structure and Function* 21(3):295–310.

Coops, Nicholas C., Chen Shang, Michael A. Wulder, Joanne C. White, and Txomin Hermosilla. 2020. "Change in Forest Condition: Characterizing Non-Stand Replacing Disturbances Using Time Series Satellite Imagery." *Forest Ecology and Management* 474:118370.

Cumming, S. G. 2001. "Forest Type and Wildfire in the Alberta Boreal Mixedwood: What Do Fires Burn?" *Ecological Applications* 11(1):97–110.

Eid, Tron, Terje Gobakken, and Erik Næsset. 2004. "Comparing Stand Inventories for Large Areas Based on Photo-Interpretation and Laser Scanning by Means of Cost-plus-Loss Analyses." *Scandinavian Journal of Forest Research* 19(6):512–23.

Eitel, Jan U. H., Lee A. Vierling, and Troy S. Magney. 2013. "A Lightweight, Low Cost Autonomously Operating Terrestrial Laser Scanner for Quantifying and Monitoring Ecosystem Structural Dynamics." *Agricultural and Forest Meteorology* 180:86–96.

Ellison, Aaron M. 1987. "Effect of Seed Dimorphism on the Density-Dependent Dynamics of Experimental Populations of Atriplex Triangularis (Chenopodiaceae)." *American Journal of Botany* 74(8):1280.

Enquist, Brian J. and Karl J. Niklas. 2001. “Invariant Scaling Relations across Tree-Dominated Communities.” *Nature* 410(6829):655.

van Ewijk, Karin Y., Paul M. Treitz, and Neal A. Scott. 2011. “Characterizing Forest Succession in Central Ontario Using Lidar-Derived Indices.” *Photogrammetric Engineering & Remote Sensing* 77(3):261–69.

Falkowski, Michael J., Michael A. Wulder, Joanne C. White, and Mark D. Gillis. 2009. “Supporting Large-Area, Sample-Based Forest Inventories with Very High Spatial Resolution Satellite Imagery.” *Progress in Physical Geography*.

Fang, Rong and Bogdan M. Strimbu. 2017. “Stem Measurements and Taper Modeling Using Photogrammetric Point Clouds.” *Remote Sensing* 9(7):716.

FAO. 2005. *Global Forest Resources Assessment 2005: Progress towards Sustainable Forest Management*. Rome, Italy.

FAO. 2010. *Global Forest Resources Assessment 2010 : Main Report.* Food and Agriculture Organization of the United Nations.

Forsman, Mona, Niclas Börlin, and Johan Holmgren. 2016. “Estimation of Tree Stem Attributes Using Terrestrial Photogrammetry with a Camera Rig.” *Forests* 7(3):1–20.

Franklin, Jerry F., Thomas A. Spies, Robert Van Pelt, Andrew B. Carey, Dale A. Thornburgh, Dean Rae Berg, David B. Lindenmayer, Mark E. Harmon, William S. Keeton, David C. Shaw, Ken Bible, and Jiquan Chen. 2002. “Disturbances and Structural Development of Natural Forest Ecosystems with Silvicultural Implications, Using Douglas-Fir Forests as an Example.” *Forest Ecology and Management* 155:399–423.

Freeman, Jonathan B. and Rick Dale. 2012. “Assessing Bimodality to Detect the Presence of a Dual Cognitive Process.” *Behavioral Research*.

Frey, Brent R., Victor J. Lieffers, Simon M. Landhäusser, Phil G. Comeau, and Ken J. Greenway. 2003. "An Analysis of Sucker Regeneration of Trembling Aspen." *Canadian Journal of Forest Research* 33(7):1169–79.

Frolking, Stephen, Michael W. Palace, D. B. Clark, Jeffrey Q. Chambers, H. H. Shugart, and George C. Hurtt. 2009. "Forest Disturbance and Recovery: A General Review in the Context of Spaceborne Remote Sensing of Impacts on Aboveground Biomass and Canopy Structure." *Journal of Geophysical Research: Biogeosciences* 114(G2).

Fulton, R. J. 1989. "Quaternary Geology of Canada and Greenland."

García, Oscar. 1992. "What Is a Diameter Distribution." Pp. 11–29 in *Proceedings of the Symposium on Integrated Forest Management Information Systems*.

Gautam, Shuva, Luc Lebel, and Daniel Beaudoin. 2017. "A Hierarchical Planning System to Assess the Impact of Operational-Level Flexibility on Long-Term Wood Supply." *Canadian Journal of Forest Research* 47(4):424–32.

Gillis, Mark D. 2001. "Canada's National Forest Inventory (Responding to Current Information Needs)." *Environmental Monitoring and Assessment*.

Gillis, Mark D. and Donald G. Leckie. 1996. "Forest Inventory Update in Canada." *Forestry Chronicle*.

Gillis, Mark D., A. Y. Omule, and T. Brierly. 2005. "Monitoring Canada's Forests: The National Forest Inventory." *The Forestry Chronicle* 81(2):214–21.

Gobakken, Terje and Erik Næsset. 2004. "Estimation of Diameter and Basal Area Distributions in Coniferous Forest by Means of Airborne Laser Scanner Data." *Scandinavian Journal of Forest Research* 19(6):529–42.

Goodbody, Tristan R. H., Nicholas C. Coops, Txomin Hermosilla, Piotr Tompalski, Grant

McCartney, and David A. MacLean. 2018. “Digital Aerial Photogrammetry for Assessing Cumulative Spruce Budworm Defoliation and Enhancing Forest Inventories at a Landscape-Level.” *ISPRS Journal of Photogrammetry and Remote Sensing* 142:1–11.

Goodbody, Tristan R. H., Nicholas C. Coops, Txomin Hermosilla, Piotr Tompalski, and Gaetan Pelletier. 2018. “Vegetation Phenology Driving Error Variation in Digital Aerial Photogrammetrically Derived Terrain Models.” *Remote Sensing* 10(10):1554.

Goodbody, Tristan R. H., Nicholas C. Coops, and Joanne C. White. 2019. “Digital Aerial Photogrammetry for Updating Area-Based Forest Inventories: A Review of Opportunities, Challenges, and Future Directions.” *Current Forestry Reports*.

Government of Alberta. 2005. *Alberta Vegetation Inventory Interpretation Standards*. Edmonton.

Gressin, Adrien, Clément Mallet, Jérôme Demantké, and Nicolas David. 2013. “Towards 3D Lidar Point Cloud Registration Improvement Using Optimal Neighborhood Knowledge.” *ISPRS Journal of Photogrammetry and Remote Sensing* 79:240–51.

Griffiths, Patrick, Tobias Kuemmerle, Matthias Baumann, Volker C. Radeloff, Ioan V Abrudan, Juraj Lieskovsky, Catalina Munteanu, Katarzyna Ostapowicz, and Patrick Hostert. 2014. “Forest Disturbances, Forest Recovery, and Changes in Forest Types across the Carpathian Ecoregion from 1985 to 2010 Based on Landsat Image Composites.” *Remote Sensing of Environment* 151:72–88.

Grumbine, R. Edward. 1994. “What Is Ecosystem Management?” *Conservation Biology* 8(1):27–38.

Hansen, Matthew C., Peter V Potapov, Rebecca Moore, Matt Hancher, S. A. A. Turubanova, Alexandra Tyukavina, David Thau, S. V Stehman, S. J. Goetz, and Thomas R. Loveland.

2013. “High-Resolution Global Maps of 21st-Century Forest Cover Change.” *Science* 342(6160):850–53.

Hapca, Adrian Ilie, Frédéric Mothe, and Jean-Michel Leban. 2007. “A Digital Photographic Method for 3D Reconstruction of Standing Tree Shape.” *Annals of Forest Science* 64(6):631–37.

Hassan, Rashid, Robert Scholes, and Neville Ash. 2005. *Ecosystems and Human Well- Being: Current State and Trends. Vol. 1. Millennium Ecosystem Assessment Series*. edited by R. Hassan, R. Scholes, and N. Ash. London, UK: Island Press.

Herrera, Pedro Javier, Gonzalo Pajares, María Guijarro, José J. Ruz, and Jesús M. Cruz. 2011. “A Stereovision Matching Strategy for Images Captured with Fish-Eye Lenses in Forest Environments.” *Sensors*.

Hilker, Thomas, Nicholas C. Coops, Darius S. Culvenor, Glenn Newnham, Michael A. Wulder, Christopher W. Bater, and Anders Siggins. 2012. “A Simple Technique for Co-Registration of Terrestrial LiDAR Observations for Forestry Applications.” *Remote Sensing Letters* 3(3):239–47.

Hilker, Thomas, Michael A. Wulder, and Nicholas C. Coops. 2008. “Update of Forest Inventory Data with Lidar and High Spatial Resolution Satellite Imagery.” *Canadian Journal of Remote Sensing* 34(1):5–12.

Holmström, Hampus, Hans Kallur, and Göran Ståhl. 2003. “Cost-plus-Loss Analyses of Forest Inventory Strategies Based on KNN-Assigned Reference Sample Plot Data.” *Silva Fennica*.

Holopainen, Markus, Mikko Vastaranta, and Juha Hyyppä. 2014. “Outlook for the next Generation’s Precision Forestry in Finland.” *Forests*.

Huang, Shongming. 1994. *Ecologically Based Individual Tree Volume Estimation for Major*

Alberta Tree Species. Edmonton.

Huang, Shongming, Shawn X. Meng, and Yuqing Yang. 2009. *A Growth and Yield Projection System (GYPSY) for Natural and Post-Harvest Stands in Alberta*. Vol. T/216. Edmonton, Canada.

Hudak, Andrew Thomas, Jeffrey Scott Evans, and Alistair Matthew Stuart Smith. 2009. "LiDAR Utility for Natural Resource Managers." *Remote Sensing* 1(4):934–51.

Isenburg, Martin. 2014. "LAStools."

Johnson, Edward A. and Kiyoko Miyanishi. 2012. "The Boreal Forest as a Cultural Landscape." *Annals of the New York Academy of Sciences*.

Johnstone, Jill F., F. S. Chapin III, J. Foote, S. Kemmett, K. Price, and L. Viereck. 2004. "Decadal Observations of Tree Regeneration Following Fire in Boreal Forests." *Canadian Journal of Forest Research* 34(2):267–73.

Kane, Van R., Robert J. McGaughey, Jonathan D. Bakker, Rolf F. Gersonde, James A. Lutz, and Jerry F. Franklin. 2010. "Comparisons between Field- and LiDAR-Based Measures of Stand Structural Complexity." *Canadian Journal of Forest Research* 40(4):761–73.

Kane, Van R., Robert J. McGaughey, James A. Lutz, Rolf F. Gersonde, Jonathan D. Bakker, and Jerry F. Franklin. 2010. "Examining Conifer Canopy Structural Complexity across Forest Ages and Elevations with LiDAR Data." *Canadian Journal of Forest Research* 40(4):774–87.

Kangas, Annika. 2010. "Value of Forest Information." *European Journal of Forest Research* 129(5):863–74.

Kangas, Annika, Rasmus Astrup, Johannes Breidenbach, Jonas Fridman, Terje Gobakken, Kari T. Korhonen, Matti Maltamo, Mats Nilsson, Thomas Nord-Larsen, Erik Næsset, and Håkan

Olsson. 2018a. “Remote Sensing and Forest Inventories in Nordic Countries–Roadmap for the Future.” *Scandinavian Journal of Forest Research*.

Kangas, Annika, Rasmus Astrup, Johannes Breidenbach, Jonas Fridman, Terje Gobakken, Kari T. Korhonen, Matti Maltamo, Mats Nilsson, Thomas Nord-Larsen, Erik Næsset, and Håkan Olsson. 2018b. “Remote Sensing and Forest Inventories in Nordic Countries–Roadmap for the Future.” *Scandinavian Journal of Forest Research*.

Kangas, Annika, Terje Gobakken, Stefano Puliti, Marius Hauglin, and Erik Næsset. 2018. “Value of Airborne Laser Scanning and Digital Aerial Photogrammetry Data in Forest Decision Making.” *Silva Fennica*.

Kao, David L., Marc G. Kramer, Alison L. Love, Jennifer L. Dungan, and Alex T. Pang. 2005. “Visualizing Distributions from Multi-Return Lidar Data to Understand Forest Structure.” *Cartographic Journal* 42(1):35–47.

Kelbe, David, Jan Van Aardt, Paul Romanczyk, Martin Van Leeuwen, and Kerry Cawse-Nicholson. 2015. “Single-Scan Stem Reconstruction Using Low-Resolution Terrestrial Laser Scanner Data.” *IEEE Journal of Selected Topics in Applied Earth Observations and Remote Sensing*.

Kennedy, Robert E., Zhiqiang Yang, Warren B. Cohen, Eric Pfaff, Justin Braaten, and Peder Nelson. 2012. “Spatial and Temporal Patterns of Forest Disturbance and Regrowth within the Area of the Northwest Forest Plan.” *Remote Sensing of Environment* 122:117–33.

Kozak, A. 1988. “A Variable-Exponent Taper Equation.” *Canadian Journal of Forest Research* 18(11):1363–68.

Krawchuk, Meg A. and Steve G. Cumming. 2009. “Disturbance History Affects Lightning Fire Initiation in the Mixedwood Boreal Forest: Observations and Simulations.” *Forest Ecology* *and Management* 257(7):1613–22.

Laamanen, Risto and Annika Kangas. 2011. “Large-Scale Forest Owner’s Information Needs in Operational Planning of Timber Harvesting - Some Practical Views in Metsähallitus, Finnish State-Owned Enterprise.” *Silva Fennica* 45(4):711–27.

Lambert, M. C., C. H. Ung, and F. Raulier. 2005. “Canadian National Tree Aboveground Biomass Equations.” *Canadian Journal of Forest Research* 35(8):1996–2018.

Landsberg, Joe, Annikki Mäkelä, Risto Sievänen, and Mikko Kukkola. 2005. “Analysis of Biomass Accumulation and Stem Size Distributions over Long Periods in Managed Stands of Pinus Sylvestris in Finland Using the 3-PG Model.” *Tree Physiology* 25(7):781–92.

Latham, Penelope A., Hans R. Zuuring, and Dean W. Coble. 1998. “A Method for Quantifying Vertical Forest Structure.” *Forest Ecology and Management*.

Leberl, Franz, Arnold Irschara, Thomas Pock, Philipp Meixner, Michael Gruber, Set Scholz, and Alexander Wiechert. 2010. “Point Clouds: LiDAR versus Three-Dimensional Vision.” *Photogrammetric Engineering & Remote Sensing* 76(10):1123–34.

Leckie, Donald G. and Mark D. Gillis. 1995. “Forest Inventory in Canada with Emphasis on Map Production.” *The Forestry Chronicle* 71(1):74–88.

van Leeuwen, Martin and Maarten Nieuwenhuis. 2010. “Retrieval of Forest Structural Parameters Using LiDAR Remote Sensing.” *European Journal of Forest Research*.

Lenihan, James M. 1993. “Ecological Response Surfaces for North American Boreal Tree Species and Their Use in Forest Classification.” *Journal of Vegetation Science* 4(5):667–80.

Letcher, Susan G. and Robin L. Chazdon. 2009. “Rapid Recovery of Biomass, Species Richness, and Species Composition in a Forest Chronosequence in Northeastern Costa Rica.” *Biotropica* 41(5):608–17.

Liang, Jingjing, Joseph Buongiorno, and Robert A. Monserud. 2005. “Growth and Yield of All-Aged Douglas-Fir - Western Hemlock Forest Stands: A Matrix Model with Stand Diversity Effects.” *Canadian Journal of Forest Research*.

Liang, Xinlian and Juha Hyyppä. 2013. “Automatic Stem Mapping by Merging Several Terrestrial Laser Scans at the Feature and Decision Levels.” *Sensors* 13(2):1614–34.

Liang, Xinlian, Juha Hyyppä, Harri Kaartinen, Markus Holopainen, and Timo Melkas. 2012. “Detecting Changes in Forest Structure over Time with Bi-Temporal Terrestrial Laser Scanning Data.” *ISPRS International Journal of Geo-Information* 1(3):242–55.

Liang, Xinlian, Juha Hyyppä, Harri Kaartinen, Matti Lehtomäki, Jiri Pyörälä, Norbert Pfeifer, Markus Holopainen, Gábor Brolly, Pirotti Francesco, Jan Hackenberg, Huabing Huang, Hyun Woo Jo, Masato Katoh, Luxia Liu, Martin Mokroš, Jules Morel, Kenneth Olofsson, Jose Poveda-Lopez, Jan Trochta, Di Wang, Jinhu Wang, Zhouxi Xi, Bisheng Yang, Guang Zheng, Ville Kankare, Ville Luoma, Xiaowei Yu, Liang Chen, Mikko Vastaranta, Ninni Saarinen, and Yunsheng Wang. 2018. “International Benchmarking of Terrestrial Laser Scanning Approaches for Forest Inventories.” *ISPRS Journal of Photogrammetry and Remote Sensing* 144(June):137–79.

Liang, Xinlian, Anttoni Jaakkola, Yunsheng Wang, Juha Hyyppä, Eija Honkavaara, Jingbin Liu, and Harri Kaartinen. 2014. “The Use of a Hand-Held Camera for Individual Tree 3D Mapping in Forest Sample Plots.” *Remote Sensing*.

Liang, Xinlian, Ville Kankare, Juha Hyyppä, Yunsheng Wang, Antero Kukko, Henrik Haggrén, Xiaowei Yu, Harri Kaartinen, Anttoni Jaakkola, Fengying Guan, Markus Holopainen, and Mikko Vastaranta. 2016. “Terrestrial Laser Scanning in Forest Inventories.” *ISPRS Journal of Photogrammetry and Remote Sensing*.

Liang, Xinlian, Ville Kankare, Xiaowei Yu, Juha Hyyppä, and Markus Holopainen. 2014. "Automated Stem Curve Measurement Using Terrestrial Laser Scanning." *IEEE Transactions on Geoscience and Remote Sensing* 52(3):1739–48.

Liang, Xinlian, Yunsheng Wang, Anttoni Jaakkola, Antero Kukko, Harri Kaartinen, Juha Hyyppä, Eija Honkavaara, and Jingbin Liu. 2015. "Forest Data Collection Using Terrestrial Image-Based Point Clouds from a Handheld Camera Compared to Terrestrial and Personal Laser Scanning." *IEEE Transactions on Geoscience and Remote Sensing* 53(9):5117–32.

Lin, Yi and Martin Herold. 2016. "Tree Species Classification Based on Explicit Tree Structure Feature Parameters Derived from Static Terrestrial Laser Scanning Data." *Agricultural and Forest Meteorology*.

Lindenmayer, David B. and Jerry F. Franklin. 2002. *Conserving Forest Biodiversity: A Comprehensive Multiscaled Approach*. Island press.

Liu, Chuangmin, Lianjun Zhang, Craig J. Davis, Dale S. Solomon, and Jeffrey H. Gove. 2002. "A Finite Mixture Model for Characterizing the Diameter Distributions of Mixed-Species Forest Stands." *Forest Science* 48(4).

Lundholm, Anders. 2018. "Evaluating Inventory Methods for Estimating Stem Diameter Distributions in Micro Stands Derived from Airborne Laser Scanning." Swedish University of Agricultural Sciences.

Luoma, Ville, Ninni Saarinen, Michael Wulder, Joanne White, Mikko Vastaranta, Markus Holopainen, Juha Hyyppä, Ville Luoma, Ninni Saarinen, Michael A. Wulder, Joanne C. White, Mikko Vastaranta, Markus Holopainen, and Juha Hyyppä. 2017. "Assessing Precision in Conventional Field Measurements of Individual Tree Attributes." *Forests* 8(2):38.

Maas, H. G., A. Bienert, S. Scheller, and E. Keane. 2008. "Automatic Forest Inventory Parameter Determination from Terrestrial Laser Scanner Data." *International Journal of Remote Sensing* 29(5):1579–93.

Magnussen, Steen and Jean Pierre Renaud. 2016. "Multidimensional Scaling of First-Return Airborne Laser Echoes for Prediction and Model-Assisted Estimation of a Distribution of Tree Stem Diameters." *Annals of Forest Science* 73:1089–98.

Maltamo, Matti and Terje Gobakken. 2014. "Predicting Tree Diameter Distributions." Pp. 177–91 in *Forestry Applications of Airborne Laser Scanning*, edited by M. Maltamo, E. Næsset, and J. Vauhkonen. Springer.

Maltamo, Matti, Erik Næsset, Ole M. Bollandsås, Terje Gobakken, and Petteri Packalén. 2009. "Non-Parametric Prediction of Diameter Distributions Using Airborne Laser Scanner Data." *Scandinavian Journal of Forest Research* 24(6):541–53.

Maltamo, Matti, P. Packalén, X. Yu, K. Eerikäinen, J. Hyyppä, and J. Pitkänen. 2005. "Identifying and Quantifying Structural Characteristics of Heterogeneous Boreal Forests Using Laser Scanner Data." *Forest Ecology and Management*.

Maltamo, Matti, A. Suvanto, and P. Packalén. 2007. "Comparison of Basal Area and Stem Frequency Diameter Distribution Modelling Using Airborne Laser Scanner Data and Calibration Estimation." *Forest Ecology and Management* 247(1–3):26–34.

McGarrigle, Elizabeth, John A. Kershaw, Michael B. Lavigne, Aaron R. Weiskittel, and Mark Ducey. 2011. "Predicting the Number of Trees in Small Diameter Classes Using Predictions from a Two-Parameter Weibull Distribution." *Forestry* 84(4):431–39.

McGaughey, Robert J. 2008. "FUSION/LDV: Software for LIDAR Data Analysis and Visualization." *United States Department of Agriculture, Forest Service, Pacific Northwest*

Research Station.

McRoberts, Ronald E., William A. Bechtold, Paul L. Patterson, Charles T. Scott, and Gregory A. Reams. 2005. "The Enhanced Forest Inventory and Analysis Program of the USDA Forest Service: Historical Perspective and Announcement of Statistical Documentation." *Journal of Forestry*.

Mikita, Tomáš, Přemysl Janata, and Peter Surovỳ. 2016. "Forest Stand Inventory Based on Combined Aerial and Terrestrial Close-Range Photogrammetry." *Forests* 7(8):1–14.

Miller, Jordan, Justin Morgenroth, and Christopher Gomez. 2015. "3D Modelling of Individual Trees Using a Handheld Camera: Accuracy of Height, Diameter and Volume Estimates." *Urban Forestry & Urban Greening* 14(4):932–40.

Ministry of Sustainable Resource Management. 2003. *Forest Inventory and Monitoring Program: Growth and Yield Standards and Procedures*. Victoria.

Mokroš, Martin, Xinlian Liang, Peter Surový, Peter Valent, Juraj Čerňava, František Chudý, Daniel Tunák, Šimon Saloň, and Ján Merganič. 2018. "Evaluation of Close-Range Photogrammetry Image Collection Methods for Estimating Tree Diameters." *ISPRS International Journal of Geo-Information* 7(3):93.

Mokroš, Martin, Jozef Výbošťok, Alžbeta Grznárová, Michal Bošela, Vladimír Šebeň, and Ján Merganič. 2020. "Non-Destructive Monitoring of Annual Trunk Increments by Terrestrial Structure from Motion Photogrammetry." *PloS One* 15(3):e0230082.

Myung, In Jae. 2003. "Tutorial on Maximum Likelihood Estimation." *Journal of Mathematical Psychology* 47(1):90–100.

Næsset, Erik. 2002. "Predicting Forest Stand Characteristics with Airborne Scanning Laser Using a Practical Two-Stage Procedure and Field Data." *Remote Sensing of Environment*

80:88–99.

Næsset, Erik. 2007. “Airborne Laser Scanning as a Method in Operational Forest Inventory: Status of Accuracy Assessments Accomplished in Scandinavia.” *Scandinavian Journal of Forest Research* 22(5):433–42.

Natural Regions Committee. 2006. “Natural Regions and Subregions of Alberta.” *Compiled by DJ Downing and WW Pettapiece. Government of Alberta. Pub*.

Natural Resources Canada. 2018. *The State of Canada’s Forests 2018*. Ottawa.

Newnham, Glenn J., John D. Armston, Kim Calders, Mathias I. Disney, Jenny L. Lovell, Crystal B. Schaaf, Alan H. Strahler, and F. Mark Danson. 2015. “Terrestrial Laser Scanning for Plot-Scale Forest Measurement.” *Current Forestry Reports* 1(4):239–51.

Niklas, Karl J., Jeremy J. Midgley, and Richard H. Rand. 2003. “Tree Size Frequency Distributions, Plant Density, Age and Community Disturbance.” *Ecology Letters*.

Oliver, Chadwick Dearing. 1981. “Forest Development in North America Following Major Disturbances.” *Forest Ecology and Management* 3:153–68.

Packalen, Petteri and Matti Maltamo. 2008. “Estimating Species-Specific Diameter Distributions and Saw Log Recoveries of Boreal Forests from Airborne Laser Scanning Data and Aerial Photographs: A Distribution-Based Approach.” *Canadian Journal of Forest Research* 38:1750–60.

Packalén, Petteri and Matti Maltamo. 2006. “Predicting the Plot Volume by Tree Species Using Airborne Laser Scanning and Aerial Photographs.” *Forest Science* 52(6):611–22.

Palahí, Marc, Timo Pukkala, and Antoni Trasobares. 2006. “Modelling the Diameter Distribution of Pinus Sylvestris, Pinus Nigra and Pinus Halepensis Forest Stands in Catalonia Using the Truncated Weibull Function.” *Forestry* 79(5):553–62.

Pan, Yude, Richard A. Birdsey, Jingyun Fang, Richard Houghton, Pekka E. Kauppi, Werner A. Kurz, Oliver L. Phillips, Anatoly Shvidenko, Simon L. Lewis, Josep G. Canadell, Philippe Ciais, Robert B. Jackson, Stephen W. Pacala, A. David McGuire, Shilong Piao, Aapo Rautiainen, Stephen Sitch, and Daniel Hayes. 2011. "A Large and Persistent Carbon Sink in the World's Forests." *Science*.

Penner, Margaret, Murray Woods, and Douglas G. Pitt. 2015. "A Comparison of Airborne Laser Scanning and Image Point Cloud Derived Tree Size Class Distribution Models in Boreal Ontario." *Forests* 6(11):4034–54.

Pfister, Roland, Katharina A. Schwarz, Markus Janczyk, Rick Dale, and Jonathan B. Freeman. 2013. "Good Things Peak in Pairs: A Note on the Bimodality Coefficient." *Frontiers in Psychology* 4(700):1–4.

Piboule, A., M. Krebs, L. Esclatine, and JC Hervé. 2015. "Computree: A Collaborative Platform for Use of Terrestrial LiDAR in Dendrometry."

Pickell, Paul D., Txomin Hermosilla, Ryan J. Frazier, Nicholas C. Coops, and Michael A. Wulder. 2015. "Forest Recovery Trends Derived from Landsat Time Series for North American Boreal Forests." *International Journal of Remote Sensing* 37(1):138–49.

Piermattei, Livia, Wilfried Karel, Di Wang, Martin Wieser, Martin Mokroš, Peter Surový, Milan Koreň, Julián Tomaštík, Norbert Pfeifer, and Markus Hollaus. 2019. "Terrestrial Structure from Motion Photogrammetry for Deriving Forest Inventory Data." *Remote Sensing* 11(8):950.

Podlaski, R. 2010. "Diversity of Patch Structure in Central European Forests: Are Tree Diameter Distributions in near-Natural Multilayered Abies-Fagus Stands Heterogeneous?" *Ecological Research* 25(3):599–608.

Popescu, Sorin C. and Kaiguang Zhao. 2008. “A Voxel-Based Lidar Method for Estimating Crown Base Height for Deciduous and Pine Trees.” *Remote Sensing of Environment* 112(3):767–81.

Pueschel, Pyare, Glenn Newnham, Gilles Rock, Thomas Udelhoven, Willy Werner, and Joachim Hill. 2013. “The Influence of Scan Mode and Circle Fitting on Tree Stem Detection, Stem Diameter and Volume Extraction from Terrestrial Laser Scans.” *ISPRS Journal of Photogrammetry and Remote Sensing* 77:44–56.

R Core Team. 2018. “R: A Language and Environment for Statistical Computing.”

Reutebuch, Stephen E., Hans Erik Andersen, and Robert J. McGaughey. 2005. “Light Detection and Ranging (LIDAR): An Emerging Tool for Multiple Resource Inventory.” *Journal of Forestry* 103(6):286–92.

Reynolds, Marion R. Jr, Thomas E. Burk, and Won-Chin Huang. 1988. “Goodness-of-FiT Tests and Model Selection Procedures for Diameter Distribution Models.” *Forest Science* 34(2):373–99.

Rickbeil, Gregory J. M., Txomin Hermosilla, Nicholas C. Coops, Joanne C. White, and Michael A. Wulder. 2017. “Estimating Changes in Lichen Mat Volume through Time and Related Effects on Barren Ground Caribou (Rangifer Tarandus Groenlandicus) Movement.” *PloS One* 12(3):e0172669.

RICOH. 2017. “RICOH THETA S.”

del Río, Miren, Hans Pretzsch, Iciar Alberdi, Kamil Bielak, Felipe Bravo, Andreas Brunner, Sonia Condés, Mark J. Ducey, Teresa Fonseca, Nikolas von Lüpke, Maciej Pach, Sanja Peric, Thomas Perot, Zahera Souidi, Peter Spathelf, Hubert Sterba, Martina Tijardovic, Margarida Tomé, Patrick Vallet, and Andrés Bravo-Oviedo. 2016. “Characterization of the

Structure , Dynamics , and Productivity of Mixed-Species Stands : Review and Perspectives." *European Journal of Forest Research* 135(23):23–49.

Roberts, Scott D., Thomas J. Dean, David L. Evans, John W. McCombs, Richard L. Harrington, and Patrick A. Glass. 2005. "Estimating Individual Tree Leaf Area in Loblolly Pine Plantations Using LiDAR-Derived Measurements of Height and Crown Dimensions." *Forest Ecology and Management*.

Rodríguez-García, Cristina, Fernando Montes, Federico Ruiz, Isabel Cañellas, and Pilar Pita. 2014. "Stem Mapping and Estimating Standing Volume from Stereoscopic Hemispherical Images." *European Journal of Forest Research*.

Roussel, Jean-Romain and David Auty. 2019. "LidR: Airborne LiDAR Data Manipulation and Visualization for Forestry Applications."

Ruiz, Luis A., Txomin Hermosilla, Francisco Mauro, and Miguel Godino. 2014. "Analysis of the Influence of Plot Size and LiDAR Density on Forest Structure Attribute Estimates." *Forests* 5(5):936–51.

Ryding, Joseph, Emily Williams, Martin Smith, and Markus Eichhorn. 2015. "Assessing Handheld Mobile Laser Scanners for Forest Surveys." *Remote Sensing* 7(1):1095–1111.

Sánchez-González, Mariola, Miguel Cabrera, Pedro Javier Herrera, Roberto Vallejo, Isabel Cañellas, and Fernando Montes. 2016. "Basal Area and Diameter Distribution Estimation Using Stereoscopic Hemispherical Images." *Photogrammetric Engineering and Remote Sensing*.

Saukkola, Atte, Timo Melkas, Kirsi Riekki, Sanna Sirparanta, Jussi Peuhkurinen, Markus Holopainen, Juha Hyyppä, and Mikko Vastaranta. 2019. "Predicting Forest Inventory Attributes Using Airborne Laser Scanning, Aerial Imagery, and Harvester Data." *Remote*

Sensing.

Seidl, Rupert, Dominik Thom, Markus Kautz, Dario Martin-Benito, Mikko Peltoniemi, Giorgio Vacchiano, Jan Wild, Davide Ascoli, Michal Petr, Juha Honkaniemi, Manfred J. Lexer, Volodymyr Trotsiuk, Paola Mairota, Miroslav Svoboda, Marek Fabrika, Thomas A. Nagel, and Christopher P. O. Reyer. 2017. “Forest Disturbances under Climate Change.” *Nature Climate Change*.

Shen, Xin, Lin Cao, Bisheng Yang, Zhong Xu, and Guibin Wang. 2019. “Estimation of Forest Structural Attributes Using Spectral Indices and Point Clouds from UAS-Based Multispectral and RGB Imageries.” *Remote Sensing*.

Sheppard, Jonathan, Christopher Morhart, Jan Hackenberg, and Heinrich Spiecker. 2016. “Terrestrial Laser Scanning as a Tool for Assessing Tree Growth.” *IForest-Biogeosciences and Forestry* 10(1):172.

Siipilehto, Jouni, Harri Lindeman, Mikko Vastaranta, Xiaowei Yu, and Jori Uusitalo. 2016. “Reliability of the Predicted Stand Structure for Clear-Cut Stands Using Optional Methods: Airborne Laser Scanning-Based Methods, Smartphone-Based Forest Inventory Application Trestima and Pre-Harvest Measurement Tool EMO.” *Silva Fennica* 50(3):1–24.

Smith, David J. 1996. *Development and Field Application of Density Management Diagrams and Size-Density Surface Models Developed for the Boreal Mixedwood Stands of Ontario*. Sault Ste. Marie, Canada.

Smith, W. Brad. 2002. “Forest Inventory and Analysis: A National Inventory and Monitoring Program.” *Environmental Pollution*.

Stinson, Graham and Joanne C. White. 2018. “What’ s the Difference between EFI and NFI ? Demystifying Current Acronyms in Forest Inventory in Canada.” *BC Forest Professional*, 10–11.

Strong, Wayne. 1992. *Ecoregions and Ecodistricts of Alberta*. Edmonton: Alberta Forestry, Lands and Wildlife, Land Information Services Division, Resource Information Branch.

Swatantran, Anu, Hao Tang, Terence Barrett, Phil Decola, and Ralph Dubayah. 2016. "Rapid, High-Resolution Forest Structure and Terrain Mapping over Large Areas Using Single Photon Lidar." *Scientific Reports*.

Taubert, Franziska, Florian Hartig, Hans-Jürgen Dobner, and Andreas Huth. 2013. "On the Challenge of Fitting Tree Size Distributions in Ecology" edited by J. P. Brody. *PLoS ONE* 8(2):e58036.

Taylor, Anthony R. and Han Y. H. Chen. 2011. "Multiple Successional Pathways of Boreal Forest Stands in Central Canada." *Ecography* 34(2):208–19.

Terrier, Aurélie, Martin P. Girardin, Catherine Périé, Pierre Legendre, and Yves Bergeron. 2013. "Potential Changes in Forest Composition Could Reduce Impacts of Climate Change on Boreal Wildfires." *Ecological Applications* 23(1):21–35.

Thomas, V., R. D. Oliver, K. Lim, and M. Woods. 2008. "LiDAR and Weibull Modeling of Diameter and Basal Area." *Forestry Chronicle* 84(6):866–75.

Toledo, José J., William E. Magnusson, and Carolina V. Castilho. 2013. "Competition, Exogenous Disturbances and Senescence Shape Tree Size Distribution in Tropical Forest: Evidence from Tree Mode of Death in Central Amazonia." *Journal of Vegetation Science* 24(4):651–63.

Tompalski, Piotr. 2012. "Wykorzystanie Wskaźników Przestrzennych 3D w Analizach Cech Roślinności Miejskiej Na Podstawie Danych z Lotniczego Skanowania Laserowego." *Archiwum Fotogrametrii, Kartografii i Teledetekcji* 23.

Tompalski, Piotr, Nicholas C. Coops, Joanne C. White, and Michael A. Wulder. 2015. “Enriching ALS-Derived Area-Based Estimates of Volume through Tree-Level Downscaling.” *Forests* 6(8):2608–30.

Tompalski, Piotr, Nicholas Coops, Peter Marshall, Joanne White, Michael Wulder, and Todd Bailey. 2018. “Combining Multi-Date Airborne Laser Scanning and Digital Aerial Photogrammetric Data for Forest Growth and Yield Modelling.” *Remote Sensing*.

Tompalski, Piotr, Joseph Rakofsky, Nicholas C. Coops, Joanne C. White, Alexander N. V. Graham, and Kyle Rosychuk. 2019. “Challenges of Multi-Temporal and Multi-Sensor Forest Growth Analyses in a Highly Disturbed Boreal Mixedwood Forests.” *Remote Sensing* 11(18).

Tompalski, Piotr, Joanne C. White, Nicholas C. Coops, and Michael A. Wulder. 2019. “Quantifying the Contribution of Spectral Metrics Derived from Digital Aerial Photogrammetry to Area-Based Models of Forest Inventory Attributes.” *Remote Sensing of Environment*.

Turner, Monica G., Daniel C. Donato, and William H. Romme. 2013. “Consequences of Spatial Heterogeneity for Ecosystem Services in Changing Forest Landscapes: Priorities for Future Research.” *Landscape Ecology* 28(6):1081–97.

Vastaranta, Mikko. 2012. “Forest Mapping and Monitoring Using Active 3D Remote Sensing.” *Dissertationes Forestales*.

Walker, Brian, Crawford S. Holling, Stephen R. Carpenter, and Ann Kinzig. 2004. “Resilience, Adaptability and Transformability in Social–Ecological Systems.” *Ecology and Society* 9(2).

Wallace, Andrew M., Aongus McCarthy, Caroline J. Nichol, Ximing Ren, Simone Morak, Daniel Martinez-Ramirez, Iain H. Woodhouse, and Gerald S. Buller. 2014. "Design and Evaluation of Multispectral LiDAR for the Recovery of Arboreal Parameters." *IEEE Transactions on Geoscience and Remote Sensing*.

Wang, Yunsheng, Matti Lehtomäki, Xinlian Liang, Jiri Pyörälä, Antero Kukko, Anttoni Jaakkola, Jingbin Liu, Ziyi Feng, Ruizhi Chen, and Juha Hyyppä. 2019. "Is Field-Measured Tree Height as Reliable as Believed – A Comparison Study of Tree Height Estimates from Field Measurement, Airborne Laser Scanning and Terrestrial Laser Scanning in a Boreal Forest." *ISPRS Journal of Photogrammetry and Remote Sensing* 147:132–45.

White, Joanne C., Nicholas C. Coops, Michael A. Wulder, Mikko Vastaranta, Thomas Hilker, and Piotr Tompalski. 2016. "Remote Sensing Technologies for Enhancing Forest Inventories: A Review." *Canadian Journal of Remote Sensing* 42(5):619–41.

White, Joanne C., Ninni Saarinen, Ville Kankare, Michael A. Wulder, Txomin Hermosilla, Nicholas C. Coops, Paul D. Pickell, Markus Holopainen, Juha Hyyppä, and Mikko Vastaranta. 2018. "Confirmation of Post-Harvest Spectral Recovery from Landsat Time Series Using Measures of Forest Cover and Height Derived from Airborne Laser Scanning Data." *Remote Sensing of Environment* 216:262–75.

White, Joanne C., Ninni Saarinen, Michael A. Wulder, Ville Kankare, Txomin Hermosilla, Nicholas C. Coops, Markus Holopainen, Juha Hyyppä, and Mikko Vastaranta. 2019. "Assessing Spectral Measures of Post-Harvest Forest Recovery with Field Plot Data." *International Journal of Applied Earth Observation and Geoinformation* 80:102–14.

White, Joanne C., Michael A. Wulder, Txomin Hermosilla, Nicholas C. Coops, and Geordie W. Hobart. 2017. "A Nationwide Annual Characterization of 25 Years of Forest Disturbance and Recovery for Canada Using Landsat Time Series." *Remote Sensing of Environment*

194:303–21.

White, Joanne C., Michael A. Wulder, Andrés Varhola, Mikko Vastaranta, Nicholas C. Coops, Bruce D. Cook, Doug Pitt, and Murray Woods. 2013. *A Best Practices Guide for Generating Forest Inventory Attributes from Airborne Laser Scanning Data Using an Area-Based Approach*. Vol. 89.

White, Joanne C., Michael A. Wulder, Mikko Vastaranta, Nicholas C. Coops, Doug Pitt, and Murray Woods. 2013. “The Utility of Image-Based Point Clouds for Forest Inventory: A Comparison with Airborne Laser Scanning.” *Forests* 4(3):518–36.

Wiant, H. V., G. B. Wood, and T. G. Gregoire. 1992. “Practical Guide for Estimating the Volume of a Standing Sample Tree Using Either Importance or Centroid Sampling.” *Forest Ecology and Management* 49(3–4):333–39.

Wirth, Christian. 2009. “Old-Growth Forests: Function, Fate and Value – a Synthesis.” Pp. 465–91 in *Old-Growth Forests: Function, Fate and Value*, edited by C. Wirth, G. Gleixner, and M. Heimann. Berlin, Heidelberg: Springer Berlin Heidelberg.

Wood, Simon N. 2001. “Mgcv: GAMs and Generalized Ridge Regression for R.” 1.

Wood, Simon N. 2017. *Generalized Additive Models: An Introduction with R*. Chapman and Hall/CRC.

Wulder, Michael A., Christopher W. Bater, Nicholas C. Coops, Thomas Hilker, and Joanne C. White. 2008. “The Role of LiDAR in Sustainable Forest Management.” *Forestry Chronicle* 84(6):807–26.

Wulder, Michael A. and Steven E. Franklin. 2003. *Remote Sensing of Forest Environments: Concepts and Case Studies*. 1st ed. edited by M. A. Wulder and S. E. Franklin. New York, USA: Springer Science+Business Media.

Wulder, Michael A., Joanne C. White, Christopher W. Bater, Nicholas C. Coops, Chris Hopkinson, and Gang Chen. 2012. “Lidar Plots — a New Large-Area Data Collection Option: Context, Concepts, and Case Study.” *Canadian Journal of Remote Sensing*.

Xu, Qing, Zhengyang Hou, Matti Maltamo, and Timo Tokola. 2014. “Calibration of Area Based Diameter Distribution with Individual Tree Based Diameter Estimates Using Airborne Laser Scanning.” *ISPRS Journal of Photogrammetry and Remote Sensing* 93:65–75.

Zenner, Eric K. 2005. “Development of Tree Size Distributions in Douglas-Fir Forests under Differing Disturbance Regimes.” *Ecological Applications* 15(2):701–14.

Zhang, L. J., K. C. Packard, and C. M. Liu. 2003. “A Comparison of Estimation Methods for Fitting Weibull and Johnson’s S-B Distributions to Mixed Spruce-Fir Stands in Northeastern North America.” *Canadian Journal of Forest Research-Revue Canadienne De Recherche Forestiere* 33(7):1340–47.

Zhang, Lianjun, Jeffrey H. Gove, Chuangmin Liu, and William B. Leak. 2001. “A Finite Mixture of Two Weibull Distributions for Modeling the Diameter Distributions of Rotated-Sigmoid, Uneven-Aged Stands.” *Canadian Journal of Forest Research* 31(9):1654–59.

Zhang, Xiao, Craig Glennie, and Arpan Kusari. 2015. “Change Detection from Differential Airborne LiDAR Using a Weighted Anisotropic Iterative Closest Point Algorithm.” *IEEE Journal of Selected Topics in Applied Earth Observations and Remote Sensing* 8(7):3338–46.

Zhang, Yu, Han Y. H. Chen, and Peter B. Reich. 2012. “Forest Productivity Increases with Evenness, Species Richness and Trait Variation: A Global Meta-analysis.” *Journal of Ecology* 100(3):742–49.

Zuur, Alain, Elena N. Ieno, Neil Walker, Anatoly A. Saveliev, and Graham M. Smith. 2009.

Mixed Effects Models and Extensions in Ecology with R. Springer Science & Business Media.